

**RIVERBANK FILTRATION: MODELING FATE OF DISSOLVED  
ORGANIC CARBON, TRANSPORT OF *ESCHERICHIA COLI* AND  
COUPLING WITH AQUIFER STORAGE TO ADDRESS TEMPORAL  
WATER SCARCITY**

A DISSERTATION SUBMITTED TO THE GRADUATE DIVISION OF THE  
UNIVERSITY OF HAWAI'I AT MĀNOA IN PARTIAL FULFILLMENT OF  
THE REQUIREMENTS FOR THE DEGREE OF

DOCTOR OF PHILOSOPHY

IN

CIVIL AND ENVIRONMENTAL ENGINEERING

AUGUST 2012

By

Laxman Sharma

Dissertation Committee:

Chittaranjan Ray (Chairperson)

Edmond Cheng

Aly El-Kadi

Henning Prommer

Michelle Teng

Ali Fares

Keywords: Riverbank Filtration, Redox Modeling, Groundwater Dissolved  
Organic Carbon, Pathogen Transport, Aquifer Storage and Recovery

## DEDICATION

I dedicate this dissertation to my family, especially....

To my parents, who always encouraged me to follow my dreams;

To my wife Bindu, for her continued support and understanding during these student days;

To my son Shantanu, with whom I wanted to spend more time but this research kept on pulling me away;

To my brother and sister, who went through turbulent times back home in Nepal while I pursued my studies here in the USA.

This is to all of you, my friends and family, for all the time I missed being with you.

## ACKNOWLEDGEMENT

First and foremost, I am grateful to my advisor, Prof. Chittaranjan Ray, who introduced me to the field of riverbank filtration and patiently guided me, providing support and challenges to keep me going on to complete my dissertation. I also acknowledge the dissertation committee members - Edmond Cheng, Aly El-Kadi, Henning Prommer, Michelle Teng and Ali Fares for their guidance and suggestions as I went through the rigors of graduate studies. Thank you for taking me under your tutelage, allowing me to be your teaching assistant and encouraging me on!

I am further indebted to Henning (CSIRO Land and Water, Perth, Australia) for his tireless effort in teaching me reactive transport modeling with PHT3D and endless sessions on Skype from Australia. I owe gratitude to Janek Greskowiak (currently at Carl von Ossietzky University of Oldenburg, Germany) for helping me the intricacies of numerical modeling and reaction kinetics. Saeed Torkzaban of CSIRO, Adelaide, South Australia helped me understand the latest in pathogen transport. Vincent Post of Flinders University, Adelaide, South Australia showed how to obtain the velocity fields from MODFLOW into PHT3D.

I must thank Paul Eckert at the Flehe waterworks, Stadtwerke Düsseldorf AG, Düsseldorf, who provided me the data set for the Rhine River RBF to work on. His help is immensely appreciated. I also acknowledge the East-West Center for awarding me the Graduate Degree Fellowship that enabled me to come to the U.S. for graduate studies. I am indebted to the Water Resources Research Center at UH and the Department of Civil and Environmental Engineering who supported me with numerous Graduate Research Assistantships. A part of the support for the chapter on riverbank filtration and aquifer and storage recovery was possible through support from the USGS.

## Abstract

Riverbank filtration (RBF) is an accepted method of treatment for water supply from rivers which markedly improves the source water quality. Pumping water from wells adjacent to water body induces surface water to infiltrate through the aquifer attenuating contaminants present in the source water. This study used field data from an operating RBF system located along the Rhine River in Düsseldorf, Germany, and carried out focused research on the fate of dissolved organic carbon and on transport of *E. coli*. Furthermore, a novel application of RBF and aquifer storage and recovery (ASR) was considered in a study to address seasonal water scarcity in the Albany region of the Georgia in US.

A reactive transport model (PHT3D) was developed to study the fate of dissolved organic carbon incorporating transient boundary conditions. Modeling residence times showed that high floods in the river reduced the travel time to the RBF well to 8 days, while low flows increased it to about 60 days. Aerobic processes with some partial denitrification occurred in the aquifer. The temporal changes in the breakthrough of dissolved oxygen were best reproduced when the temperature dependency of the biogeochemical processes was explicitly considered. The results showed that seasonal temperature changes superimposed by changes in residence time strongly affected the extent of redox reactions along the flow path.

Microbial transport is modeled in groundwater using the advection-dispersion transport equation adding on the processes of attachment, detachment and inactivation processes. The rates defined by these processes are velocity dependent and cannot be used directly for a transient RBF model. An approach to handle such transient conditions is developed using colloid filtration theory and the concepts of single collector contact efficiency and verified on a benchmark 1-D study. The model is extended to the Rhine River RBF system. The transport of *E-coli* and coliforms was successfully modeled.

The RBF-ASR study showed the viability of obtaining excess river flows through RBF and storing it a deeper aquifer to be recovered later. Geochemical changes were also investigated. The overall study contributes to our understanding of the various processes involved in RBF and subsurface flows.

# Table of Contents

Acknowledgement .....	i
Abstract .....	ii
List of Tables .....	vi
List of Figures.....	vii
<b>CHAPTER 1. INTRODUCTION.....</b>	<b>1</b>
1.1 Background on riverbank filtration.....	2
1.1.1 Pollutants in riverbank filtration.....	3
1.1.2 Processes occurring in riverbank filtration.....	5
1.1.3 Factors affecting performance of RBF systems .....	11
1.1.4 Conclusion.....	13
1.2 Scope and Objectives.....	14
1.3 Publications from this study.....	18
<b>CHAPTER 2. ELUCIDATING TEMPERATURE EFFECTS ON SEASONAL VARIATIONS OF BIOGEOCHEMICAL TURNOVER RATES DURING RIVERBANK FILTRATION .....</b>	<b>19</b>
Abstract .....	19
2.1 Introduction.....	20
2.2 Study site .....	23
2.2.1 Hydrogeology.....	24
2.2.2 Geochemical characteristics.....	25

2.3 Modeling of seasonal flow dynamics and nonreactive transport behavior .....	26
2.3.1 Conceptual model and numerical model set up.....	26
2.3.2 Non-reactive transport model.....	29
2.3.3 Residence time simulations .....	30
2.4 Reactive transport model .....	31
2.4.1 Reaction network.....	31
2.4.2 Boundary conditions.....	33
2.5 Results and discussion .....	33
2.5.1 Chloride and heat Transport.....	33
2.5.2 Residence time simulations .....	35
2.5.3 Spatial and temporal variability of redox and secondary reactions.....	37
2.6 Summary and Conclusions .....	43
<b>CHAPTER 3. MODELLING OF FIELD-SCALE E-COLI TRANSPORT DURING RIVER BANK FILTRATION.....</b>	<b>45</b>
Abstract .....	45
3.1 Introduction.....	46
3.1.1 Objective: .....	48
3.1.2 Background literature on microbial removal.....	48
3.2 Incorporation of pathogen transport capabilities into PHT3D.....	53
3.2.1 Governing equations for pathogen transport .....	53
3.3 Model evaluation with column experiments.....	58
3.3.1 Model code verification using original method .....	59
3.3.2 Model verification using 1-D column experiments.....	62

3.4 Evaluation for field-scale transport.....	65
3.4.1 Study site .....	65
3.4.2 Model Setup .....	65
3.4.3 Results and discussion.....	67
3.5 Conclusions.....	73
<b>CHAPTER 4. A COMBINED RBF AND ASR SYSTEM FOR PROVIDING DRINKING WATER IN WATER SCARCE AREAS.....</b>	<b>75</b>
Abstract .....	75
4.1 Introduction.....	76
4.2 Review of Past Relevant Work.....	78
4.3 Methods and Procedures .....	80
4.4 Results and Discussion .....	90
4.4.1 The RBF subsystem.....	90
4.4.2 The ASR subsystem.....	92
4.4.3 Pyrite Oxidation and Arsenic mobility .....	94
4.5 Conclusions and Future Research Recommendations .....	95
<b>CHAPTER 5. CONCLUSION AND RECOMMENDATIONS.....</b>	<b>97</b>
<b>Appendix A: PHT3D database modifications and PHT3D_PH.DAT file for modeling DOC transport .....</b>	<b>103</b>
<b>Appendix B: PHT3D database modifications and PHT3D_PH.DAT for modeling microbial transport.....</b>	<b>107</b>
<b>REFERENCES.....</b>	<b>122</b>

## LIST OF TABLES

Table 1: Redox reactions for conversion of organic matter and the potential Gibbs free-energy changes at pH equal to 7.....	9
Table 2: Initial concentrations in the model and range of concentrations in the river and the groundwater (mol/L). ....	28
Table 3: Parameter values used in defining the reaction kinetics. ....	37
Table 4: Input parameters used in modeling 1-D column transport for the two soils.....	59
Table 5: A comparison of the fitted parameters for the benchmark case... ..	60
Table 6: Constant parameters used in modeling 1-D column transport for the two soils.....	63
Table 7: Fitted parameters for the two soil columns using filtration theory applicable to both velocities of flow for the columns. ....	65
Table 8: Constant parameters used in modelling RBF microbial transport. ....	67
Table 9: Aqueous components as model inputs from charge balanced data set. ....	87
Table 10: Pumping Schedule .....	88
Table 11: Maximum concentrations of various aqueous species in RBF and ASR water.....	92

## LIST OF FIGURES

Fig. 1: Schematics of horizontal and vertical RBF wells (Ray et al., 2002).....	2
Fig. 2: Schematic diagram of processes affecting water quality during bank filtration .....	5
Fig. 3: Location of the Flehe water works along Rhine River in Düsseldorf, Germany. The modeled x-section of the Rhine River, the observation wells and RBF well are shown. The alignment of other wells along the Rhine in the right bank is also shown by black dots, the position of the dots are only indicative and do not represent actual wells. ....	22
Fig. 4: Cross-section of the study site showing the pumping well and the observation wells near the right bank of the river. ....	23
Fig. 5: Seasonal temperature variations of the Rhine River water and the filtrate at the RBF well. ....	24
Fig. 6: Model extent, grid discretization, hydraulic conductivity zones and hydraulic boundary conditions used in the numerical model. The well is located in the North-East (right bank) side of the model. GHB = General Head Boundary, $K1 = 1.04 \times 10^{-6}$ m/s, $K2 = 9.26 \times 10^{-4}$ m/s, $K3 = 3.01 \times 10^{-3}$ m/s, $K4 = 6.37 \times 10^{-3}$ m/s, $K5 = 5.79 \times 10^{-5}$ m/s and $K6 = 5.79 \times 10^{-4}$ m/s.....	27
Fig. 7: Observed and simulated breakthrough curves of temperature and chloride at the observation well B and at the RBF well. ....	34
Fig. 8: Simulated groundwater age distribution (age since start of simulation) $t = 68$ days. The clogging layer is shown in bold line in the middle portion of the river bed. ....	36

Fig. 9: Simulated groundwater age distribution (age since start of simulation) $t = 340$ days. The clogging layer is shown in bold line in the middle portion of the river bed. ....	36
Fig. 10: Simulated (lines) and observed (o) concentrations of DOC and dissolved oxygen. Red lines show the reactive transport results in comparison with the results of non-reactive simulations (black lines). The dashed lines indicate the Rhine river concentrations. ....	38
Fig. 11. Simulated (lines) and observed (o) concentrations of nitrate (N(5)) and sulphate (S(6)). Red lines show the reactive transport results in comparison with the results of non-reactive simulations (black lines). The dashed lines indicate the Rhine River concentrations. The concentrations of S(6) for the reactive simulations and the corresponding non-reactive simulations do not differ and appear as a single line. ....	39
Fig. 12: Simulated and measured concentrations of Ca, C(4) and pH levels at the observation points B1 and B2 .....	41
Fig. 13: a) Observed and simulated concentrations of dissolved oxygen at B1 for various assumptions of temperature in redox modeling, (b) Extent of biodegradation at B1 in terms of transferred electrons (see text), and (c) simulated age/residence time of water at the observation point B1. ....	43
Fig. 14: Comparison of data, Hijnen's results and our modeled MS2 breakthrough curves for Castricum soils loaded with two different velocities (code verification) .....	61
Fig. 15: Comparison of data, Hijnen's fitted and our modeled MS2 breakthrough curves for Roosteren soils loaded with two different velocities (code verification). ....	61

Fig. 16: Comparison of original fitted MS2 breakthrough curves with our modeled results for Castricum soil using filtration theory concepts. ....	64
Fig. 17: Comparison of original fitted MS2 breakthrough curves with our modeled results for Roosteren soil using filtration theory concepts. ....	64
Fig. 18: E-coli and coliform concentrations measured in the river water and the observed values at the RBF well. ....	66
Fig. 19: Simulated (green lines) and observed (red ×) E-coli and Coliforms shown in reference to the concentration in river (black line) in the saturated observation points B 1- 3 and the changing river water level (blue lines) (detection limit > 1 MPN/100 mL).....	69
Fig. 20: Simulated (green lines) and observed (red ×) E-coli and Coliforms shown in reference to the concentration in river (black line) in the intermittently saturated observation points B 4 -6 and the changing river water level (blue lines) (detection limit > 1 MPN/100 mL) .....	70
Fig. 21: E-coli concentration in the river and the aquifer at different times.....	71
Fig. 22: Coliforms concentration in the river and the aquifer at different times .....	72
Fig. 23: Possible location of the ASR site east/north-east of the City of Albany, Georgia, USA. ....	82
Fig. 24: Aquifers in the Albany area .....	84
Fig. 25: Two dimensional grid models for depicting RBF (top) and ASR (bottom).....	86
Fig. 26: Concentration time series data at the RBF pumping well. The pump is turned off during the periods 230-410 and 590-770 days. ....	91

Fig. 27: Concentration time series data at the ASR well. The pump is injecting RBF water into the deeper aquifer in the periods 0- 230 days and 410-590 days, and extracting at other times.....93

Fig. 28: Concentration time series plot at the ASR well for the second case when pyrite oxidation is considered. The pump is injecting RBF water into the deeper aquifer in the periods 0 - 230 days and 410-590 days, and extracting at other times. ....95

## **CHAPTER 1. INTRODUCTION**

Growing population, competing demand for resources, improved standards of living, and various other external causes and environmental concerns have placed greater demands on the available supply of safe drinking water. UNESCO reports that over 1.1 billion people do not have access to safe water (Keast and Johnston, 2008). Communities along rivers have always depended upon surface water as their primary source of drinking water. Surface water quality is often impaired by agricultural runoff, municipal outfalls and industrial discharges that introduce a complex variety of contaminants and pollutants. Groundwater is often over-exploited. Alternate water supply and management options are required to increase water reuse, reduce capital cost and provide less energy-intensive systems. Riverbank filtration (RBF) is a mechanism in which wells placed alongside rivers (or lakes) or driven below them are pumped to induce surface water to flow through the aquifer to the wells. As water is induced to travel through the aquifer, the natural processes of filtration, straining, adsorption, mixing and other important biological and geochemical processes attenuate these contaminants and pathogens thereby markedly improving the source water quality (Ray et al., 2002a).

Many cities in Europe (e.g., Belgrade, Berlin, Bratislava, Bonn, Budapest, Dusseldorf, Hamburg, Köln, etc.) along the major rivers (Rhine, Elbe, Danube, etc.) have utilized the natural process of riverbank filtration for more than a century (Schubert, 2002b). More recently, cities in the US (e.g., Cedar Rapids, Iowa; Cincinnati, Ohio; Louisville, Kentucky; Jacksonville, Illinois; Lincoln, Nebraska and Sonoma County, California) have also implemented the approach. RBF has a potential to supply water to more than 67 million people in US and is gradually being considered in other countries around the world, e.g., India, Korea and Egypt (Ray, 2008). Compared to using surface water directly, RBF provides water that is more consistent in quality, requiring a lesser amount of subsequent treatment processes and disinfection. RBF is often used as a pre-treatment method followed by other treatment options. In some cases, it may be the only treatment option followed by chlorination and fluoridation before being distributed to the consumers. Widespread surface water contamination and the possible impacts of such contamination on drinking water supplies are forcing utilities to look for better quality

water sources. A greater interest and scrutiny is being placed on the functioning of RBF schemes (Tufenkji et al., 2002; Weiss et al., 2005) as possible sources for water supply. Constructing new conventional water treatment facilities and maintaining them are getting more expensive. RBF schemes provide an alternative option reducing operating costs and thus can be an attractive choice in both the developed and developing nations around the world.

### 1.1 Background on riverbank filtration

RBF is an attractive option in riparian areas that have aquifers hydraulically connected to the rivers. Depending upon the location and orientation of the wells, the RBF wells are classified as vertical or horizontal wells as shown in Fig. 1 below.

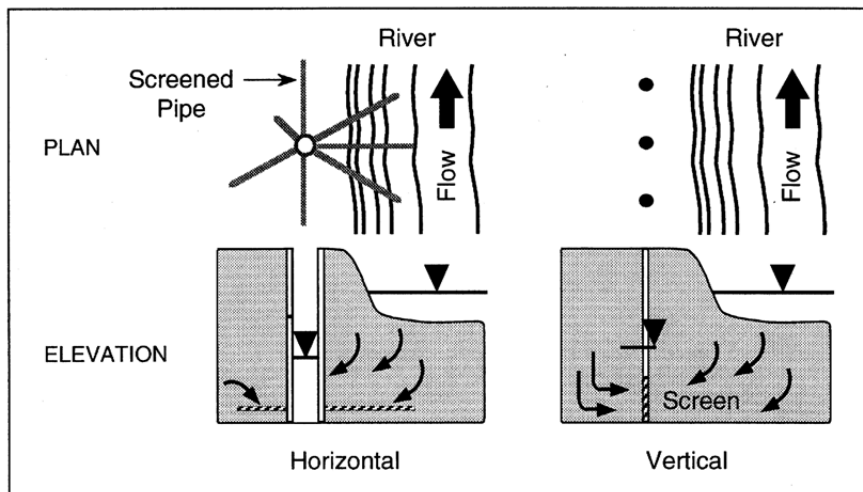


Fig. 1: Schematics of horizontal and vertical RBF wells (Ray et al., 2002).

Vertical wells are drilled adjacent to the riverbank with vertical well screens. The horizontal wells have horizontal lateral collectors extending radially from a large-diameter caisson. Some of these laterals may even extend below the riverbed. The vertical wells mostly capture horizontal flows while horizontal wells capture vertical flows (Schijven et al., 2003). The choice of horizontal or vertical wells is affected by the aquifer thickness and the desired pumping capacity (Ray, 2002). Horizontal wells are preferred over vertical wells when the aquifers are thin, and when the pumping needs are higher. Utilities with existing treatment plants often use horizontal wells as a pre-

treatment before full-scale treatment. The laterals underneath the river have their well screens nearer to the riverbed and thus the infiltrating water has shorter a flow path. Microorganisms are more likely to breakthrough in to the laterals from the river (Schijven et al., 2003). Wells are preferably placed on an inner part of meander (Schubert, 2002a), the convex bank, as it intercepts more subsurface cross flows.

### **1.1.1 Pollutants in riverbank filtration**

RBF remove a variety of pollutants in the source water to improve source water quality. The scope of contaminants of concern that are present, removed or attenuated by riverbank filtration can be classified into physical, chemical or microbiological in nature, as described below.

#### *Physical contaminants*

Turbidity and temperature are the major physical contaminants in river waters. Turbidity is a common indicator of water quality and filtration performance. Turbidity can be due to presence of particulate colloids, algae and decaying organic matter. High turbidity in source water can cause problems as it can favor transport of microorganisms and chemicals by providing sorption sites for them. Presence of decaying organic matter can aid in the formation of disinfection by-products (DBPs) if it gets into the water disinfection phase. DBPs are potentially carcinogenic substances. Temperature can also be a concern, if it is altered through disposal of heated water such as those from power plants and industrial centers. Temperature controls the solubility of oxygen, affects coagulation and flocculation processes, and other physiological/biological activities of microorganisms. Temperature influences reaction kinetics, solubility and other chemical and physical properties of subsurface water and its constituents.

#### *Chemical contaminants*

Chemical contaminants include a wide range of products in waterways including pH, inorganics, natural organic matter (NOM), synthetic organic compounds, pharmaceuticals and personal care products (PPCPs). The pH of water defines numerous bio-geochemical processes in water and in the subsurface environments. When pH is changed from its optimum value of around 7.4, it can cause problems such as disrupting the physiology of

aquatic flora and fauna in rivers and lake waters. During subsurface transport processes, pH plays a large role in redox reactions, dissolution of matrix such as that of calcite, and leaching of heavy metals.

Inorganic pollutants are also major problems in aquatic environments. These include chlorides, bromides, and nutrients for plants (e.g. nitrogen, phosphorus and potassium). Bromine and chlorine, in the presence of natural organic matter, can form potentially carcinogenic DBPs. Runoff from agricultural lands can contain fertilizers (source of plant nutrients - nitrogen, phosphorus and potassium), municipal outfalls contain soap products containing phosphorus and these pose major problems in aquatic environments. Excess nitrogen and phosphorus lead to algal blooms in surface waters increasing the presence of decaying organic matter, depleting dissolved oxygen in water and increasing turbidity. Manganese and iron are also minerals that lead to discoloration and taste issues not palatable to the public apart from increasing hardness of water.

Synthetic organic compounds, e.g., pesticides and herbicides are chemicals of concern known to be dangerous if consumed. NOM can form carcinogenic DBPs, such as haloacetic acids (HAA) and trihalomethanes (THM). High concentrations of NOM increase the amount of dissolved organic carbon in water that can trigger a chain of reactions of redox processes consuming dissolved oxygen or other electron acceptors (Appelo and Postma, 2006). This can lead to development of anoxic conditions, release of metals and even gases in the aquifer.

PPCPs, including medicines, cosmetics, and fragrances, are low level pollutants (micropollutants) that, mostly, are easily dissolved in water and are suspected to affect physiological processes and behavior. PPCPs are reported to have changed function and structure of algae (Wilson et al., 2003).

#### *Microbiological pollutants*

Biological pollutants in water include viruses, bacteria, protozoa and algae; many of these are pathogenic - water posing a major concerns for health and wellbeing of life. These pathogens can cause severe diseases with health concerns, wide spread epidemics, and even death. Viruses are unicellular organisms, 20~120 nm in size, and may persist in

filtrate water if the RBF system is not functioning or designed well. Hepatitis virus, rotavirus, adenovirus, etc. are some of the common examples viruses that can cause life-threatening diseases.

Presence of fecal bacteria indicates sewage contamination of water bodies and these can cause severe life threatening diseases and epidemics. *Escherichia coli* (*E. coli*), *Legionella*, *salmonella* etc. are some of the examples. Protozoa are waterborne parasites such as the *Cryptosporidium parvum* and *Giardia lamblia*. *Cryptosporidium parvum* are most resistant to disinfection and their oocysts remain stable for months. These cause abdominal pain, cramp, fever and diarrhea severely compromising health and well-being of the population. Algae increases decaying matter in water, which depletes oxygen, introduces odor and changes the taste of water. The size and shape of the microbial pollutants along with their behavior when exposed to aquifer grains and the prevalent water chemistry are important characteristics that define their fate and transport in aquifers.

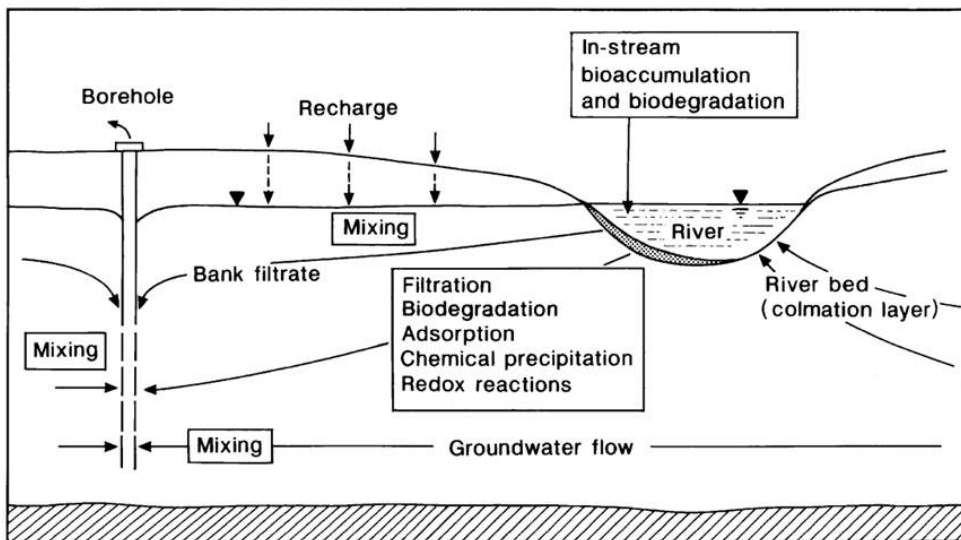


Fig. 2: Schematic diagram of processes affecting water quality during bank filtration (source: Hiscock and Grischek, 2002)

### 1.1.2 Processes occurring in riverbank filtration

Rivers and lakes, source waters for RBF systems, can contain high amounts of physical, chemical or biological contaminants. RBF should be able to remove these contaminants

or reduce them to acceptable limits. Removal of pathogenic organisms – virus, bacteria and protozoa – is crucial for human health and livelihood. RBF is known to be an effective protection barrier because microorganisms and pathogens are removed quite efficiently from the infiltrating water primarily through the processes of straining, attachment and inactivation or decay (Schijven et al., 2003). The natural process of attenuation of the contaminants in the river water depends strongly upon site-specific hydro-geochemical conditions. Processes of filtration, adsorption, precipitation, redox reactions and mixing occur as the water travels from the river to the RBF well through the aquifer as depicted in Fig 2 (Hiscock and Grischek, 2002).

#### *Physical processes*

The physical processes aiding removal of contaminants are filtration, straining, dispersion, adsorption and mixing with ambient groundwater. Filtration and straining are responsible for removing particulate material and microbes in water as it flows through aquifer grains (Bradford et al., 2003; Harvey et al., 1993). These are the main mechanisms of turbidity removal. Straining occurs when particles, abiotic or biotic, get physically trapped in pores due to their larger size stopping them from passing through the media. Even viruses and smaller pathogens can be strained if they are adsorbed to larger particles such as parasites, bacteria and other finer grains of the media (Bradford et al., 2006b; Foppen and Schijven, 2006; Sen, 2011). Bridging effects can also occur when smaller particles come up together and are blocked in pore throats that are smaller than their collective sizes. Sedimentation and trapping at dead end-pores can also occur, immobilizing moving particles. Hydrodynamic dispersion can have a dual effect on contamination levels by attenuating peak concentrations and spreading the concentration front such that some fraction of the particulates arrive earlier than conservative tracers.

The major component in retardation or removal of contaminants is adsorption, which is described as attachment of contaminants to solid grains (Barry et al., 2002). Adsorption occurs when contaminants or particulates are attached to the aquifer grain surfaces and is an important phenomenon in colloidal removal (Ryan and Elimelech, 1996). Adsorption is also affected by chemical and biological processes. Aquifers contain fine materials, such as clays and organic matter, which can adsorb a variety of contaminants.

Adsorption on the micro-scale is described as more of a physico-chemical process involving colloid filtration theory (Ryan and Elimelech, 1996) using concepts of single collector contact efficiency (SCCE) describing the likelihood of smaller particles colliding with a larger soil grain and getting attached. This theory suggests that the removal efficiency of granular media for microbes sized 1- 3  $\mu\text{m}$  is the lowest (Yao et al., 1971), showing that the bacteria and smaller protozoa in that size range have the greatest probability of traveling the furthest. Additional concepts of Derjaguin-Landau-Verwey-Overbeek (DLVO) theory (Hermansson, 1999) and van der Waal's forces (Tufenkji and Elimelech, 2003) have also been used in describing the process of adsorption. Attached particles can also get detached, where hydrodynamic forces are believed to come into play (Johnson et al., 2001). Adsorption and desorption have been described by both equilibrium and kinetic processes depending upon the flow properties and time scales involved.

Another important physical process is the mixing of water with the ambient groundwater that helps to attenuate and mitigate sudden impulse of pollutants (shock loads). This is a major advantage of RBF systems, compared to conventional treatment systems, which cannot handle shock loads and the input stream has to be carefully regulated. Mixing can also moderate extremes in temperature that can help maintain other physiological activities of microbes or stabilize concentration of gases and minerals.

#### *Biological processes*

Biological processes occurring in subsurface transport include biodegradation with aerobic, facultative and anaerobic bacteria, which are affected by growth, motility, competition, and predation among living organisms. Living organisms in the aquifer breakdown organic matter to meet metabolic needs and consume substrates (Phanikumar et al., 2005). Microorganisms catalyze chemical breakdown of certain compounds to obtain energy for their survival. This process can be aerobic, consuming dissolved oxygen rapidly within a short distance of infiltration if the organic loading is high enough, and then it can be followed by denitrification and other sequential redox reactions. Strongly reducing conditions can develop causing dissolution of iron and manganese from the aquifer matrix, and even release arsenics from arsenopyrites, if present, causing

further chemical contamination of the filtrate water (Greskowiak et al., 2005; Wallis et al., 2010). Different species of microorganisms may predominate depending upon the redox condition of the system.

A number of field studies or site monitoring activities have documented reduction of pathogens, surrogates, and indicators in RBF systems proving their performance. A one year study of three operating RBF facilities, located in the US along the Ohio, Missouri, and Wabash Rivers report that total coliforms were rarely detected in the well waters (Weiss et al., 2005). While average concentrations of total coliforms ranged from  $7.5 \times 10^5$  to  $4.6 \times 10^6$  MPN/L at the three sites, coliforms were detected only at two wells in one of the sites, and the reductions in coliforms concentrations were observed to be 5.5 and 6.1 log units relative to the river water.

Gollnitz et al. (2003) report findings from an RBF well field of Greater Cincinnati Water Works, Ohio, USA after analyzing long-term data (over 10 years) and an intensive monitoring of 20 months at two RBF production wells and 10 observation wells. RBF was found to be highly effective in removing pathogenic microbes with all surrogate concentrations maintaining at least 3.5-log reductions. Similar results of a 3-log reduction in average bacterial spores concentration have also been noted (Ray et al., 2002b) for a 50 feet travel distance to a collector well in Louisville, KY, USA. Daily monitoring of total coliforms in the river and the collector well in the same RBF facility in a later year showed removal ranging from 0.9 to more than 6 log units (Wang, 2003). The river water coliform concentrations ranged from 9 MPN/100 mL to 165,200 MPN/100 mL, whereas that at the collector well had very little positive detection, most of which were 1 MPN/100 mL or less.

### *Chemical processes*

A host of chemical processes may prevail, depending on the type of chemicals existing in the subsurface. Examples include ion exchange wherein electrolytes exchange ions and form complexes. Clay materials, humic acids and organic materials have high exchange capacities for heavy metal cations, and trap them in the soil matrix. These processes are sensitive to pH and salinity (Appelo and Postma, 2006). Consumption of substrates,

mineralization of organic compounds, and redox reactions of metals in solutions are also chemical processes. Agglomeration, coagulation, and flocculation of dispersed contaminants and microbes can also aid in removal of those materials within soil pores. Sometimes, when reduced species release metals, such as arsenic, these can be attached to oxyhydrates when the pH is suitable through surface complexation (NRC, 2007; Petrunic et al., 2005). This can precipitate out the metals in the subsurface.

Redox processes are very important chemical processes of any RBF or managed aquifer recharge systems. Water contains redox sensitive species such as  $O_2$ ,  $NO_3^-$ ,  $Mn^{4+}$ ,  $Fe^{2+}$ ,  $SO_4^{2-}$ ,  $H_2S$  or  $CH_4$ . Degradation of the DOC present in the infiltrating water provides the major driving force for redox changes as microorganisms catalyze reactions to gain energy for maintenance and growth (Lovley and Chapelle, 1995). The microorganisms preferentially catalyze the reactions releasing the highest energy. The stoichiometry of the reactions and the sequential removal of electron acceptors is given below ranked according to the amount of Gibbs free-energy changes ( $\Delta G_o(W)$ ) at pH equal to 7 (Champ et al., 1979) with the dissolved organic matter represented by the compound  $CH_2O$ .

Table 1: Redox reactions for conversion of organic matter and the potential Gibbs free-energy changes at pH equal to 7 (Champ et al., 1979).

Reaction	Stoichiometry	$\Delta G_o(W)$ kcal/mol
Respiration	$CH_2O + O_2 \rightarrow CO_2 + H_2O$	-120
Denitrification	$5CH_2O + 4NO_3^- + 4H^+ \rightarrow 5CO_2 + 2N_2 + 7H_2O$	-114
Mn(IV) reduction	$CH_2O + 2MnO_2(s) + 4H^+ \rightarrow 2Mn^{2+} + 3H_2O + CO_2$	-81
Fe (III) reduction	$CH_2O + 4Fe(OH)_3(s) + 8H^+ \rightarrow 4Fe^{2+} + 11H_2O + CO_2$	-28
Sulfate reduction	$CH_2O + SO_4^{2-} + H^+ \rightarrow HS^- + 2H_2O + 2CO_2$	-25

The sequence of reactions occurring at a location may be limited or partial depending upon the availability of degradable dissolved organic carbon or electron donors. The reaction is temperature dependent (Kirschbaum, 1995), kinetically controlled and often described by Monod-type rate expressions.

### *Riverbed clogging*

Clogging is the formation of a low permeability layer in the riverbed made of sedimentary or organic material. Water from the river infiltrates into the aquifer under the stresses created by the pump heads, but suspended solids cannot infiltrate the aquifer and are trapped and deposited in the upper layer of the aquifer or are embedded in between the larger particles. Microbial and chemical processes also help harden the clogging layer (Schubert, 2002). Precipitation of solutes or metals such as iron-manganese hydroxides or growth of bacterial cells in pores binds the surface into a more cohesive layer. High loads of organics in the river water can lead to chemical clogging beneath the infiltration zone. Often these clogged materials get so well armored that they cannot be removed by the river current. Clogging is understood to be a dynamic process governed not only by varying pumping rates but also by the flow dynamics of the river and the quality of river water (Schubert, 2002).

The clogged areas tend to expand from the well-side bank to the middle of the riverbed. In general, as the RBF operates, a clogging layer is formed on the riverbed near the source zone of the pumping well that reduces infiltration rates and decreases the production yield from the well field as also observed in the River Rhine RBF site at the Flehe water works in Dusseldorf, Germany (Schubert, 2002). A positive result of clogging is related to the increase of filtration efficiency, which enhances the ability to filter out particulates.

River flooding effects on RBF schemes are generally expected to lead to (1) reduced clogging due to erosion caused by greater scouring and decreasing filtering efficiency, or (2) short-circuiting of the flow paths as it circumvents the armored clogged zone, which leads to rapid infiltration from areas of higher conductivity zones. This shortens the travel path and the contact time between the contaminants and the aquifer matrix so that the reduction or attenuation of contaminants is incomplete and a breakthrough can occur. Such a microbial breakthrough occurs in the Rhine River RBF site at the Flehe water works when high flood occurs (see Chapter 3).

### **1.1.3 Factors affecting performance of RBF systems**

Riverbank filtration is a natural contaminant attenuation process whose performance depends on hydrogeological conditions, well design and placement factors, and most importantly, source water concentrations (Ray, 2002; Wang et al., 2002).

#### *Hydrogeological conditions*

##### Aquifer properties and hydraulic connection

For an RBF to be feasible, the river must be hydraulically connected to the aquifer. This means that any water drawn from the aquifer will be replenished by the infiltrating water from the river. The RBF wells are most successful in fluvial or alluvial aquifers along rivers or in unconsolidated sand and gravel deposits along lakes and reservoirs. Aquifers with very high hydraulic conductivity, or having fissures and cracks through which preferential flows can occur (i.e. having dual porosity) can cause earlier breakthrough of contaminants and undermine the RBF operation. Too low hydraulic conductivities also reduce yield, create more stress on pumps, and create larger drawdowns at wells and even unsaturated zones around abstraction zones (Su et al., 2007).

Research in microbial transport has shown that attachment mechanisms of pathogens and their ultimate inactivation may be facilitated by heterogeneous material that have some positive attraction to pathogens, which increases availability of favorable attachment sites (DeFlaun et al., 1997; Scheibe et al., 2007). Negatively charged microbes, such as coliforms, can easily attach to minerals such as iron oxyhydroxides, which have more positively charged surfaces. Anisotropy and non-homogeneity can certainly affect the dispersion and flow patterns in an aquifer affecting contaminant breakthroughs.

##### Travel distance and time

The quality of water is often related to the distance between the river water and the screen of the pumping well, which is the apparent travel distance. Travel distance and time are important factors that control the adequacy of maintaining interactions between the infiltrating water and the aquifer matrix. Short distance would mean lesser time for attenuation and not enough time for degradation of organic compounds. When the wells

are placed too far away, the contribution of river water in the filtrate will be reduced; it will consist mainly of groundwater.

In Europe, setback (travel) distances are typically specified to ensure RBF performance. However, in The Netherlands, a 60 day travel or residence time is mandated for water to be recovered from subsurface zones (Schijven et al., 2003). In US, for the horizontal wells where the laterals are placed closer and beneath the river, the travel distance is relatively short allowing rapid flow of water to the RBF wells. This has prompted the U.S. Environmental Protection Agency to classify RBF systems as groundwater under the direct influence of surface water which requires the utilities to treat the filtrate as surface water.

#### *Source water characteristics*

The RBF performance may be affected by source water characteristics. Water bodies with higher concentrations of contaminants will have more likelihood for the contaminant to persist through filtration and breakthrough with the filtrate. Concentrations or type of pollutants can be river or area specific. For example, rivers through forests have large amount of vegetative decay residues in water and those through industrial areas may have spills and trace chemicals. Catchment areas also define the presence of pollutant. For example, rivers passing through agricultural lands, pasturelands may indicate a larger than normal concentrations of *E. coli*, hormones, antibiotics, pesticides (Verstraeten et al., 1999) and fertilizer residues. Rivers that pass through geological zones with clays have higher problems with turbidity, and this can result in persistent microbes in the filtrate.

#### *River and lake hydrodynamics*

River and lake hydrodynamics also play a part in the RBF performance. In terms of rivers, hydraulic factors including the velocity profile, depth of flow can affect the formation or removal of clogging layers affecting the quality of filtrate. Wide shallow rivers may meander and change their thalweg, rendering altered distances to RBF well and changing the overall performance. Flood levels can shorten flow paths to the wells and reduce water's residence time in subsurface zone causing breakthrough of pathogens

and contaminants as discussed under hydrogeological conditions above. Rapid increase in flow with extreme floods can erode the clogging layer or even overflow banks to damage RBF wells, equipment and appurtenances.

#### *Management actions*

Pumping rates affect the quality of water abstracted. Low rates would likely reduce infiltration from the river and the bulk of the water may originate from the groundwater. The quality of the filtrate will then be dominated by the ambient groundwater. On the other hand, if the pumping rates are too high, then greater amount of river water will be drawn in along with an increase in the loading on the RBF system. This may result in breakthroughs of contaminants, turbidity and even lead to development of unsaturated zone around the abstraction points. This, in turn, increases stresses on pumps and reduce production of water. A temporary impoundment in rivers can reduce flow velocities in the reservoir and cause greater sedimentation and deposition. This can lead to a reduction in yield as observed in the Russian River RBF plant operated by the Sonoma County Water District (Su et al., 2007) due to the placement of inflatable dams to impound water.

#### **1.1.4 Conclusion**

The description above shows that the RBF is a complex processes to ensure supply of better quality water to communities. It is important to analyze the processes and mechanisms through which contaminants in the surface water are attenuated as the surface water infiltrates into the aquifer and travels through it. Flow conditions and the imposed river water quality in a functioning RBF system are dynamic and transient in nature. Any process-based detailed study of RBF systems need to incorporate these transient conditions and the dynamic characteristics of the boundary conditions and the flow fields within the aquifer to represent the RBF system. A modeling study, based on the abovementioned approach, using data from a full-scale operating RBF system would give the opportunity to analyze and understand some of these processes. This study attempts to fulfill that need along with an application of the RBF to address seasonal water scarcity with an example of coupling it with an aquifer storage and recovery (ASR) system. The transient nature of hydrodynamic conditions imposed by the river flow

stages, concentration of microbes and various species dissolved in the water, their fate as water infiltrates through the riverbed and the riverbank into the aquifer, along with the interactions in the aquifer, are carefully scrutinized and modeled in this study.

## 1.2 Scope and Objectives

The overall objective of this study is to analyze the different processes in a RBF system and carry out modeling studies to enable a better understanding of the RBF systems. The study includes a brief background description on RBF, which highlights the major pollutants, processes and factors affecting the performance of RBF systems (Chapter 1). The study further carries out three focused areas of research related to RBF; (1) transient redox modeling of the fate of dissolved organic carbon in a full scale performing system; (2) modeling transport of pathogenic bacteria (*E. coli*) in an RBF system; (3) integrating RBF with an aquifer storage and recovery to system to assess the possible water quality changes therein.

### 1. Transient redox modeling of a full scale RBF scheme for degradation of organic carbon

This study intends to fill a gap in the existing body of literature by carrying out a detailed quantitative analysis of time dependent biogeochemical dynamics of RBF systems by developing and applying a process-based reactive transport model. To date no detailed, model-based quantitative analysis of the temporal biogeochemical dynamics of RBF systems has been undertaken.

Surface waters contain dissolved organic matter and other redox sensitive aqueous species which infiltrate into the aquifer. When the existing chemical equilibrium of the groundwater in the aquifer is disturbed by the infiltrating water and its constituent species, a set of physical, chemical changes take place, including aerobic and anaerobic degradation of organic matter (Champ et al., 1979; Barry et al., 2002) under the presence of suitable microbes. Bourg and Bertin (1993) used groundwater mixing and bacterial degradation of organic matter to explain observed reduced zones in River Lot of France. Greskowiak et al. (2005b) used spatial and temporal distribution of the redox reactions below an artificial recharge pond near Lake Tegel in Germany to explain oxidation of

sulphides and dissolution of calcite. Seasonality, represented by temperature, was also shown to affect the reaction rates and the redox dynamics of phenazone in the same study. Microbes play a catalytic role in degradation of organic matter and it is known that temperature regulates microbial activity. Temperature also needs to be included in any RBF modelling. It is commonly used as a tracer to aid in modeling surface water groundwater interactions (Stonestrom and Constantz, 2003; Blasch et al., 2007; and Constantz, 2008), in groundwater flow modeling (Anderson, 2005) and has been modeled as a chemical species undergoing sorption and desorption (Prommer and Stuyfzand, 2005) a deep well injection in a pyritic aquifer.

Altered redox regimes in aquifers can set off different geochemical reactions affecting aqueous speciation, mobility of metals, metalloids, pesticides and other contaminants. Different redox zonation can occur in RBF aquifers which can affect the water quality of the RBF filtrate as well as the fate and transport of micropollutants.

The study aims at linking dynamic flow processes with the effects of varying temperature, reaction kinetics and the resulting overall biogeochemical rates at riparian aquifer. Specific objectives are to identify and quantify the interactive, dynamic physical and chemical processes influencing water quality changes within the hyporheic zone and the extraction wells in an RBF system under seasonally changing hydrological and raw/river water geochemical conditions. Data were obtained from a well-documented field site in the lower Rhine Valley near Düsseldorf (Germany) to develop and test a process-based reactive transport model.

## 2. Modeling transport of pathogenic bacteria (*E. coli*) in an RBF system

Microbial transport equations are investigated to include transient velocity and other related terms to be incorporated into a numerical model. The fate and transport of colloids and microbes in saturated media have been historically studied and reviewed in the literature (Foppen and Schijven, 2006; Ginn et al., 2002; Lawrence and Hendry, 1996; Ryan and Elimelech, 1996; Schijven and Hassanizadeh, 2000; Sen, 2011; Tufenkji, 2007). A bulk of the research has focused on the pore-scale processes and laboratory columns in controlled scenarios.

Most often, 1-D numerical models are fit to the breakthrough curves and are used to estimate various transport parameters (Bradford et al., 2003; Hijnen et al., 2005) that are different for different flow velocities. Most of the column studies were conducted with a single uniform flow velocity, i.e. a single column was operated at a single velocity, and limited in scope to one-dimensional. In contrast, field-scale pathogen transport is commonly affected by (i) the geological and geochemical heterogeneity of natural aquifer systems and (ii) complex and dynamically changing boundary conditions, such as river level fluctuations. Both factors induce significant spatial and temporal variations in groundwater flow velocities and, therefore, in estimates of the pathogen transport parameters. However, the impact of the combined spatial and temporal variations in groundwater velocities on pathogen fate and transport were not analyzed to date, and specifically, no numerical modeling study of pathogen transport in a full-scale RBF system exist to our knowledge.

Specific objectives are to develop a versatile pathogen transport model that is capable of handling transient flow conditions within the aquifer and test previously developed approaches. The developed model is to be applied to a benchmark study to demonstrate the accuracy of the modeling tool (reproduce previously published model results and data for column-scale experiment). This fully dynamic microbial transport model approach is to be finally used or tested on a fully functioning RBF scheme subject to transient flow conditions in simulating *E. coli* transport.

### 3. A combined RBF and ASR

The world is increasingly under stress as the water basins and aquifers are being over-exploited. This has brought in scarcity of water in developed as well as developing countries stifling economic growth. A large investment is required for construction of water treatment plants and distribution system. This lack of funds may be the reason for water scarcity in many developing nations, even though no physical shortage of water may be occurring. In developed countries and arid regions around the world, the actual limitations of water supply round the year may be causing physical scarcity. The availability of surface runoff during seasonal excesses can occur followed by a period of

dry spell. Surface storage schemes for the seasonally available water may be the alternative but it is often rendered ineffective due to high evaporation and other losses in arid zones, limitations of storage areas and other environmental concerns with reservoirs. A possible method can be used to store the seasonal water in underground aquifers and retrieve it when needed. Surface water with all its contaminants cannot be injected directly into the aquifers, because contamination of aquifers may take place. Water treatment, often to drinking water standards, is required before it can be injected into the aquifers. RBF may provide a solution in this aspect because the RBF filtrate provides water that is much cleaner and safer than the direct surface water.

This study looks at the possibility of a novel combination of riverbank filtration and aquifer storage recovery to address water shortage issues with reference to the Albany region of Georgia in US. The Georgia State Water Plan (EPD, 2008) outlines surface water storage, inter-basin transfer, and aquifer storage and recovery (ASR) as three main water supply management options to address water scarcity issues. RBF filtrate is sought to be used as source water for an ASR system, which injects water into the deeper aquifer during times of excess flows in the Flint River, and extract it during the drier season. The objective of this part of the study is to carry out a numerical modeling to investigate the possibility of such a scheme and to model the possible water quality changes occurring therein.

The results of the study on the fate of dissolved organic carbon has been published as a peer reviewed journal article (Sharma et al., 2012) in the Journal of Hydrology and the third study on combined RBF and ASR has also been published (Sharma and Ray, 2011) in the proceedings of a workshop. The second study on microbial transport is being finalized for publication. Because these are or are meant to be stand-alone publications, some of the introductory material and references may appear to be repetitive.

### **1.3 Publications from this study**

The proposed methods, results and findings have been presented in a number of meetings, discussions, workshops and conferences. The following are the publications made from this study.

1. Sharma, L., Greskowiak, J., Ray, C., Eckert, P. and Prommer, H., 2012. Elucidating temperature effects on seasonal variations of biogeochemical turnover rates during riverbank filtration. *Journal of Hydrology*, 428-429 : 104-115.
2. Sharma, L. and Ray, C., 2011. A combined RBF and ASR system for providing drinking water in water scarce areas. In: C. Ray and M. Shamrukh (Editors), *Riverbank filtration for water security in desert countries. NATO Science for Peace and Security Series C: Environmental Security*. Springer Netherlands, pp. 29-49.

## **CHAPTER 2. ELUCIDATING TEMPERATURE EFFECTS ON SEASONAL VARIATIONS OF BIOGEOCHEMICAL TURNOVER RATES DURING RIVERBANK FILTRATION<sup>1</sup>**

### **Abstract**

Riverbank filtration (RBF) is a mechanism by which undesired substances contained in infiltrating surface waters are attenuated during their passage across the riverbed and its underlying aquifer towards production wells. In this study, multi-component reactive transport modeling was used to analyze the biogeochemical processes that occur during subsurface passage at an existing RBF system - the Flehe Waterworks located along the Rhine River in Düsseldorf, Germany. The reactive transport model was established on the base of a conservative solute transport model for which temperature and chloride data served as calibration constraints. The model results showed that seasonal temperature changes superimposed by changes in residence time strongly affected the extent of the redox reactions along the flow path. The observed temporal, especially seasonal, changes in the breakthrough of dissolved oxygen were found to be best reproduced by the model when the temperature dependency of the biogeochemical processes was explicitly considered. High floods in the Rhine drastically reduced the travel time to the RBF well from an average travel time of 25-40 days to less than 8 days. On the other hand, low flow conditions increased the subsurface residence times between the Rhine River and the RBF well to about 60 days. The model results revealed that short term changes in the terminal electron acceptor consumption (biodegradation extent) were solely attributed to fluctuations in residence time, while more gradual changes in biodegradation extent were due to both seasonal variations of the river water temperature and gradual changes in residence time.

---

<sup>1</sup> Note: This chapter has already been published as an original research article in the Journal of Hydrology: Laxman Sharma, Janek Greskowiak, Chittaranjan Ray, Paul Eckert, Henning Prommer. Elucidating temperature effects on seasonal variations of biogeochemical turnover rates during riverbank filtration, Journal of Hydrology, Volumes 428–429, 27 March 2012, Pages 104-115, ISSN 0022-1694, 10.1016/j.jhydrol.2012.01.028.

## 2.1 Introduction

Riverbank filtration (RBF) is a mechanism by which undesired substances contained in infiltrating surface waters are attenuated during their passage across the riverbed and its underlying aquifer towards collector wells (Ray et al., 2002a). Riverbank filtration wells for public water supply have been widely used in Europe for more than a century (Schubert, 2002a) and for more than half a century in the United States (Ray et al., 2002a). Water in the aquifer below or adjacent to the water bodies is typically harvested using vertical or horizontal collector wells. This yields, in general, cleaner water that is more consistent in quality and requires a lesser amount of subsequent treatment and disinfection compared to using the surface water as a direct source (Eckert and Irmscher, 2006). The quality of surface water is often affected by agricultural runoff, industrial discharges and municipal outfalls which introduce a large variability of contaminants in the source water. During the subsurface passage the infiltrating water is subjected to a combination of physical, chemical, and biological processes such as filtration, sorption and biodegradation that can significantly improve the raw water quality (Hiscock and Grischek, 2002; Kuehn and Mueller, 2000; Ray et al., 2002). The quality improvements obtained by bank filtration may allow for significant reductions of turbidity, microbial contaminants, natural organic matter (Wang et al., 2002; Weiss et al., 2004), organic trace pollutants (Grünheid et al., 2005) such as pesticides (Ray et al., 2002c) and pharmaceutical residues (Massmann et al., 2008; Petrovic et al., 2009). On the other hand, hydrogeological or geochemical factors such as long flow paths and high sedimentary organic matter (SOM) concentrations or high dissolved organic carbon (DOC) concentrations in the raw, i.e., in the river water can cause adverse redox reactions that deteriorate the water quality by inducing the reductive dissolution of minerals and the associated increase of, for example, manganese and iron (Bourg et al., 2002) as well as trace metal concentrations in the infiltrated water.

During RBF the pumping-induced infiltration of surface waters typically affects the redox conditions in the hyporheic zone, resulting from DOC/SOM being degraded while sequentially consuming the terminal electron acceptors (TEAP) dissolved oxygen, nitrate, manganese and iron(hydr)oxides and sulfate. (Barry et al., 2002; Champ et al., 1979).

This sequential consumption of electron acceptors along the flow path of infiltrating river water and the development of distinct redox zones towards more reducing conditions in downstream direction has been documented for many cases. Bourg and Bertin (1993) used groundwater mixing and degradation of organic matter to explain the observed reducing zones in an aquifer adjacent to the Lot River (France). More recently Kedziorek et al. (2008) confirmed through geochemical modeling for the same site the occurrence of redox reactions and also showed that they affected groundwater quality away from the river bank.

Where hydrochemical monitoring covered longer time periods it was shown, in many cases, that redox gradients and zonation undergo strong temporal variations. Jacobs et al. (1988), for example, documented significant seasonal water quality changes along a saturated river-groundwater infiltration flow path. Similar to an RBF situation, a spatially and temporally varying redox zonation was also found below an artificial pond near Lake Tegel, Germany (Greskowiak et al., 2005a). For that site it was demonstrated that the redox zonation and its changes were driven by seasonally varying, temperature-dependent organic matter degradation. A complete removal of the PhAC phenazone was shown to occur when the aquifer remained aerobic, during colder months. It was substantially more persistent during the warmer months when anaerobic conditions dominated (Greskowiak et al., 2006; Massmann et al., 2008). Similarly, temperature dependent reactions of the key reductants were shown to be crucial for successfully modeling the redox zonation created by the injection of oxic surface water into a deep pyritic aquifer (Prommer and Stuyfzand, 2005). In their case, the consideration of heat transport that accounted for strong seasonal temperature variations was also shown to be highly valuable for an improved calibration of redox changes. Other cases also showed the use of temperature measurements to aid groundwater flow modeling (Anderson, 2005) and in modeling groundwater surface water interactions (Blaschke et al., 2003; Constantz, 2008; Doppler et al., 2007; Doussan et al., 1994; Stonestrom and Constantz, 2003).

Despite a continuously increasing interest in surface water/groundwater interactions, to date no detailed, model-based quantitative analysis of the temporal biogeochemical dynamics of RBF systems has been undertaken, linking dynamic flow processes with the effects of varying temperature, reaction kinetics and resulting overall biogeochemical turnover rates at the river groundwater interface. The objective of the present paper is to fill this gap and to identify and quantify the interactive, dynamic physical and chemical processes impacting water quality changes within the hyporheic zone and the extraction wells in an RBF system under seasonally changing hydrological and raw/river water hydrochemical conditions. We use data from a well-documented field site in the lower Rhine Valley near Düsseldorf (Germany) to develop and test a process-based reactive transport model.

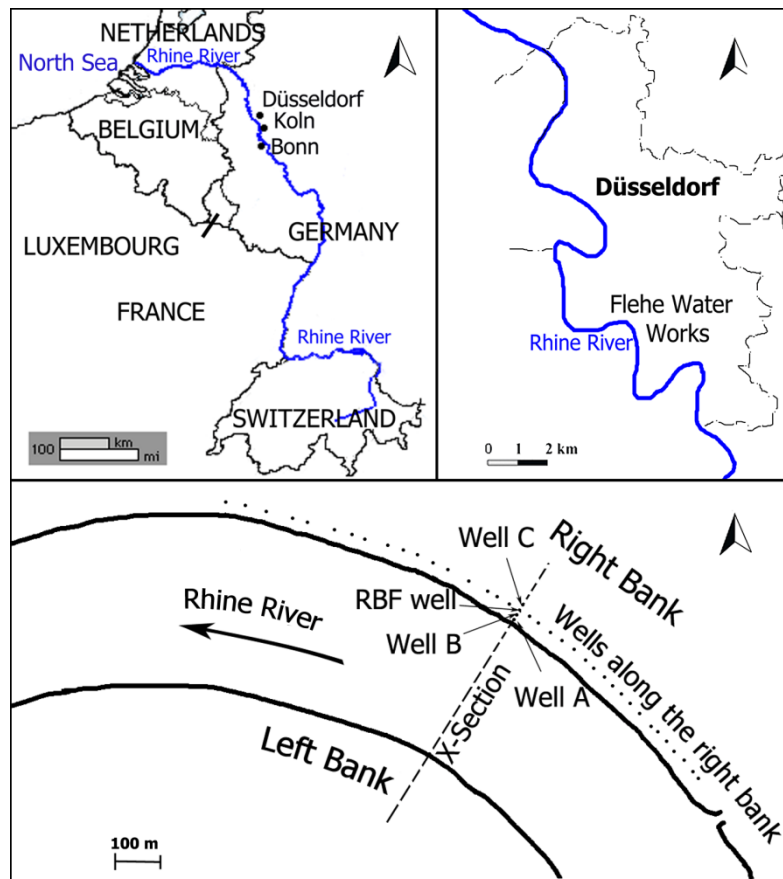


Fig. 3: Location of the Flehe water works along Rhine River in Düsseldorf, Germany. The modeled x-section of the Rhine River, the observation wells and RBF well are shown. The alignment of other wells along the Rhine in the right bank is also shown by black dots, the position of the dots are only indicative and do not represent actual wells.

## 2.2 Study site

The RBF site used for our modeling study is the Flehe Waterworks well field, situated on the Eastern bank of the Rhine River (see Fig 3) in the outer side of the river bend between river kilometers 730.7 and 732.5 (Eckert et al., 2005; Schubert, 2002; Sontheimer, 1980). The Rhine River is at the site 400 m wide, has a median discharge of 2100 m<sup>3</sup>/s, a hydraulic gradient of 0.2 m/km and a flow velocity of 1-1.4 m/s. The data analyzed by our study were collected between January 2003 and May 2004. During this period the highest recorded flood level was 36.35 m (above mean sea level) and the lowest observed level was 27.44 m. The median flow occurs at river levels of approximately 29.8 m (see Fig 4).

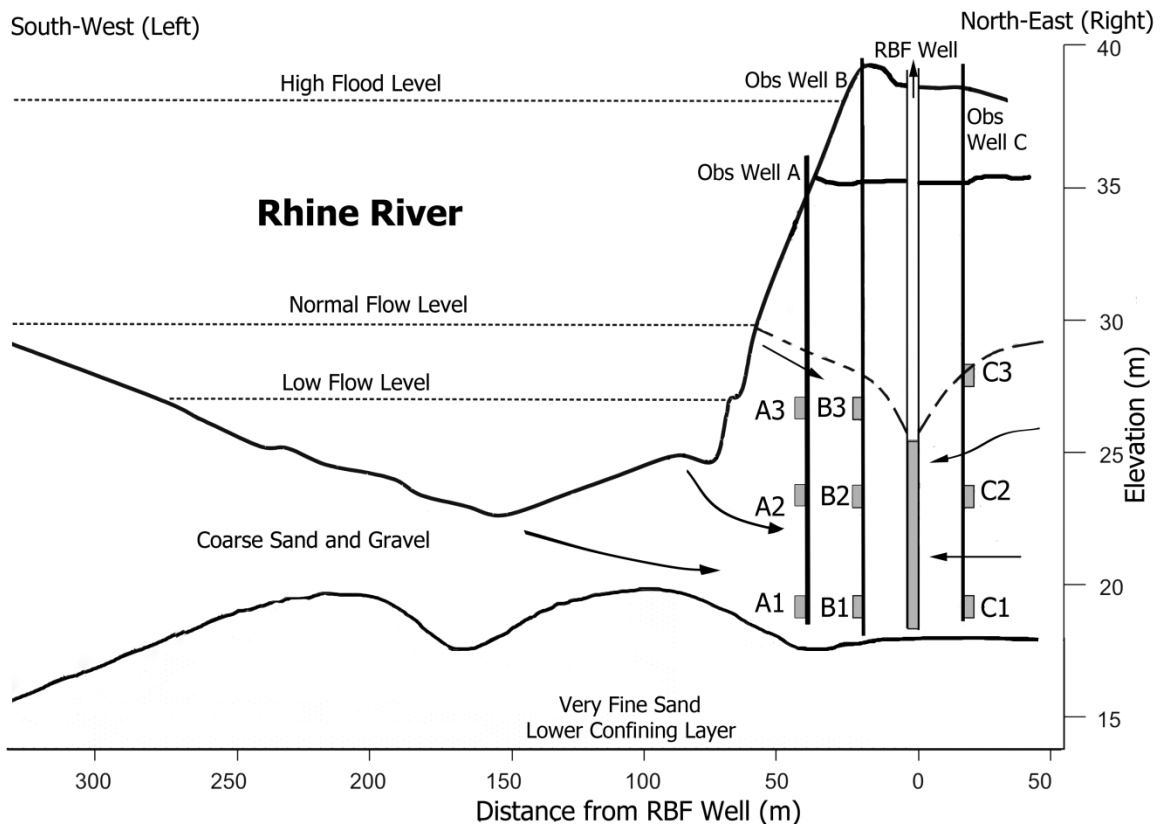


Fig. 4: Cross-section of the study site showing the pumping well and the observation wells near the right bank of the river.

The RBF system consists of a gallery of wells located 60 m from the bank. The wells are typically 0.60 m in diameter, 22 to 28 m deep with 15 m screen lengths and interconnected by siphon pipes. The design capacity of the well field is 44,000 m<sup>3</sup>/d, but the actual pumpage during the period of our study varied between 34 and 1480 m<sup>3</sup>/h (816 - 35,520 m<sup>3</sup>/d) including a number of short shut off periods. In total, 50 wells are located linearly in a reach of 1400 m parallel to the river on the North-East bank.

In the river water the temperature fluctuates seasonally between a minimum of 3 °C and a maximum of 27 °C and between 7 °C and 21 °C in the infiltrated water (see Fig 5). A distinct lag is apparent between the river temperature extremes of the river and the infiltrated water.

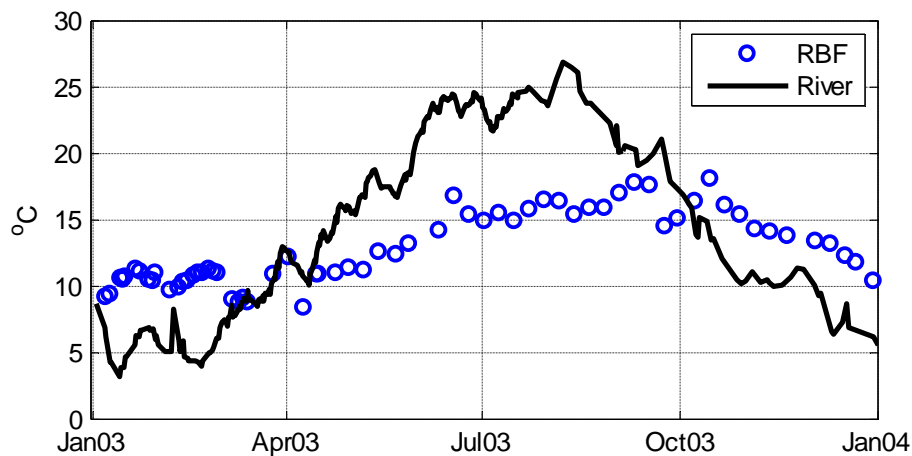


Fig. 5: Seasonal temperature variations of the Rhine River water and the filtrate at the RBF well.

### 2.2.1 Hydrogeology

The aquifer targeted by the RBF system consists of sandy gravely Pleistocene sediments with an underlying confining layer of very fine Tertiary sands. The thickness of the aquifer at the Flehe site varies between 15 and 25 m (Schubert, 2002) as shown in Fig 4. The aquifer is exposed and hydraulically connected to the Rhine River. The average hydraulic conductivity of the aquifer is reported to range between  $4 \times 10^{-3}$  m/s and  $2 \times$

$10^{-2}$  m/s (Schubert, 2002). The riverbed at the site was previously reported to contain zones affected by riverbed clogging (Eckert and Irmischer, 2006; Schubert, 2002) whereby the permeability of the clogged zones was estimated to be as low as  $1 \times 10^{-8}$  m/s and to affect mainly the riverbank (North-East) in the proximity of the wells. This zone was estimated in 1987 (Schubert, 2002) to extend to about 80 m, while a semi-clogged zone extended for another 100 m towards the center of the river with a higher permeability of about  $3 \times 10^{-3}$  m/s. The region beyond that up to the opposite bank (South-West) is reported to contain a movable bed and again somewhat higher permeability between  $4 \times 10^{-3}$  and  $2 \times 10^{-2}$  m/s. The clogging layers were reported to comprise of two distinct sub-layers, a mechanical layer due to in-trapping of suspended solids between the grains of the aquifer and a chemical layer formed due to precipitates. High loads of biodegradable substances in the river water were hypothesized to be responsible for the formation of this chemical layer beneath the infiltration areas where strong changes in redox-potential and pH values were expected to induce the precipitation of minerals such as siderite ( $\text{FeCO}_3$ ) that successively reduced the available pore space (Schubert, 2002). However, since 1987, the extraction rates of the pumping wells, turbidity and organic loads in the Rhine River have decreased substantially. Therefore, the severity and extent of clogging has therefore successively been reduced (Grischek et al., 2010). The now more oxic conditions that prevail in the Rhine River preclude the presence of an excessive chemical clogging layer that was assumed to be present earlier.

### **2.2.2 Geochemical characteristics**

The aquifer matrix consists largely of silicate sand and gravel. The geochemical analyses of 17 individual core samples, taken from three boreholes in the vicinity of the transect, showed that the average total carbon in the aquifer was about 0.14% (ranging from 0.33% to 0.02%) of which about 0.03% was inorganic. The average total sulfur content was generally less than 0.02% (mostly pyrites). The top soil, as expected, contained more carbon, up to 3.5%, the majority of it being the organic variety.

The water quality of the aquifer water was mostly monitored through two multilevel observation wells located at a distance of 40.2 m (well A) and 20.4 m (well B), respectively, from the production well towards the center of the river (Fig 4). Another multilevel observation well (well C) is located at 18.1 m North-East from the production well (Fig 4). Each observation well consists of three separate observation locations (1 - 3) numbered from the bottom towards the top located at elevations of 18.5, 23, and 26.5 m respectively. No hydro-geochemical data were available for observation well A.

## **2.3 Modeling of seasonal flow dynamics and nonreactive transport behavior**

### **2.3.1 Conceptual model and numerical model set up**

A vertical, cross-sectional model of unit width located along a streamline passing the observation wells was constructed to approximate the flow between the river, across the bank and towards the RBF well. The USGS model MODFLOW (Harbaugh et al., 2000) was used for the flow simulations while conservative transport of chloride (Cl<sup>-</sup>) and heat transport was simulated with the multi-species transport simulator MT3DMS (Zheng and Wang, 1999).

The cross-section was discretized into a grid of 390 m length in x-direction (335 m towards the river and 55 m towards the bank side of the pumping well located on the inland side of the model) and a total thickness of 25 m in z-direction. The bottom elevation of the model is positioned at 14 m above sea level while the top elevation is located at 39 m above sea level. The selected regular grid spacing was 5 m in x-direction and 0.5 m in z-direction. The selected grid and its boundaries are shown in Fig 6. The river is represented by a zone of high hydraulic conductivity in the top part of the model. The clogging layers are approximated by a 0.5 m thick layer with reduced hydraulic conductivities at the river bed near the pumping well. The model shows a confining unit at the bottom with a low hydraulic conductivity. The aquifer is shown in two layers in the intermediate depths; the hydraulic conductivities and the zonation of these, as well as that of the clogging layers, were adjusted during calibration.

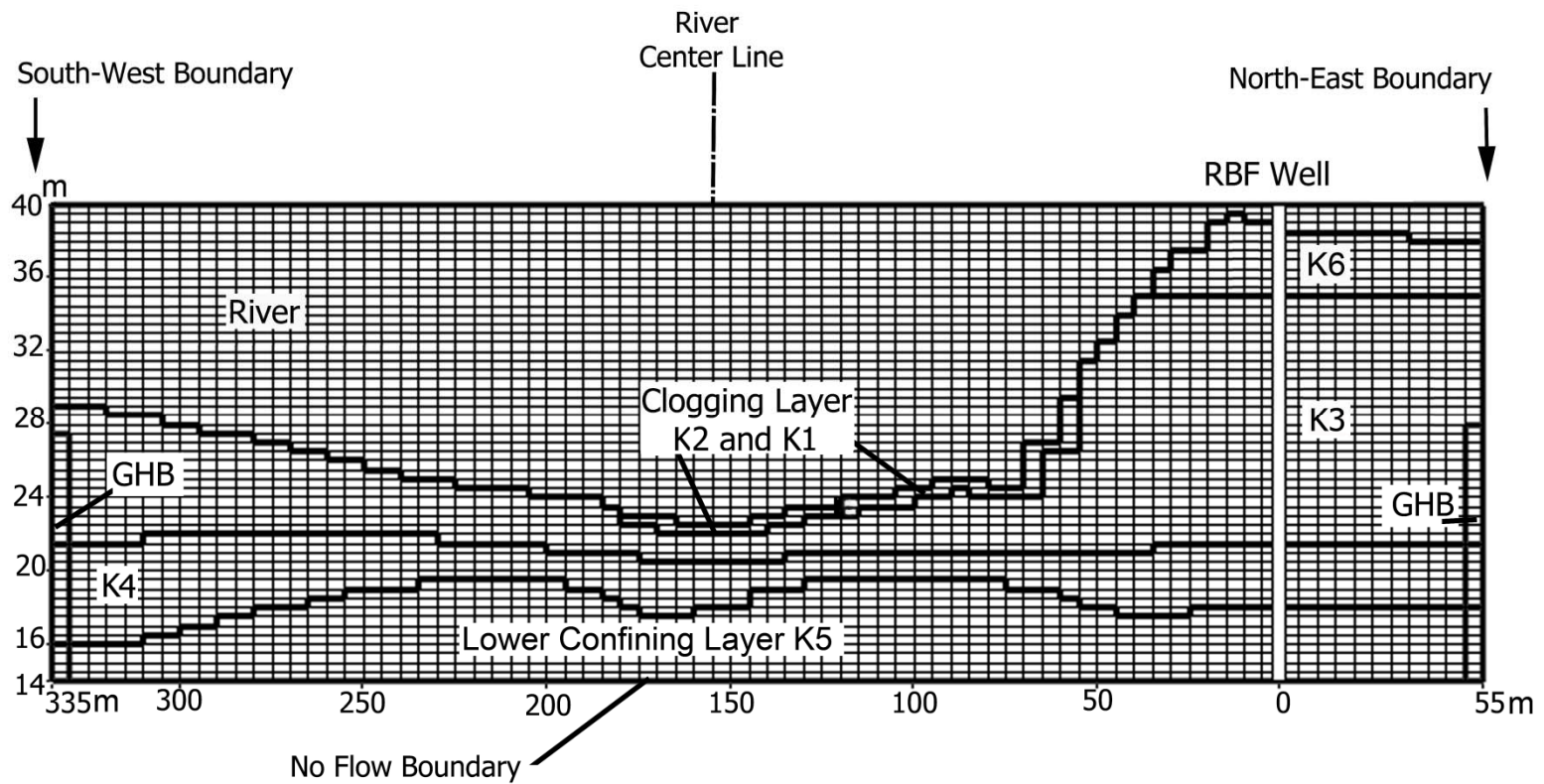


Fig. 6: Model extent, grid discretization, hydraulic conductivity zones and hydraulic boundary conditions used in the numerical model. The well is located in the North-East (right bank) side of the model. GHB = General Head Boundary,  $K1 = 1.04 \times 10^{-6}$  m/s,  $K2 = 9.26 \times 10^{-4}$  m/s,  $K3 = 3.01 \times 10^{-3}$  m/s,  $K4 = 6.37 \times 10^{-3}$  m/s,  $K5 =$  and  $5.79 \times 10^{-5}$  m/s and  $K6 = 5.79 \times 10^{-4}$  m/s.

Table 2: Initial concentrations in the model and range of concentrations in the river and the groundwater (mol/L).

Aqueous Component <sup>a</sup>	Initial Concentration (mol/L) <sup>b</sup>	River Water (mol/L) <sup>b</sup>		Groundwater (mol/L) <sup>b</sup>	
		min	max	min	max
Orgc	$5.56 \times 10^{-5}$	$1.50 \times 10^{-4}$	$4.00 \times 10^{-4}$	$4.50 \times 10^{-5}$	$1.00 \times 10^{-4}$
Tmp	14	3.2	26.9	13.2	14.0
O(0)	$1.77 \times 10^{-4}$	$4.13 \times 10^{-4}$	$8.35 \times 10^{-4}$	$6.25 \times 10^{-6}$	$4.13 \times 10^{-4}$
Ca	$1.98 \times 10^{-3}$	$1.32 \times 10^{-3}$	$1.97 \times 10^{-3}$	$1.70 \times 10^{-3}$	$2.88 \times 10^{-3}$
Mg	$4.34 \times 10^{-4}$	$3.88 \times 10^{-4}$	$5.97 \times 10^{-4}$	$2.92 \times 10^{-4}$	$6.50 \times 10^{-4}$
Na	$1.45 \times 10^{-3}$	$8.27 \times 10^{-4}$	$2.91 \times 10^{-3}$	$1.10 \times 10^{-3}$	$4.44 \times 10^{-3}$
K	$1.06 \times 10^{-4}$	$8.19 \times 10^{-5}$	$1.66 \times 10^{-4}$	$6.22 \times 10^{-5}$	$1.41 \times 10^{-4}$
Fe(2)	0	0	0	0	0
Fe(3)	$1.25 \times 10^{-6}$	$6.99 \times 10^{-8}$	$1.06 \times 10^{-5}$	$6.99 \times 10^{-8}$	$1.25 \times 10^{-6}$
Mn(2)	0	0	0	0	0
Mn(3)	$5.46 \times 10^{-7}$	$1.13 \times 10^{-7}$	$1.24 \times 10^{-6}$	$1.13 \times 10^{-7}$	$2.11 \times 10^{-6}$
Cl	$1.07 \times 10^{-3}$	$6.84 \times 10^{-4}$	$3.12 \times 10^{-3}$	$1.52 \times 10^{-5}$	$2.80 \times 10^{-3}$
C(4) <sup>c</sup>	$4.53 \times 10^{-3}$	$2.30 \times 10^{-3}$	$3.63 \times 10^{-3}$	$4.05 \times 10^{-3}$	$7.15 \times 10^{-3}$
C(-4)	0	0	0	0	0
S(6)	$5.17 \times 10^{-4}$	$4.79 \times 10^{-4}$	$9.37 \times 10^{-4}$	$4.69 \times 10^{-4}$	$9.48 \times 10^{-4}$
S(-2)	0	0	0	0	0
N(5)	$1.82 \times 10^{-4}$	$8.87 \times 10^{-5}$	$2.63 \times 10^{-4}$	$5.81 \times 10^{-5}$	$2.29 \times 10^{-4}$
N(3)	0	0	0	0	0
N(0)	0	0	0	0	0
Amm	0	$1.11 \times 10^{-6}$	$1.17 \times 10^{-5}$	0	0
pH	7.3	7.8	8.7	6.8	8.0
Alkalinity <sup>c</sup>	$4.10 \times 10^{-3}$	$2.27 \times 10^{-3}$	$3.72 \times 10^{-3}$	$4.10 \times 10^{-3}$	$5.74 \times 10^{-3}$

<sup>a</sup> Values in brackets indicate valence states

<sup>b</sup> Temperature (Tmp) in °C and pH dimensionless

<sup>c</sup> In the reactive transport simulations C(4) was considered as aqueous component, not alkalinity.

The inland flow boundary condition at the North-East (right) boundary of the model domain was defined as a general head boundary (GHB), i.e., 3rd type boundary, which permits two way flow, defined by the head difference across the boundary. A time series of groundwater head data was generated for 516 days from the weekly observations recorded at a well located at 195 m distance inland from the pumping well, i.e., outside the model region and used for the North-East (right) flow boundary condition. At the South-West (left) boundary a general head boundary was introduced below the river and was positioned well beyond the center of the river. The hydraulic head of this boundary

was set as equivalent to the North-East (right) boundary. The bottom boundary was assumed to be a no-flow boundary. The cells located below the minimum water level in the river area were defined as constant head boundaries, whereby the constant heads correspond to the measured transient river stage data. The pumping wells and their rates were defined as a specified flux boundary, whereby the rates were defined per meter of the reach parallel to the river. The initial heads over the model domain were obtained from the average heads determined from the multilevel observation wells. A model spin-up period of 60 days was used to remove any biases introduced by the adopted initial conditions in the model. The simulation period of 516 days was discretized into 531 individual stress periods.

### **2.3.2 Non-reactive transport model**

Based on the computed transient flow field, chloride and heat transport were simulated. Following comparable earlier studies (Greskowiak et al., 2006; Prommer and Stuyfzand, 2005) the simulations of the temperature considered advective-dispersive transport of heat and heat exchange with the sediment matrix but neglected heat conductance within the matrix itself. It was assumed to have little impact compared to the transport by advection and dispersion. The retardation of temperature was approximated by equilibrium controlled linear isotherm with an adsorption coefficient of  $2 \times 10^{-7}$  L/mg (Parkhurst and Appelo, 1999)Zheng, 2010) corresponding to a retardation coefficient of 2.24. Variations in temperature can in principle also cause changes in density and viscosity which could then affect the groundwater flow process. However, for temperature variations below a range of 15 °C, the effects were reported to be small (Ma and Zheng, 2010) and thus neglected. For simplicity our flow and transport modeling study assumes constant density, constant viscosity and also time invariant hydraulic conductivities. The latter was assumed to be valid for the entire simulation period. A flood event that may have been substantial enough to change the river bed's hydraulic conductivity had only occurred at the very beginning of the considered time period, i.e., during the model spin-up phase.

The observed and interpolated data for chloride concentrations and the temperature in the Rhine River were used to define their values in cells representing surface water in the model as one of the boundary conditions. The chloride and temperature observed at the three discrete depth of monitoring well C (located 18 m North-East from the RBF well) were taken to define the North-East (right) boundary condition. These values were almost uniform, the temperature averaged 13.5 °C (ranging from 13.2 to 14 °C), while the chloride data averaged  $9.50 \times 10^{-4}$  mol/L (ranging from  $1.76 \times 10^{-4}$  to  $1.43 \times 10^{-3}$  mol/L). The same set of groundwater data was used to describe the South-West (left) boundary underneath the river. The initial concentrations in the model domain were set to the initial values observed at the corresponding observation points.

During model calibration the hydraulic conductivities and extent of their zones were varied to initially obtain an acceptable fit between the simulated and the observed chloride data, and then refined further using the measured temperature data as calibration constraints.

### **2.3.3 Residence time simulations**

The calibrated model was used to analyze and illustrate groundwater travel times. These simulations were also carried out with MT3DMS, whereby a zeroth-order irreversible production rate without sorption (Zheng, 2010) was incorporated to account for the steadily increasing age of the groundwater. Using an initial age of 0 at the start of the simulation, the simulated travel time at any particular instance is denoted by the residence time or age of water in days since the start time of the model simulation; however, this is not the real age of the groundwater. The simulation of the age distribution can indicate zones where water of little residence time dominates and/or zones where water is more stagnant. In the RBF case, the simulated age of the groundwater represents the total contact time between the infiltrating surface water and the subsurface environment.

## **2.4 Reactive transport model**

The coupled transport and biogeochemical processes were simulated with the MODFLOW/MT3DMS/PHREEQC-based multi-component reactive transport model PHT3D (Prommer et al., 2003), which employs a non-iterative sequential operator splitting approach for a coupled simulation of physical transport and reactive processes. In all simulations the temporal discretization was selected and tested to eliminate temporal operator split errors. Transport parameters estimated in the non-reactive transport simulations were utilized unchanged in the subsequent reactive transport simulations. A site-specific reaction network that translates the conceptual hydrogeochemical model into a numerical model was formulated and implemented into the PHREEQC/PHT3D reaction database (see Appendix A).

### **2.4.1 Reaction network**

In RBF systems, organic matter contained in the infiltrating water and the aquifer sediment generally provides the major driving force for a spatial and temporal redox zonation. The degradation of organic matter is thermodynamically linked to the sequential removal of electron acceptors. The geochemical data from the Flehe site indicated that conditions within the RBF systems were mostly aerobic or denitrifying. In contrast to earlier years, when the Rhine River carried higher DOC loads, elevated levels of manganese or iron do not occur today.

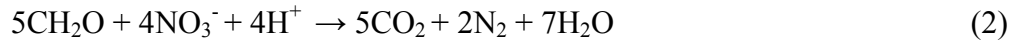
The observed data indicated that a constant recalcitrant residual fraction of about  $9 \times 10^{-5}$  mol/L DOC remained in the infiltrated water, unaffected by the hydrological and physico-chemical dynamics of the river. During initial model runs it showed that the degraded amount of DOC contained in the river water alone did not explain the corresponding consumption of oxygen and nitrate. This suggested that another source of reduction capacity must exist in the aquifer. Underpinned by the results of sediment analyses, SOM was assumed to be present in the aquifer and its degradation contributing to the overall consumption of the terminal electron acceptors (Greskowiak et al., 2006; Kedziorek et al., 2008). In the model, SOM was allowed to degrade while the DOC

originating in the river water was only allowed to degrade until the measured recalcitrant concentration was reached.

The aerobic degradation of DOC/SOM is



while DOC/SOM coupled to denitrification is described by



These degradation processes are kinetically controlled and described in the model by a Monod-type rate expression (Barry et al., 2002; Brun and Engesgaard, 2002; Lensing et al., 1994):

$$r_{DOC/SOM} = f_T \left[ r_{ox} \left( \frac{C_{ox}}{K_{ox} + C_{ox}} \right) + r_{nitr} \left( \frac{C_{nitr}}{K_{nitr} + C_{nitr}} \right) \times \left( \frac{K_{inh\_ox}}{K_{inh\_ox} + C_{ox}} \right) \right] \quad (3)$$

where  $r_{ox}$  and  $r_{nitr}$  are rate constants with respect to dissolved oxygen and nitrate, respectively.  $C_{ox}$  and  $C_{nitr}$  are the concentrations of dissolved oxygen and nitrate.  $K_{ox}$  and  $K_{nitr}$  denote the half saturation constants for dissolved oxygen and nitrate.  $K_{inh\_ox}$  is an inhibition constant, while  $f_T$  is a factor that incorporates the effect of temperature on the degradation rates, as proposed by e.g., Kirschbaum (1995) for soil organic matter and as applied by Greskowiak et al. (2006). The temperature correction factor,  $f_T$  at a specific temperature  $T$  (in °C) is:

$$f_T = \exp \left[ \alpha + \beta T \left( 1 - 0.5 \frac{T}{T_{opt}} \right) \right] \quad (4)$$

where,  $\alpha$  and  $\beta$  are fitting parameters and  $T_{opt}$  is the optimal temperature at which the degradation rate is fastest, which is taken to be 35 °C.

The consumption of electron acceptors was automatically accounted for by using a partial equilibrium approach (PEA). The PEA assumes the oxidation step (e.g., of DOC) as rate-limiting step described by a kinetic reaction (e.g., Brun and Engesgaard, 2002; McNab and Narasimhan, 1994; Postma and Jakobsen, 1996), which allows the electron accepting step to be approximated by an instantaneous equilibrium reaction. This concept was successfully used for a range of closely related reactive transport problems in which DOC and/or SOM degradation was simulated, e.g., by Greskowiak et al. (2005b) and Prommer et al. (2006).

Precipitation and dissolution of minerals was not seen to affect the hydrochemical composition along the flow path significantly and was therefore excluded in the modeled reaction network.

#### **2.4.2 Boundary conditions**

The ambient groundwater and the imposed river water compositions used in the model were defined on the basis of the measured water compositions (Table 2). The measured compositions were slightly adjusted to obtain charge-balanced aqueous solutions. While the raw data set did not include observations for total inorganic carbon (TIC), it was estimated indirectly with PHREEQC from the measured alkalinity data and corresponding pH measurements. Temporal variations in the measured river water quality were reflected in the model by an appropriate adjustment of the water compositions for each defined stress period. The composition of the groundwater entering via the two general head boundaries was constructed for each stress period on the basis of the observed groundwater composition at monitoring well C (Table 2).

### **2.5 Results and discussion**

#### **2.5.1 Chloride and heat Transport**

After calibration of hydraulic conductivities and dispersivities, the observed chloride concentrations and the temperature dynamics in the three filter screens of monitoring well B could be adequately simulated by the non-reactive transport simulations (Fig 7).

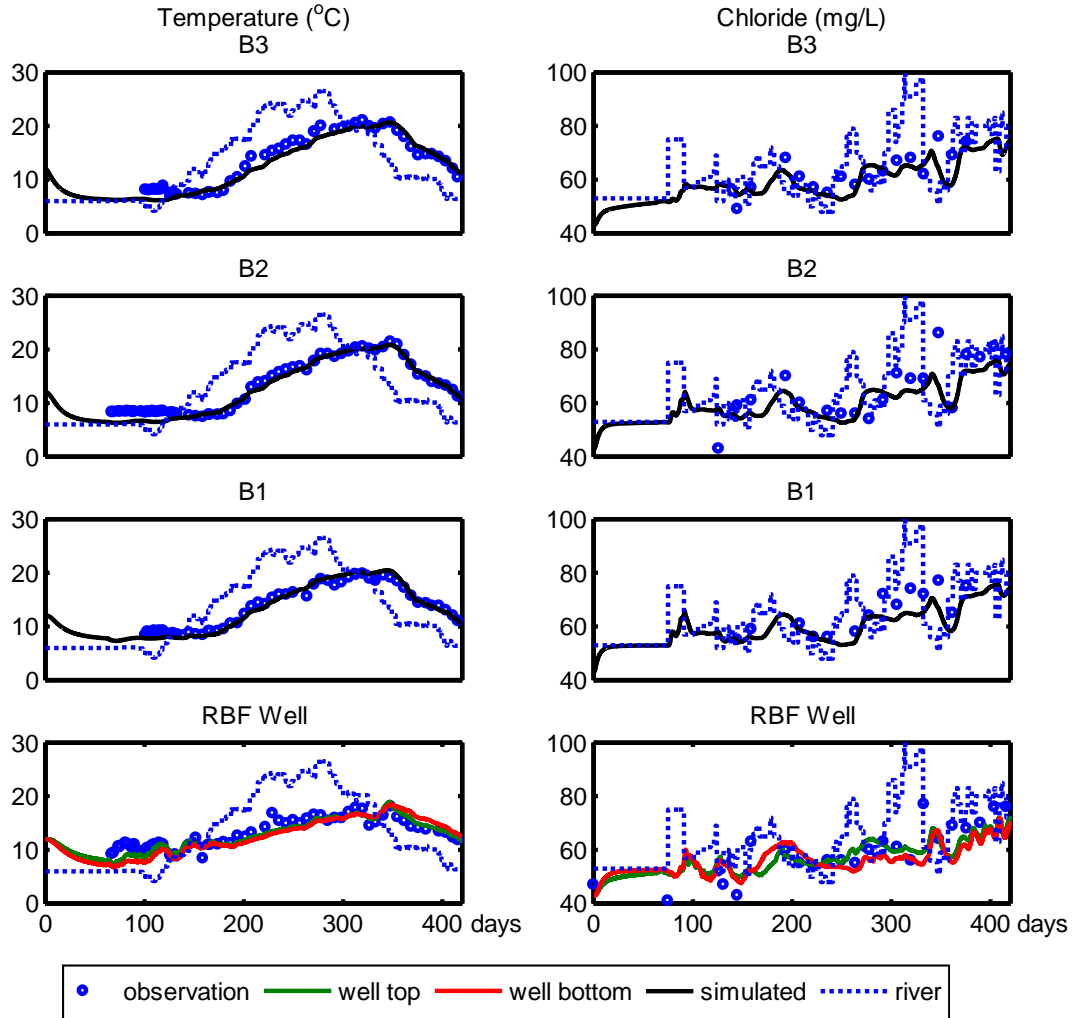


Fig 7. Observed and simulated breakthrough curves of temperature and chloride at the observation well B and at the RBF well.

The results show, as expected, that the temperature variations are more attenuated at the deeper observation point (B1) than at the upper depth levels (B2 and B3), while there is still a considerable seasonal variability in the filtered water temperature. At the RBF well, the simulation is shown for both the top and bottom of the well. It should be noted that the pumping well observations are subject to considerable intermixing and turbulence within them. The ultimate water composition of the pumped water depends on the relative contribution of each of the two fractions in terms of water fluxes and chemical composition. The model simulations only reproduce the monitored water composition if (i) the hydraulic conditions on both sides of the RBF well and (ii) the quality of the

pumped waters on both sides are approximated well enough by the model. From the comparison of simulated and observed chloride concentrations and temperature within the RBF well (Fig 7), it can be concluded that the model captures the relative contributions of landside and river side water fluxes in the RBF well very well.

The calibrated clogging layer distribution and hydraulic conductivities are depicted in Fig 6, showing the position of the clogging layers (marked as K1 and K2) with equivalent hydraulic conductivities of  $1.04 \times 10^{-6}$  m/s and  $9.26 \times 10^{-4}$  m/s respectively with a thickness of 0.50 m. The aquifer is represented by two layers of different hydraulic conductivities ( $K3 = 3.01 \times 10^{-3}$  m/s and  $K4 = 6.37 \times 10^{-3}$  m/s). Delineating a higher conductive zone in the lower part of the RBF aquifer improved the fit between the observed and simulated values in the borehole B and the RBF well. The zone K6 is the top soil, and K5 is the confining unit at the bottom with low conductivities of  $5.79 \times 10^{-4}$  m/s and  $5.79 \times 10^{-5}$  m/s respectively.

### **2.5.2 Residence time simulations**

Simulation of groundwater age, as mentioned earlier, illustrates the dynamic nature of the distribution of the residence time of the infiltrating water. The age distribution becomes distinctly different depending upon the stage of the river water. During high flows, when the water levels rise up and above the clogged zones, more water originating from the river and with lower residence time arrives at the RBF well. During a flooding event, such as that occurring at ~67 days after the start of the simulation, the infiltrating water travels rapidly around the clogging layer towards the well flowing through the previously unsaturated zone with a high pore velocity of up to 10 m/d. Fig 8 shows the age distribution of infiltrating water at 68 days, a day after the flood peak. The age of the water reaching the top screen of the RBF well is greatly reduced from an average age of 40 days to approximately 8 days.

An example for a low river stage period is shown in Fig 9 at 340 days from the start of the simulation. At this period, the age of water entering the RBF well is significantly older, around 60 days. The water withdrawn by the RBF well is characterized by an

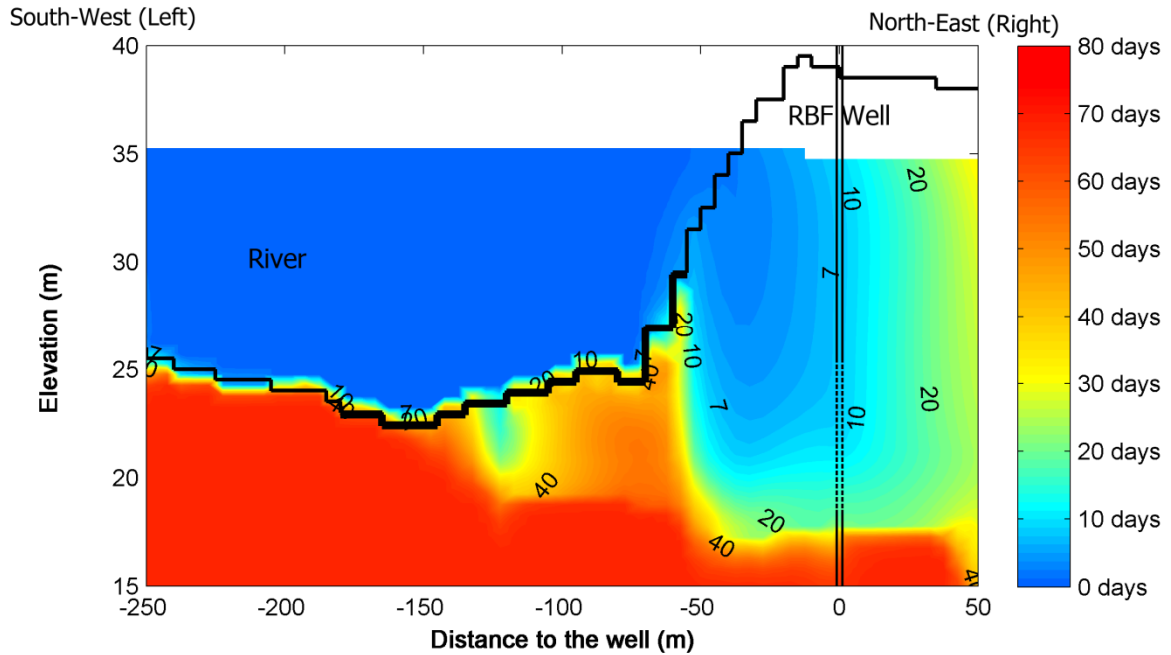


Fig. 8: Simulated groundwater age distribution (age since start of simulation)  $t = 68$  days. The clogging layer is shown in bold line in the middle portion of the river bed.

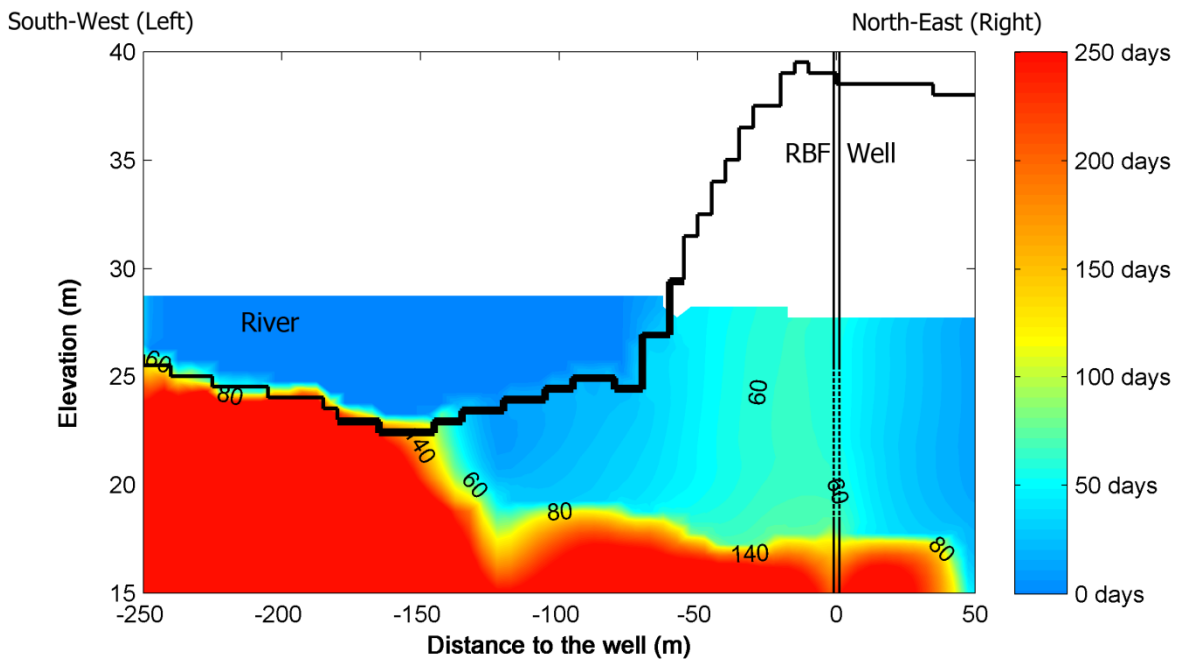


Fig. 9: Simulated groundwater age distribution (age since start of simulation)  $t = 340$  days. The clogging layer is shown in bold line in the middle portion of the river bed.

increased subsurface residence time and a major portion of the area between the river and the RBF well contains such water. This provides more time for the consumption of the electron acceptors. Fig 9 also shows that at this instant groundwater from the North-East (right) boundary is contributing more to the flow at the RBF well. In reality this water is of course older as it is mostly recharged at larger distances within the well capture zone. Instead, the simulated age indicates the travel time since entering the model domain at the North-East (right) boundary.

### 2.5.3 Spatial and temporal variability of redox and secondary reactions

The observed and simulated concentrations of the major ions, dissolved oxygen and DOC were compared for the observation points at monitoring well B and the RBF pumping well by calibrating the parameters that control the reaction kinetics (see Table 3).

Table 3: Parameter values used in defining the reaction kinetics.

Parameter	Degradation of DOC	Degradation of SOM
Rate constants (Eq. (3))		
$r_{ox}$	$1.3 \times 10^{-9}$ mol/L/s	$1.90 \times 10^{-11}$ mol/L/s
$r_{nitr}$	$8.0 \times 10^{-10}$ mol/L/s	$1.20 \times 10^{-11}$ mol/L/s
Half saturation constants (Eq. (3))		
$K_{ox}$	$2.94 \times 10^{-4}$ mol/L	$1.00 \times 10^{-5}$ mol/L
$K_{nitr}$	$1.55 \times 10^{-4}$ mol/L	$1.00 \times 10^{-5}$ mol/L
Inhibition constant (Eq. (3))		
$K_{inh\_ox}$	$1.00 \times 10^{-5}$ mol/L	$1.00 \times 10^{-5}$ mol/L
Temperature factor (Eq. (3))		
$\alpha$	-1.50	-1.50
$\beta$	0.18	0.18
$T_{opt}$	35 °C	35 °C

These parameters are determined from model calibration and adopted from literature (Appelo and Postma, 2006; Greskowiak et al., 2006; Prommer and Stuyfzand, 2005).

Fig 10 shows both the observed and the simulated concentrations of DOC and dissolved oxygen for the three different screens of observation well B (B1-B3) and for the RBF pumping well. For the latter, the simulation results are plotted for the top of the RBF well screen as well as the bottom of the screen. These plots also show the results of the corresponding conservative transport simulations in which all biogeochemical reactions

were disabled. The nonreactive case shows simulated oxygen concentrations at the observation points comparable to those found in the river water. In contrast, in the reactive simulations in which DOC and SOM are degraded, oxygen is successively consumed along the flow path between the river bed and the RBF well. In monitoring

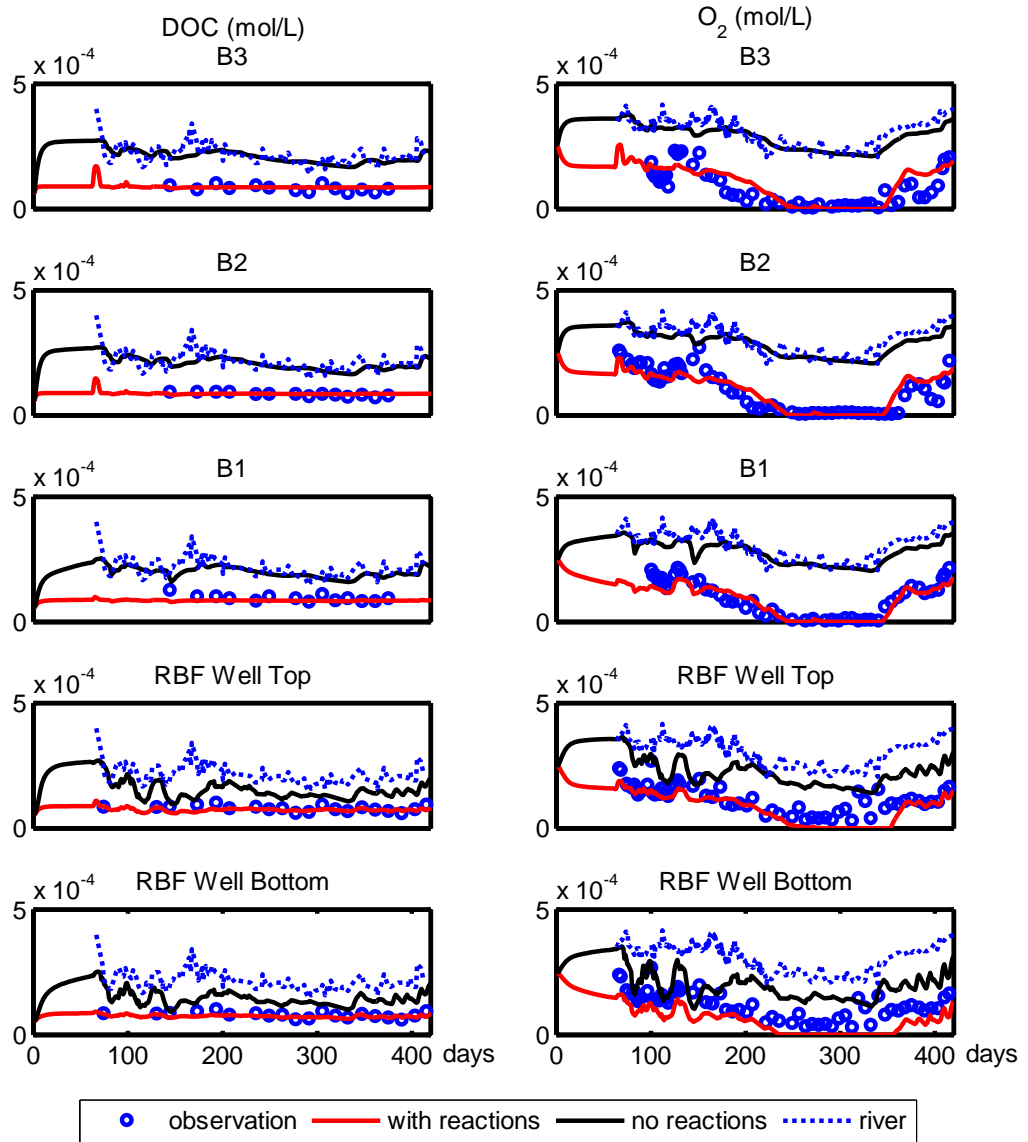


Fig. 10: Simulated (lines) and observed (o) concentrations of DOC and dissolved oxygen. Red lines show the reactive transport results in comparison with the results of non-reactive simulations (black lines). The dashed lines indicate the Rhine river concentrations.

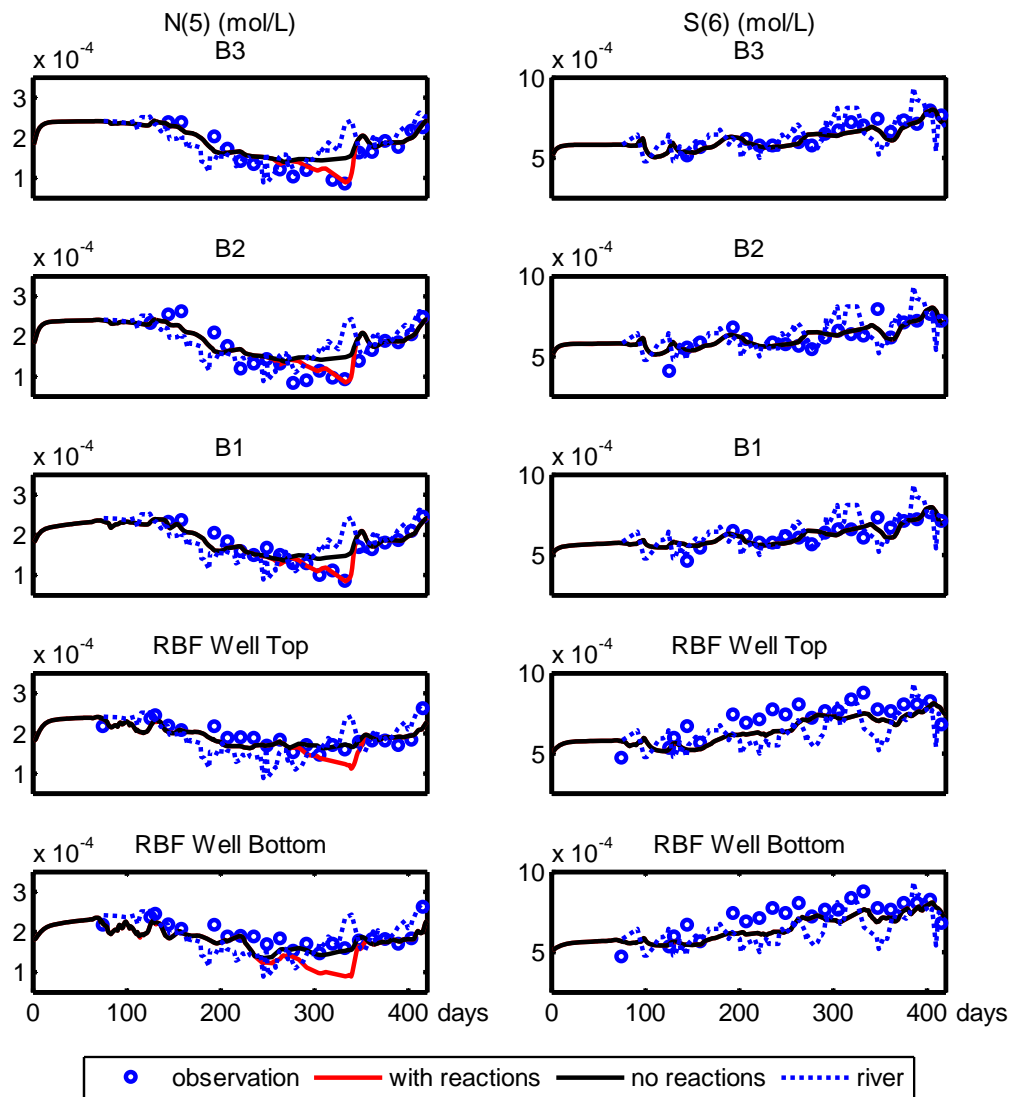


Fig. 11: Simulated (lines) and observed (o) concentrations of nitrate (N(5)) and sulphate (S(6)). Red lines show the reactive transport results in comparison with the results of non-reactive simulations (black lines). The dashed lines indicate the Rhine River concentrations. The concentrations of S(6) for the reactive simulations and the corresponding non-reactive simulations do not differ and appear as a single line.

well B, oxygen is present for most of the time, i.e., between day 0 and day 230 and then again from day 350 after the start of the simulation. Between day 230 and 350 (June-September 2003), oxygen became fully depleted in close proximity to the river bed (results not shown) and thus before the infiltrate's arrival at B1-B3 and at the RBF well, respectively (Fig 10). During this period, anoxic, denitrifying conditions develop (Fig

11). While conservative and reactive simulations produce similar nitrate breakthrough concentrations before day 230 and after day 350, respectively, the simulation results diverge between day 230 and day 350. Thereby, the reactive simulations, in which denitrification coupled to oxidation of DOC/SOM is active, provide a much better fit to the observed data.

Note, that from the available data it was not possible to uniquely reconstruct where the SOM was consumed (and at what rate). In the absence of a detailed characterization of SOM within the aquifer, we made the simplifying assumption of a homogeneous distribution. If SOM had been assumed to be predominantly present in the colmation zone, the calibrated maximum degradation rate constants would have been higher to compensate for the effect that along the remaining travel path less or no SOM degradation occurs. Our calibrated model gives therefore only one of multiple possible realizations of how the degradation processes may have occurred, i.e., other combinations of SOM distribution and SOM reaction rate constants could possibly also have explained the measured data.

Fig 11 also demonstrates that measured sulfate breakthrough curves are well-matched even though sulphate reduction was not considered in the model. This illustrates that presumably no sulfate reduction, and even more unlikely, methanogenesis, has occurred under the investigated hydraulic conditions. Further, protons produced by aerobic organic matter degradation appeared not to be buffered, e.g., by calcite dissolution. The pH decrease, TIC increase and the stable calcium concentrations were adequately reproduced by the model without accounting for calcite dissolution. These are shown Fig 12 at the observation well in points B1 and B2.

In contrast to the variable temperature simulation, simulations with constant temperatures of 5 °C, 15 °C and 25 °C were not able to reproduce the drastic seasonal change in dissolved oxygen concentration at all (only shown for B1, Fig 13a). The 5°C simulation overestimates the measured dissolved oxygen concentrations during summer, while on the other hand the 25 °C simulation cannot account for the high concentrations observed

during winter. Employing the mean of the observed temperature, the simulation results of the 15 °C simulation were, as expected, closest to the variable temperature simulation.

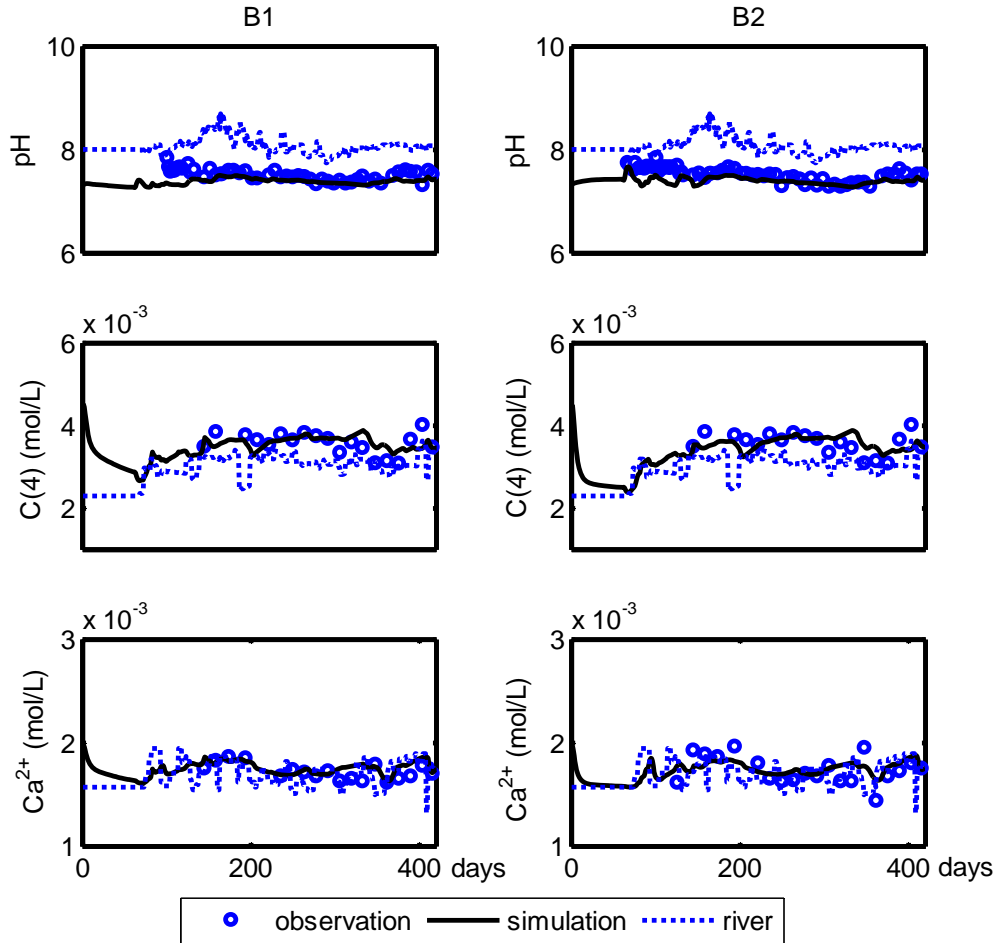


Fig. 12: Simulated and measured concentrations of Ca, C(4) and pH levels at the observation points B1 and B2.

However, the variable temperature simulation provides overall still a clearly better fit to the data, specifically for the earlier phase of the simulation (days ~100 to ~150), but also between ~day 250 and day 300, when the model correctly predicts complete oxygen depletion. It should be noted that the two coefficients employed in the temperature correction function  $f_T$  (Equation (4)) were taken from Greskowiak et al. (2006) without any further adjustments.

To approximate and analyze the extent of biodegradation that has occurred along the flow path between the river bed and a particular observation point (i.e., monitoring well) the amount of electrons transferred from DOC/SOM to the electron acceptors oxygen and nitrate were computed from

$$ET(t) = \sum_{i=1,2} \Delta C_i(t) \times Eeq_i \quad (5)$$

where  $\Delta C_i$  is the differences in electron acceptor concentrations between reactive and non-reactive simulation and  $Eeq_i$  is the corresponding half reactions of the redox reactions (1) and (2), respectively.

The comparison of the extent of biodegradation under constant temperatures (Fig 13b) and the residence time (Fig 13c) simulated at the monitoring wells (only shown for B1) can illustrate the impact of the residence times alone. If the flow velocity would have been constant, the residence time and thus the extent of biodegradation under constant temperatures would have been constant, too. However, in reality this was not the case. Instead, the flow velocity continuously varied throughout the simulation. Thus, the simulated variations in the extent of biodegradation for constant temperatures (Fig 13b) can be attributed to the variations in residence times (Fig 13c). This is, for example, the case for the variations in the biodegradation extent between 50 and 150 days after the start of the simulation. These variations also occur in the variable temperature simulation and thus it becomes clear that their main cause was due to changes in residence time. Similarly, the strongly changing biodegradation extent between 310 and 380 days after the start of the simulation were also mainly caused by changes in residence time rather than temperature. Related to this, the observed short occurrence of denitrifying conditions between day 300 and 340 after the start of the simulation resulted from the temporary increase in residence time. This means, the short term variations in the extent of biodegradation under varying temperature (Fig 13b) are mainly due to the variations in residence times, while the longer term, i.e., seasonal variations can be attributed to both, temperature and residence time effects.

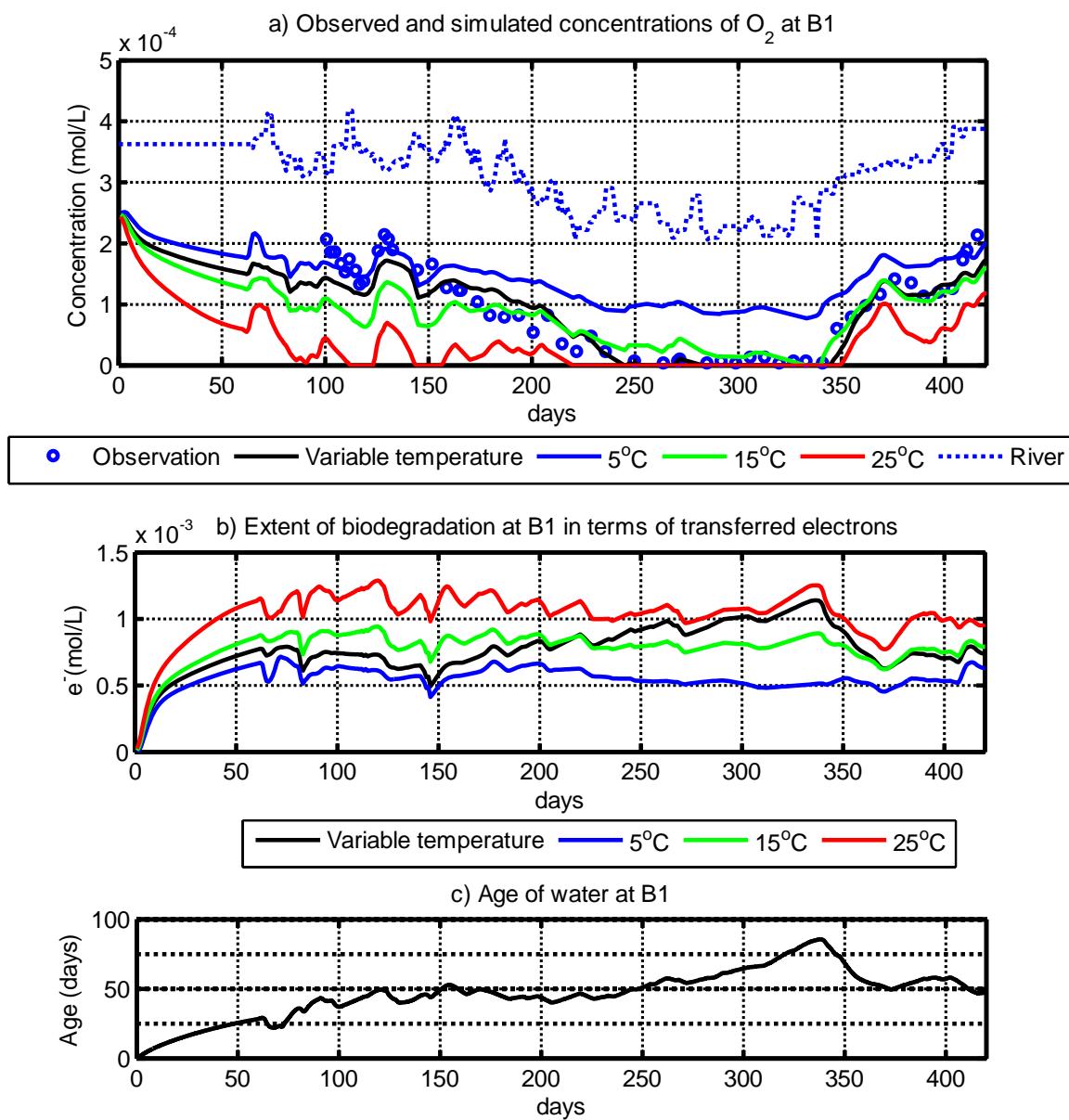


Fig. 13: a) Observed and simulated concentrations of dissolved oxygen at B1 for various assumptions of temperature in redox modeling, (b) Extent of biodegradation at B1 in terms of transferred electrons (see text), and (c) simulated age/residence time of water at the observation point B1.

## 2.6 Summary and Conclusions

In the present study a process-based reactive transport model was developed to analyze and explain the dynamically changing hydrochemical processes at one of the riverbank filtration sites operating along the Rhine River. At this site, the predominant processes

were aerobic respiration and, for a shorter period, partial denitrification in the river bank, leading to considerable variability in dissolved oxygen and nitrate concentrations at the monitoring and the production wells. Our results demonstrate that seasonal temperature changes in combination with drastic changes in residence time strongly affected the extent of biodegradation and thus electron acceptor consumption along the flow path.

Higher biodegradation rates and thus more reducing conditions were present at higher temperatures during summer, while low temperatures decreased the microbial activity and led to a breakthrough of dissolved oxygen at the monitoring and production wells. The observed strong seasonal changes in breakthrough of dissolved oxygen concentrations was better predicted when biodegradation rate constants were made dependent on temperature, compared to simulations where the effect of temperature was neglected (constant temperature simulations).

Flood events in the Rhine River and the higher hydraulic gradients caused drastically reduced travel times (~7 days) to the RBF well, compared to average travel times of 25-40 days. On the other hand, low flow conditions increased the residence time of the infiltrating water to more than 60 days to emerge in the RBF well. The latter were responsible for the temporary shift to denitrifying conditions that were observed during this period. In general, short term variations in the extent of electron acceptor consumption rates resulted from rapid changes in residence time rather than gradual changes in temperature.

The present study elucidates and quantifies biodegradation and the development and extent of redox zones, and how they respond to the highly transient hydrological and physico-chemical variations that are representative of, but not limited to, the Flehe RBF site. Such an understanding about temporally changing extents of oxic and anoxic zones in RBF systems, as well as the residence time in these zones, is crucial for assessing the breakthrough behavior of redox sensitive trace organic compounds, which are recognized as a concern in drinking water production areas.

## CHAPTER 3. MODELLING OF FIELD-SCALE *ESCHERICHIA COLI* TRANSPORT DURING RIVER BANK FILTRATION

### Abstract

Rivers and lakes, source waters for RBF systems, can contain high concentrations of microbial pathogens. Therefore, the fate and transport of pathogens in an RBF system is of common interest. Microbial transport is modeled in groundwater using the advection-dispersion transport equation adding on the mass-transfer processes of attachment, detachment and inactivation often approximated with linear kinetic reaction expressions. The rates defined by these processes are velocity dependent and could not be used directly for a transient RBF model where the velocity fields are constantly changing.

The concepts of the classical colloid filtration theory and the advection dispersion transport equations were combined together to develop a procedure to incorporate the transient flow fields and the dynamic boundary conditions in a multicomponent reactive transport model using PHT3D and MODFLOW. This enabled the use of a single set of parameters to describe the breakthrough of microbes even for different flow velocities. The approach was verified on a published benchmark 1-D study in which column experiments were run at different velocities.

This approach is extended to model the transport of *E. coli* and Coliforms in a large full scale operating RBF scheme. The model was able to replicate the occurrence of the breakthrough during high floods as well as the non-occurrence during other times. The processes of detachment, incorporation of biological and physiological processes such as growth, morbidity, starvation, active adhesion and microbial mobility are components that have been simplified or excluded in the model could be improved in the future.

### 3.1 Introduction

Riverbank filtration has been an accepted method of (pre)treatment for water supply from rivers (or lakes) which markedly improves the source water quality (e.g., Ray et al., 2002b). Pumping water from wells located adjacent to or below a river or a lake induces surface water to infiltrate through the aquifer to the wells attenuating contaminants and pathogens present in the source water (Sontheimer, 1980; Tufenkji et al., 2002; Schijven et al., 2003; Gollnitz et al., 2003). Depending on situations surface waters can contain elevated concentrations of pathogenic contaminants – viruses, bacteria and protozoa while water utilities must supply water that meets the stipulated water quality standards, such as those prescribed by the National Primary Drinking Water Regulations in US (EPA, 2009). The bacteria of common interest, *Escherichia coli* (*E. coli*), are gram-negative, facultative anaerobe rod-shaped faecal coliforms and commonly found in the intestines of animals and humans. The diameter ranges from 1.1 to 1.5  $\mu\text{m}$  and the length typically varies from 2.0 to 6.0  $\mu\text{m}$  in size (Prescott et al., 1996). The presence of *E. coli* in water is a strong indication of recent sewage or animal waste contamination and, therefore, it is commonly used as a biological indicator for contamination (Edberg et al., 2000).

The ultimate source of pathogenic bacteria is excretion from human, cattle and various domestic and wild animals. These pathogens are present in source waters due to surface runoff from watersheds (Oliver et al., 2005), overflows and leakages from cesspits and septic tanks (Ferguson et al., 2003), land application of manure (Pachepsky et al., 2006) and wastewater effluents (Fong et al., 2007). The concentrations of total coliforms, *E. coli* or enterococci in sewage range up to 10 million cells per 100 mL (Geldreich, 1996). Pathogens were ranked as the number one cause for impairment of rivers and streams in US, rendering 31% of the assessed rivers and streams to be contaminated (EPA, 2010). Almost half of this impairment is attributed to presence of *E. coli*. It is only natural that a greater scrutiny be placed on the performance of RBF systems as they draw water from water bodies that are so widely contaminated with *E. coli*. It is, therefore, important to understand the transport and fate of these bacteria in an RBF system. Modeling studies that assist with the interpretation of experimental studies at laboratory and field-scale can

provide important insights into the mechanisms of the transport and attenuation. For the present study, we modified the biogeochemical transport model PHT3D to allow for the simulation of pathogenic contaminants and tested the model against experimental data from laboratory and field investigations. For the latter, we selected data collected at the Flehe water works, where a large RBF system is located along the Rhine River in Dusseldorf (Germany).

The Flehe Water Works has been using riverbank filtration since 1870 as the major source for public water supply drawing water from the right bank of River Rhine (Schubert, 2002; and Eckert and Irmscher, 2006). Using a comprehensive field data set from the Flehe site, a recent reactive transport modeling study (Sharma et al., 2012) investigated the major hydrogeochemical processes, and particularly the transient redox conditions that occurred in response to the variability of the degradation of dissolved organic carbon. The study showed the importance of the transient conditions that occur in the RBF system, especially the fluctuating river water level, dynamically changing residence times, boundary conditions and the redox conditions of the aquifer. The present study builds upon the above-mentioned flow and reactive transport models to further investigate and analyze the microbiological transport phenomena that occur during riverbank filtration. Microbiological monitoring data including the total coliforms and *E. coli* concentrations at the river, RBF pumping well and a number of observation points were obtained from the waterworks and used in this study.

Though there are scores of related saturated column modeling studies, no actual field scale numerical modeling of microbial transport of RBF scheme is reported in the literature. Most of the column studies are conducted with a fixed uniform velocity, and these typically look at one-dimensional problems, whereas the RBF systems are more dynamic with constantly varying water levels, pumping rates, velocity fields as well as changing water quality parameters. Flow characteristics differ not only in time but also vary within the aquifer domain. The classical filtration theory (Yao et al., 1971; Tufenkji and Elimelech, 2003) uses flow velocity as one of the parameters to compute single collector contact efficiency and attachment or sticking rates. Because the velocities are constantly changing, these rates are also varying within the aquifer and over time.

Incorporation of such a transient data set to determine effects of a number of velocity dependent processes at the local (micro) level and integration of its effect over a dynamic system such as the RBF is a task that is possible only through numerical modeling. It is desirable to identify the dominant processes, formulate a numerical model incorporating these processes, and simulate such a model with a real field scenario. No numerical modeling of pathogen transport of a full scale RBF exists to our knowledge. This study addresses this gap by improving and testing the previously existing multi-component reactive transport model PHT3D (Prommer et al., 2003), which couples the widely used solute transport model MT3DMS (Zheng and Wang, 1999) with the geochemical model PHREEQC (Parkhurst and Appelo, 1999).

### **3.1.1 Objective:**

- Develop a versatile model that allows to integrate, and test previously developed approaches.
- Apply to a benchmark model to demonstrate accuracy of modeling tool (reproduce previously published model results and data for column-scale experiment).
- Test/evaluate the model for a RBF scheme subject to transient flow conditions.

### **3.1.2 Background literature on microbial removal**

The fate and transport of colloids and microbes in saturated media has been widely studied and discussed in the literature (e.g. Corapcioglu and Haridas, 1984; Harvey, 1997; Ginn et al., 2002; Tufenkji, 2007; Bradford et al., 2006a and 2007; Foppen and Schijven, 2006; Sen, 2011) where the major processes have been described to be influenced by advection, dispersion, attachment, detachment, straining and growth and inactivation processes. The attachment processes have been described in the above-mentioned review papers in various forms of equilibrium, kinetic and irreversible processes. Straining is often described by “clean-bed” filtration theory as a physical trapping of microbes in pore throats that are smaller than the microbes. Growth and inactivation processes are often deemed insignificant in groundwater microbial modeling

with assumptions of oligotrophic conditions. This is also needed to simplify the numerical approaches as modeling living organisms and biological processes are too complex such that it is hard to specify any definitive correlations between bacterial properties and transport (Ginn et al., 2002). Growth or decay may not be significant for short column studies, where the time scales are smaller, but their effect would be important in field scale studies where the time scales are much larger. It is usually addressed by incorporating net decay rates (John and Rose, 2005), which may or may not be different for the aqueous (free microbes) or solid (attached microbes) phases.

Classical colloid filtration theory (CFT) has been traditionally used to describe irreversible attachment of colloids focusing on the probability of colliding with a collector surface and remaining attached which depends upon the shape and size of the colliding particles and collectors (Yao et al., 1971; Rajagopalan and Tien, 1976; Tufenkji and Elimelech, 2003). This theory was applied to and found to reasonably account for a natural-gradient tracer test and the down-gradient transport of indigenous bacteria in a small scale (7 m) field experiment (Harvey and Garabedian, 1991). The colloid filtration theory has been extended further to include dynamics and kinetics of deposition (Ryan and Elimelech, 1996; Torkzaban et al., 2007) incorporating Derjaguin-Landau-Verwey-Overbeek (DLVO) theory (Hermansson, 1999). Further development has looked at existence of favorable and unfavorable colloidal interactions (Tufenkji and Elimelech, 2004), attachment processes (Ding, 2010; Foppen et al., 2010 and Bradford et al., 2011) and straining (Bradford et al., 2006; Foppen et al., 2005; Foppen et al., 2007; Bradford et al., 2007 and Torkzaban et al., 2008) incorporating effects of grain size and interstitial velocity (Syngouna and Chrysikopoulos, 2011), solution chemistry (Schinner et al., 2010; Kim and Walker, 2009) or even microbial physiology and characteristics (Simoni et al., 1998, Lutterodt et al., 2009; Bolster et al., 2006) etc. A bulk of the research has focused on the pore-scale processes and laboratory columns in controlled scenarios. The column experiments mostly involve obtaining breakthrough curves of microspheres or microbes through various media such as quartz sand, glass beads, and undisturbed and re-compacted soil cores. Most often, the results of 1-D numerical models are fitted to the breakthrough curves and are used to estimate various transport parameters.

There have been a number of studies that have extended the theory and experiments to larger columns or field scales where greater environmental variables come into play such as aquifer and microbial heterogeneity, and distribution of microbial characteristics affecting transport parameters, e.g. sticking (attachment), detachment, straining and inactivation or decay coefficients. Harvey et al. (1993) determined in a field experiment that sorption was mainly responsible for immobilization of microbe-sized colloids and that straining appeared to be primarily responsible in flow-through columns repacked with the same aquifer sediments. It was concluded that the physical variability in aquifer sediment structure can be an important factor in microbial transport. DeFlaun et al. (1997) report results of a field experiment in a sandy aquifer with a 30 m flow cell using native bacteria with low adhesion to sediments where a breakthrough was observed at a distance of 4 m though the bulk of the injected biomass was retained within 0.5 m of the source. It was suggested that the single strain of bacteria could have subpopulations with distinctly different transport properties, some capable traveling far and others not.

Schijven et al. (1998) showed, through injection and recovery field experiments in coastal dunes in The Netherlands, that the faecal indicator bacteria concentration was reduced by approximately an order of magnitude within 2 m of travelling. Hijnen (2005) performed column experiments using natural soil and water of an infiltration site with fine sandy soil, and an RBF site with fluvial gravel soil. It was concluded that detachment and retardation played significant roles in microbial transport while the contribution of straining varied and made difficult the task of up-scaling column test results to field scales. Levy et al. (2007) looked at bacterial transport through 32 intact cores of glacial-outwash aquifer sediments and report kinetic detachment occurring due to the observation of extending tailings. They also attempted to develop regression relationships based on the sediment characteristics to predict bacterial transport as an alternative to colloid filtration theory. Zhang et al. (2001) studied bacterial attachment and detachment kinetics in a well instrumented field scale and suggest that the laboratory determined kinetic constants might under-predict the extent of microbial transport, which was also reported by others (Hall et al., 2005, Scheibe et al., 2011).

Some literatures were found to have studied microbial subsurface transport analysing groundwater contamination subject to sewage effluent irrigation (Wall et al., 2008) and setback distances of wells from septic tanks (Pang et al., 2004). These cases involve releasing very large amounts of pathogen, exceeding by far the typical environmental levels, in surface waters and involve coarse-grained aquifers with very high yields and faster travel speeds. Rapid surface water-groundwater interchange was also noted to cause ground water contamination in South Bass Island, Ohio, USA (Fong et al., 2007) where a severe episode of microbiological contamination of Lake Erie (USA) caused wide scale groundwater contamination in the adjoining aquifer. Each of the 16 tested drinking water supply wells in the island was found to be positive for both total coliform and *E. coli*.

A number of field studies or site monitoring has documented reduction of pathogens, surrogates and indicators in RBF systems. A one year study (Weiss et al., 2005) with monthly sampling of river water and production wells in three full-scale riverbank filtration (RBF) facilities, located in the United States along the Ohio, Missouri, and Wabash Rivers for microbial monitoring report that total coliforms were rarely detected in the well waters. For two wells in one of the sites, where the coliforms could be detected, the reductions were 5.5 and 6.1 log units relative to the river water. Most of these studies have a problem in quantifying the contribution of RBF because the microbes are often below detection limits in the RBF filtrates or the ambient groundwater, as was noted by Partinoudi and Collins (2007) at four different RBF sites in USA. It was suggested that site characteristics such as travel time and distance between the river and the extraction well were important factors affecting efficiency of reduction/removal processes. The log removal rates were reported (Partinoudi and Collins, 2007) as more than 2.72 and 1.00 for total coliforms and *E. coli* respectively. It was also pointed out that the observed log removal rates were low because of low concentrations in the source water and that it did not mean low removal potential.

Gollnitz et al. (2003) report findings from an RBF well field of Greater Cincinnati Water Works (Ohio, USA) after analysing long-term data (over 10 years) and an intensive monitoring for a 20 month period at two RBF production wells and 10 observation wells.

RBF was found to be highly effective in removing pathogenic microbes with all surrogate concentrations maintaining at least 3.5 log reductions. Similar results of a 3 log reduction in average bacterial spore's concentration have also been noted (Ray et al., 2002c) for a 15 m travel distance to a collector well in Louisville, KY, USA. Daily monitoring of total coliforms in the river and the collector well in the same RBF facility in 2000 (Wang, 2003) resulted in a removal capability ranging from 0.9 to more than 6 log units. The river water coliform concentrations ranged from 9 MPN/100 mL to 165,200 MPN/100 mL, whereas that at the collector well had very few positive detections, most of which were 1 MPN/100 mL or less.

Field study augmented with column experiments in The Netherlands (Medema and Stuyfzand, 2002) showed that the passage of micro-organisms in basin recharge, deep well injection and RBF through saturated soils most effectively reduced all micro-organisms within a distance of one to six meters. In two of the three RBF sites which had sand and clayey deposits, bacteria and viruses were removed by more than 4 log units. In the third site, a gravel based aquifer along the River Meuse, very low numbers of coliforms broke through to the pumping well during extreme flood events. This was attributed to low inactivation during cold winter and faster travel times brought about by shorter travel distance and higher hydraulic gradients during flood events.

Schijven et al. (2003) give a comprehensive overview of the processes and examples of RBF performance in areas from around the world. The most important processes for removal of pathogens, similar to 1-D columns, are described to be attachment of microbes to soil and pathogen inactivation. Additional processes occurring are straining, sedimentation in pores and colloid filtration. Other factors, particular to the RBF, were listed as climatic/hydrologic conditions, siting of wells, bed and the bank material, and the groundwater flow fields. The authors reported that the reduction in concentrations of microbes could be compromised by short travel paths, high heterogeneity, coarse matrices, high hydraulic gradients, and the resulting high velocities. Hendry et al. (1999) showed that relative concentrations in breakthrough curves are generally higher for higher velocities, but no clear relationship was evident as it was bacteria specific; some bacteria reach their maximum breakthrough potential in very low velocities, while others

peak at considerably higher velocities. Using an example of a fictitious stationary well field, Foppen and Schijven (2006) demonstrated how spatially variable transport parameters (such as attachment rate and straining rate coefficients) might be considered in existing standard transport codes such as MT3DMS (Zheng and Wang, 1999) and used it to model the transport of *E. coli* in groundwater. Applying colloid filtration theory, they considered the spatially variable flow velocities to compute spatially varying but used temporally constant attachment rate coefficients. However, to date the impact of the combined spatial and temporal variations in groundwater velocities as they occur during riverbank filtration were not analyzed to date and specifically no numerical modeling study of pathogen transport in a full-scale RBF system is reported in the available literature.

## 3.2 Incorporation of pathogen transport capabilities into PHT3D

### 3.2.1 Governing equations for pathogen transport

Microbial transport in porous media can be described by the well-known advection–dispersion transport equation (Corapcioglu and Haridas, 1984; Tan et al., 1994; Scheibe et al., 2007) adding the processes of microbial attachment, inactivation and release being assumed as linear kinetic reaction model between the microbes in aqueous phase and those attached to the aquifer solid surfaces. The one dimensional form (along x-axis) can be written including the mass transfer terms (Foppen et al., 2005; Hijnen et al., 2005) for the aqueous phase is:

$$\frac{\partial C}{\partial t} = D \frac{\partial^2 C}{\partial x^2} - v \frac{\partial C}{\partial x} - k_{att} C - \mu_1 C + k_{det} \frac{\rho_B}{\theta} S \quad (6)$$

Where,  $C$  is the mass concentration in aqueous phase [ $ML^{-3}$ ],  $D$  is hydrodynamic dispersion coefficient [ $L^2T^{-1}$ ],  $v$  is the interstitial (pore water flow) velocity [ $LT^{-1}$ ],  $k_{att}$  is the attachment rate coefficient [ $T^{-1}$ ],  $k_{det}$  is the detachment rate coefficient of the species from the attached phase to the aqueous phase [ $T^{-1}$ ],  $\mu_1$  is the inactivation rate in solution phase [ $T^{-1}$ ],  $\rho_B$  is the bulk density of the porous medium [ $ML^{-3}$ ],  $\theta$  is the porosity of the medium and  $S$  is the mass concentration attached to the aquifer grains [ $MM^{-1}$ ].

For the attached phase, assuming linear kinetic reaction model, the equation is,

$$\frac{\partial S}{\partial t} = \frac{\theta}{\rho_B} k_{att} C - k_{det} S - \mu_s S \quad (7)$$

where,  $\mu_s$  is the inactivation rate in solution phase [ $T^{-1}$ ]. The mass terms can also be replaced by the number of microbes, to look at number of microbes attached or detached, in which case the porosity and the bulk density terms would not be required in the above two equations.

Many studies have often neglected the detachment term, which slowly releases attached microbes in low concentrations over an extended period, deeming it insignificant, but it can be important where even low concentrations need to be monitored, e.g. in drinking water supply wells.

The attachment rate is the most important factor for attenuation of free microbes in filtrate water and often has been determined using column experiments and numerical methods to fit the observed breakthrough curves. This essentially yields a specific value applicable only for the flow rate at which the experiment was carried out. Process based definition of attachment of microbes to solid grains can be done using CFT relating attachment coefficients to local velocity and employing the concepts of single collector contact collector efficiency (Ryan and Elimelech, 1996) as follows (Foppen and Schijven, 2006).

Attachment rate coefficient,

$$k_{att} = \frac{fv\theta}{4} (\eta_0 \alpha_{tot}) \quad (8)$$

where,  $\alpha_{tot}$  is the overall sticking efficiency. The term “overall” attachment efficiency is used to depict that the efficiencies can be different within a particular soil type due to inherent heterogeneity (Johnson et al., 1996), and the representative efficiency is an overall efficiency. This sticking efficiency, also called the empirical attachment efficiency  $\alpha$ , defines the fraction of collisions (contacts) between suspended particles and

collector grains that result in attachment because not all collisions will result in attachment (Tufenkji and Elimelech, 2004).  $\alpha_{tot}$  is obtained, when the geochemical composition of the sediment and the grain surface charge heterogeneity are known using the equation,

$$\eta = \eta_0[\lambda\alpha_f + (1 - \lambda)\alpha_u] = \eta_0\alpha_{tot} \quad (9)$$

where,

$\eta$  = single collector removal efficiency (SCRE),

$f$  = specific surface area of the porous medium ( $\text{m}^{-1}$ ) =  $6(1 - \theta)/(\theta a_c)$ , assuming spherical grains of the media.

$\eta_0$  = single collector contact efficiency (SCCE),

$\lambda$  = dimensionless heterogeneity parameter defining the fraction of aquifer grains composed of minerals favoring attachment,

$\alpha_f$  = attachment (sticking) efficiency at favorable site  $\sim 1$  as it most probably attaches at the favourable site, and

$\alpha_u$  = attachment (sticking) efficiency at unfavorable site.

The dimensionless parameter  $\eta$  (SCRE) defines the ratio of the rate of particles striking a collector to the rate of particles approaching the collector. The SCCE,  $\eta_0$ , is a semi-empirical parameter for predicting filtration efficiency (Rajagopalan and Tien, 1976) and estimated from physical considerations.

An alternate method to determine this parameter,  $\alpha$ , is through column experiments using the media for which the parameter is to be determined using Eq. (10) below.

$$\alpha = -\frac{2}{3} \frac{a_c}{(1-\theta)L\eta_0} \ln\left(\frac{C}{C_0}\right) \quad (10)$$

In this equation,  $a_c$  is median diameter of the collector or the aquifer grain,  $L$  is the length of the packed column, and  $C/C_0$  is the relative concentration at the outlet compared to the concentration at the inlet of the column.

The heterogeneity factor,  $\lambda$ , for *E. coli* is determined from the fact that the microbe is mostly negatively charged and the positively charged grains in the aquifer would be the favourable sites for attachment. Such sites are present due to presence of iron hydroxides and calcites (Foppen and Schijven, 2006).

Another mechanism through which some of the microbes get removed from the aqueous phase and that is not included in equations above is due to straining. This occurs when the microbes are too large to pass through pore throats and are irreversibly stuck. The straining rate coefficient is estimated (Foppen and Schijven, 2006) using straining contact efficiency,  $\eta_{str}$ , and the straining correction factor,  $\alpha_{str}$ , in a form similar to the attachment rate coefficient as,

$$k_{str} = \frac{fv\theta}{4} (\eta_{str} \alpha_{str}) \quad (11)$$

where,  $\eta_s \sim 2.7(a_p/a_c)^{3/2}$

$a_p$  = diameter of the bacteria (m)

$a_c$  = median of the grain size distribution (diameter of the collector (m))

The SCCE is best estimated by the correlation equation given by Tufenkji and Elimelech (2003), given below, which defines it as a algebraic sum of efficiencies for mechanisms of diffusion, interception and gravity and includes hydrodynamic effects and van der Waal's forces in deposition of colloids.

$$\eta_0 = 2.4A_s^{1/3} N_R^{-0.081} N_{Pe}^{-0.715} N_{vdW}^{0.052} + 0.55A_s N_R^{1.675} N_A^{0.125} + 0.22N_R^{-0.24} N_G^{1.11} N_{vdW}^{0.053} \quad (12)$$

where,  $A_s = [2(1 - p^5)/2 - 3p + 3p^5 - 2p^6]$  with  $p = (1 - \theta)^{1/3}$

$N_R$ , the aspect ratio =  $(a_p/a_c)$

$N_{Pe}$ , the Peclet number =  $(v a_c/D_B)$

$D_B$  = Coefficient of diffusion due to Brownian motion =  $kT/(3\pi\omega a_p)$

$k$  = Boltzmann's constant =  $1.2806 \times 10^{-23} \text{ JK}^{-1}$

$T$  = absolute temperature in Kelvin

$\omega$  = dynamic viscosity of water =  $9.85 \times 10^{15} T^{-7.7}$  for  $T$  in the range of 273 ~ 303 in Kelvins (Matthess, 1982).

$N_{vdW}$ , van der Waal's number =  $H/kT$ ,

$H$  = Hamaker constant, assumed constant =  $6.5 \times 10^{-21}$  J

$k$  = Boltzmann's constant =  $1.2806 \times 10^{-23}$  JK<sup>-1</sup>

$T$  = absolute temperature in Kelvin

$N_A$ , the attraction number =  $(H/12\pi\omega a_p^2 v \varepsilon)$

$N_G$ , the gravity number =  $(2ga_p^2(\rho_p - \rho_{fl})/9\omega v \varepsilon)$

$\rho_p$  = particle density (kg m<sup>-3</sup>) ~1050 kg m<sup>-3</sup>

$\rho_{fl}$  = fluid density (kg m<sup>-3</sup>) ~1000 kg m<sup>-3</sup>

The final form modified form of the Eq. (6) incorporating all the relevant processes, including straining and where  $k_{att}$  is defined by Eq. (8) using CFT based parameters is obtained as follows.

$$\frac{\partial C}{\partial t} = D \frac{\partial^2 C}{\partial x^2} - v \frac{\partial C}{\partial x} - k_{att} C - k_{str} C - \mu_1 C + k_{det} \frac{\rho_B}{\theta} S \quad (13)$$

The third, fourth and fifth terms on the right side of the equation define attachment, straining, and inactivation rates respectively. These three terms reduce the concentration of the free microbes in the aqueous phase, while the last term on the right side increases it as detached microbes from the solid phase come into the aqueous phase.

It is seen in the above equations that pore water velocity is an important parameter in defining transport, attachment or sticking, straining, and the estimation of the SCCE in the equations shown above. When an RBF system is pumping water, the flow fields will be dynamic and the actual water velocity will be changing in space and time around the soil grains. Assuming a single constant or average velocity will give only a single value

to the parameters describing the transport processes; this would yield erroneous results incapable of representing a dynamic process. Apart from velocity, temperature will also be changing in the aquifer, assumed primarily through mechanisms similar to sorption and desorption as water travels through the aquifer (Sharma et al., 2012). We propose to incorporate changes in velocity, and temperature, so that the transient nature of the parameters can be fully included in modeling microbial transport.

The Eq. (7) and Eq. (13) are coupled by the attachment and detachment rates. While the advection and diffusion terms, and the temperature retardation process can be conventionally handled by MODFLOW, the remaining processes of attachment, detachment, straining and inactivation are translated into a geochemical reaction code as a rate block in the database file to be solved numerically by PHT3D (see Appendix B).

### **3.3 Model evaluation with column experiments**

This section describes the methodology used in setting up the verification process. Our formulation is initially tested on a published column study of microbial transport (Hijnen et al., 2005). The verification is two is carried out in two steps, (i) to verify the code /numerical procedure by using the original authors' model and (ii) to verify the proposed model results. Hijnen's study carried out column experiments using saturated soil obtained from two different sites in The Netherlands - (1) Castricum, an artificial recharge site in the coastal dunes (fine sandy soil) along river Lek, and (2) Roosteren, an RBF site in a fluvial gravel aquifer along river Meuse.

Soil columns, 0.50 m long 0.09 m in diameter, were subject to different velocity of flowing water in separate columns. The Castricum columns were subject to velocities of 0.46 m/d and 0.92 m/d, while the Roosteren soil columns were operated at higher velocities of 0.90 m/d and 2.49 m/d. After equilibrating the columns with their source river water for 7 days, all the columns were spiked with a MS2 phage concentration of  $1.6 \times 10^9$  plaque-forming particles (PFP)  $L^{-1}$ (average) for 24 hours and then flushed with their respective source river waters.

### 3.3.1 Model code verification using original method

Our first test was to see if our model procedure set-up in MODFLOW/PHT3D was able to replicate the author's results with the author's data and model. A numerical model of 0.5 m long and of unit thickness was considered for simulating 1-D transport. The 0.5 m length was discretized into 50 cells, each 0.01 m thick. Other model parameters are given in Table 4. The flow pattern was replicated by introducing an injection well at the most upstream cell with a suitable flow rate to achieve the observed flow velocity. Loading of the MS2 phage for 24 hours and the subsequent flushing was simulated with two stress periods of 1 day and 29 days, respectively.

Table 4: Input parameters used in modeling 1-D column transport for the two soils.

	<u>Castricum Soil (fine sandy soil)</u>		<u>Roosteren Soil (fluvial gravel)</u>	
Flow velocity (md <sup>-1</sup> )	<b>0.46</b>	<b>0.92</b>	<b>0.90</b>	<b>2.49</b>
porosity	0.36	0.36	0.32	032
pore water velocity (md <sup>-1</sup> )	1.27	2.54	2.81	7.77
grain size, a <sub>c</sub> (m)	1.8 × 10 <sup>-4</sup>	1.8 × 10 <sup>-4</sup>	5 × 10 <sup>-4</sup>	5 × 10 <sup>-4</sup>
dispersivity (m)	0.238	0.167	2.287	18.44

Source: Hijnen et al. (2005)

Altogether seven species were considered in the PHT3D simulation - MS2 virus, chloride, sodium, temperature, pH and pe as the six mobile species and one immobile form of MS2 as attached to solids (aquifer soil grains). The MS2 species were set-up as kinetic species to enable attachment and detachment.

We used the advection-dispersion based Eq. (6) and (7) directly fitting the four parameters  $k_{att}$ ,  $k_{det}$ ,  $\mu_l$  and  $\mu_s$  via the reaction rate block set up through PHT3D. The net changes in concentration in the aqueous phase as well as the solid phase were calculated at every reaction time step. This was determined by the algebraic sum of the rates

corresponding to the above-mentioned four parameters, noting their contributions as positive (increasing the concentration) or negative (decreasing the concentration). The attachment and detachment rates coupled the concentrations in the aqueous and the solid (attached) phases.

The result of this computational process is shown in Table 5, Fig. 14 and Fig.15. The figures show the relative concentrations of the breakthrough curve with respect to pore water velocity. During the trial and fitting process, it was seen that the curve was most sensitive to the attachment coefficient. It defined the peak of the breakthrough curve, which decreased with an increase in the attachment coefficient. The detachment coefficient defined the abscissa of the point where the decay slope intercepted the falling limb of the breakthrough curve. Of the two decay coefficients, the model was most sensitive to  $\mu_s$ , it defined the slope of the tailing curve.

The fitted parameters are almost identical to those in the benchmark problem for both cases of Castricum soil (Table 5). For the Roosteren, significant differences occur in the attachment rates for both velocities, and for the detachment rate for the 2.46 m/d velocity case. The overall fitting in terms of the peak magnitude and the tailing slopes were identical.

Table 5: A comparison of the fitted parameters for the benchmark case.

	<b>Hijnen</b>	<b>Our Modeling</b>	<b>Hijnen</b>	<b>Our Modeling</b>
<b>Castricum Soil</b>	<b>0.46 m/d</b>		<b>0.92 m/d</b>	
	$k_{att}$	0.724	0.724	0.622
$k_{det}$	0.004	0.004	0.009	0.0025
$\mu_l$	0.120	0.120	0.120	0.120
$\mu_s$	0.056	0.056	0.098	0.095
<b>Roosteren Soil</b>	<b>0.90 m/d</b>		<b>2.46 m/d</b>	
	$k_{att}$	2.385	2.125	4.509
$k_{det}$	0.004	0.004	0.004	0.0011
$\mu_l$	0.106	0.106	0.106	0.106
$\mu_s$	0.069	0.065	0.076	0.076

Units are in  $\text{hr}^{-1}$ .

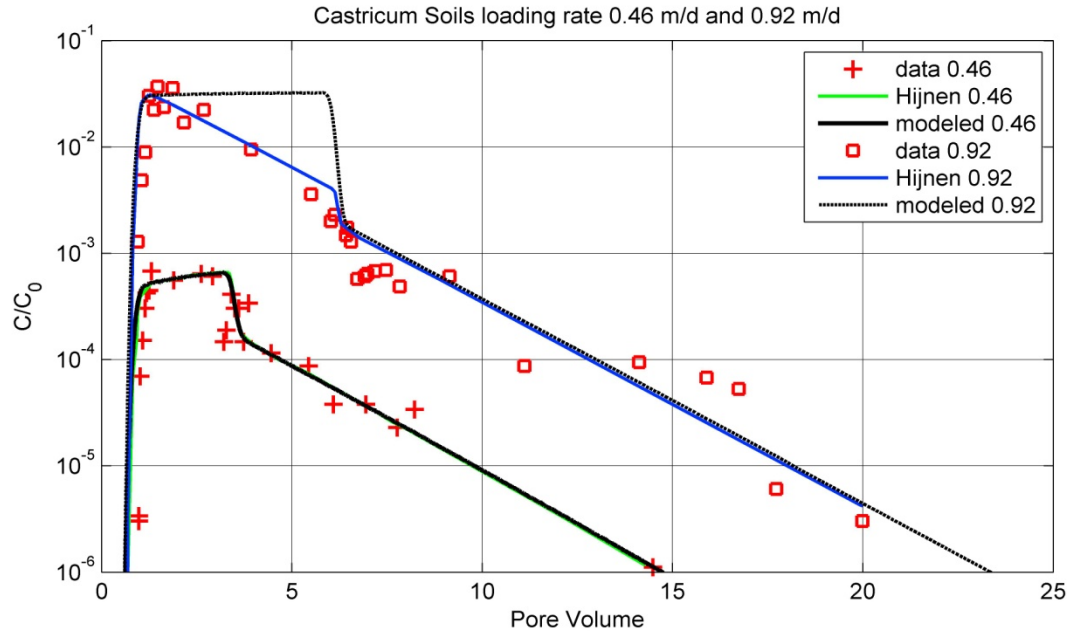


Fig. 14: Comparison of data, Hijnen's results and our modeled MS2 breakthrough curves for Castricum soils subjected to two different velocities (code verification).

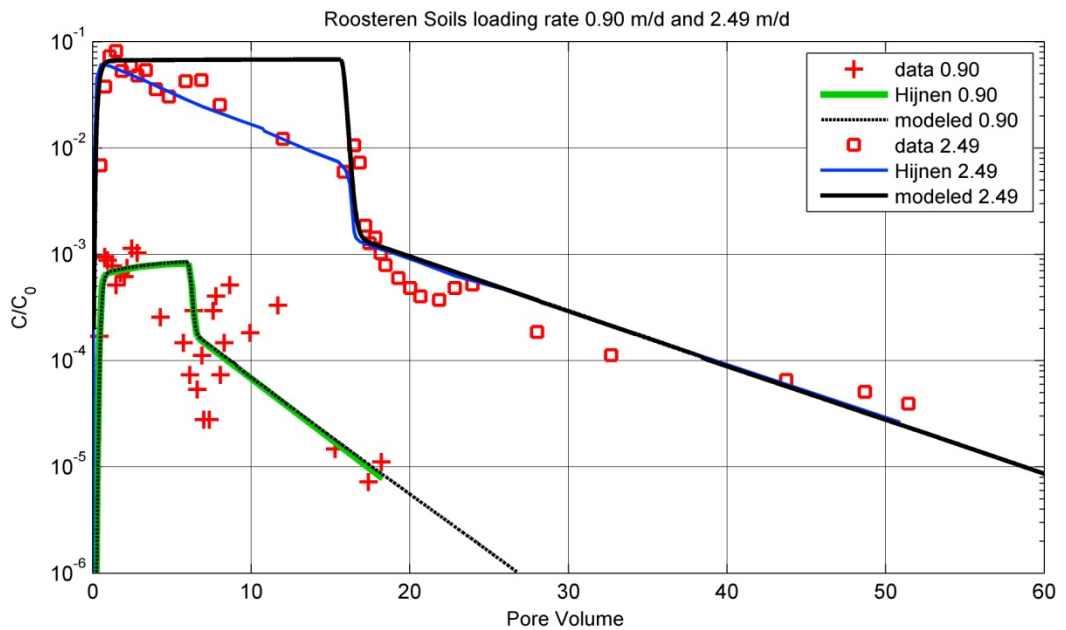


Fig. 15: Comparison of data, Hijnen's fitted and our modeled MS2 breakthrough curves for Roosteren soils subjected to with two different velocities (code verification).

The benchmark breakthrough curves fitted by Hijnen et al (2005) for the faster moving cases in each soil type show a rapid decline in concentration even when the column is still being spiked. This must be an error, as it suggests that the concentration of the spiking microbe, MS2 is not constant but decreasing exponentially, though the authors report constant spiking concentrations. We tried to fit the MS2 curve assuming an exponential decay function and it appeared to match the results of the faster loading case (2.49 m/d), but that would not match the case of the slower loading case (0.49 m/d). Our breakthrough curves are theoretically plausible for assumption of constant spiking concentration. Nevertheless, the perfect match for the slow moving cases, and match observed at the rising part of the curve, the peak and the final tailings in all cases, proves that our model code computation is acceptable and reproduces benchmark results.

### **3.3.2 Model (CFT based) verification using 1-D column experiments**

The second step in model verification was to see if our approach in model conceptualization, process description and the computational procedures would produce results similar to the benchmark. Our attempt is to fit the breakthrough curves of each soil type at two different velocities with only one set of parameters so that we have velocity independent parameters. Then we do not have to redefine different parameters for each velocity as in the case of  $k_{att}$  in Table 4, where it is different for different velocities of flow even for the same soil and site.

The experimental data for the benchmark study was then modeled using Eqs. (7) – (13) including all the processes of attachment and straining (incorporating CFT concepts), detachment and inactivation. This was, again done by modifying the reaction rate block section in the PHT3D database file. Porosity, flow rates through any particular grid cell in all three directions, and the grid cell dimensions were “called” from the MODFLOW into the PHT3D for each reaction time step. The rate block is used to calculate the pore water velocity at each grid level so that the local velocities at each grid cell are incorporated in the numerical calculation while running the model. The additional parameters used in the calculations are listed in Table 6.

Table 6: Constant parameters used in modelling 1-D column transport for the two soils.

Grain size, $a_c$ (Castricum)	$1.8 \times 10^{-4}$ m	MS2 diameter, $a_p$	$2.1 \times 10^{-8}$ m
Grain size, $a_c$ (Roosteren)	$5 \times 10^{-4}$ m	Hamaker Constant, H	$6.2 \times 10^{-21}$ J
Boltzmann's constant, k	$1.3806 \times 10^{-23}$ JK <sup>-1</sup>	gravity constant, g	9.81 ms <sup>-2</sup>
Particle density (MS2)	1085 kgm <sup>-3</sup>	Fluid density (water)	999.7 kgm <sup>-3</sup>

The result of modeling 1-D column study with our approach incorporating colloid filtration theory is given in Figs 16 and 17. For a given hydrodynamic condition, the estimates of heterogeneity factor ( $\lambda$ ) in Eq. (9), the detachment and inactivation (decay) coefficients (Eq. 13) are input as fitting variables until the observed concentrations match the breakthrough curves. The same set of parameters was fitted to the two different breakthrough curves for a site. The fitted parameters  $\lambda$ ,  $k_{det}$ ,  $\mu_l$  and  $\mu_s$  are given in Table 7. The other parameters of favourable attachment efficiency,  $\alpha_f$ , unfavorable attachment efficiency,  $\alpha_u$  and sticking efficiency  $\eta_{str}$  are kept fixed at 1, 0.0007 and 0.01 (values from the literature ) as these contribute the least and/or negligible.

For the Castricum soil columns, the peak and the overall shape is approximated reasonably well. The faster loading case in Castricum (for 0.92 m/d) underestimates the peak somewhat, while the tailing slope is slightly flatter. For the 0.49 m/d case, the peaking curve and the initial falling limb is well replicated, the decay rate is slightly steeper than the previously fitted rate.

For the Roosteren 2.49 m/d case, the upper curve in Fig 17, the fit is almost identical. For the slower loading case, i.e. the lower curve in the plot, the peak is replicated well but the falling limb of the breakthrough curve falls below the previous fit before sloping away at the decay rate. The slope of the decaying curve is well replicated, though its location or abscissa is not replicated. The fitted parameters are shown in Table 6.

Straining is reported to be least important mechanism for MS2 virus transport in sub-surface (Ginn et al., 2002) due to its diminutive size in comparison to soil grain sizes. It is to be noted that the rate coefficients for detachment, and both the inactivation processes are all similar to the previously fitted parameters given in Table 4.

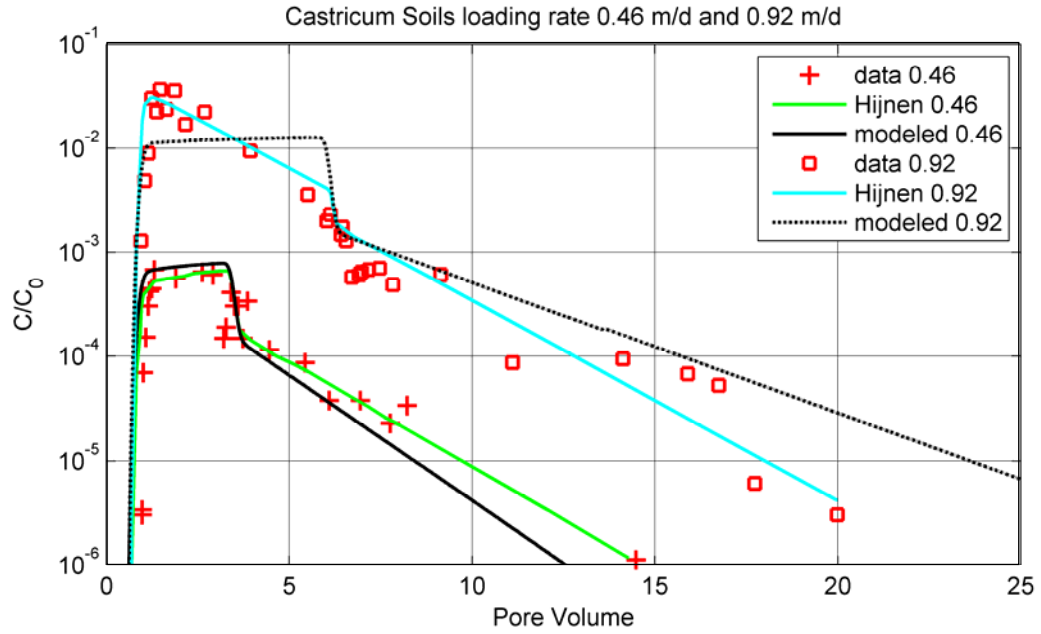


Fig. 16: Comparison of original fitted MS2 breakthrough curves with our modeled results for Castricum soil using filtration theory concepts.

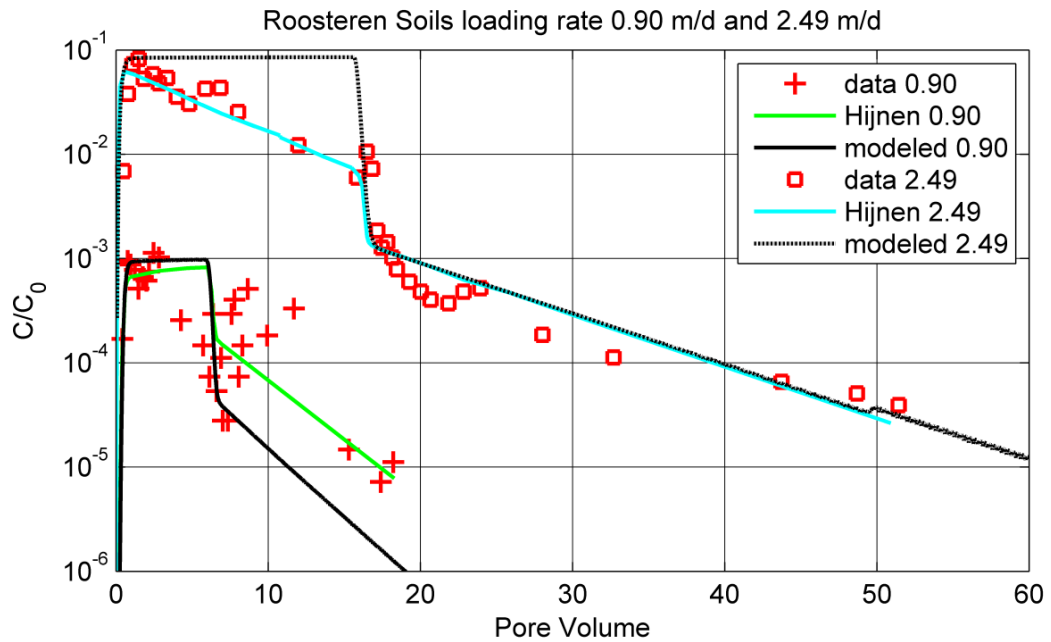


Fig. 17: Comparison of original fitted MS2 breakthrough curves with our modeled results for Roosteren soil using filtration theory concepts.

Table 7: Fitted parameters for the two soil columns using filtration theory applicable to both velocities of flow for the columns.

	$\lambda$	$k_{det}$ (h <sup>-1</sup> )	$\mu_l$ (h <sup>-1</sup> )	$\mu_s$ (h <sup>-1</sup> )
Castricum soils	0.0155	0.003	0.11	0.065
Roosteren soils	0.05	0.0012	0.25	0.08

The results achieved above are acceptable if one recognizes the fact that though the soil columns were obtained from the same location, there would be inherent variability due to the properties of soil itself as well as the sampling, handling, column packing and experimentation errors. If the fitting were to be done only to a single curve, a better fit would have been possible.

### 3.4 Evaluation for field-scale transport

#### 3.4.1 Study site

The RBF site modeled is located at the Flehe Waterworks well field, situated on the Eastern bank of the Rhine River (described in Chapter 2 and in Sharma et al., 2012). The system consists of 50 RBF wells located linearly along a 1400 m reach of the riverbank such that a 2-D approximation can be made. A calibrated MODFLOW/PHT3D model for the redox modeling of degradation of organic carbon in the Rhine RBF was already developed and has been discussed showing the importance of residence time of infiltrating water and seasonal effects Chapter 2 (and also at Sharma et al., 2012). The same numerical model is further developed to include microbial transport.

#### 3.4.2 Model Setup

A vertical cross section across a part of the River Rhine and the Eastern bank is used for the model as shown in Fig 4 (Chapter 2). The total length in  $x$ -direction is 390 m and it is 25 m in vertical direction. It is discretized for numerical modeling (see Fig 6, Chapter 2) with individual grids measuring 5 m in  $x$ -direction and 0.5 m in the vertical direction. The river bed and a portion of the right bank has been reported to be variably affected by riverbed clogging (Section 2.2.1) and this is represented by a 0.5 m thick layer with lower

hydraulic conductivities than the aquifer to represent spatially varying clogged river bed and riverbank. The model extent, grid discretization, zonation of hydraulic conductivities and the boundary conditions are shown in Fig 6 (Chapter 2). The model is set up for a total of 514 days (1 January 2003 to 15 April 2004), with 531 stress periods. This period includes 60 days of model run-up period in the beginning to remove start-up biases. For reference purposes, day 61 in the model and output plots is January 1, 2003.

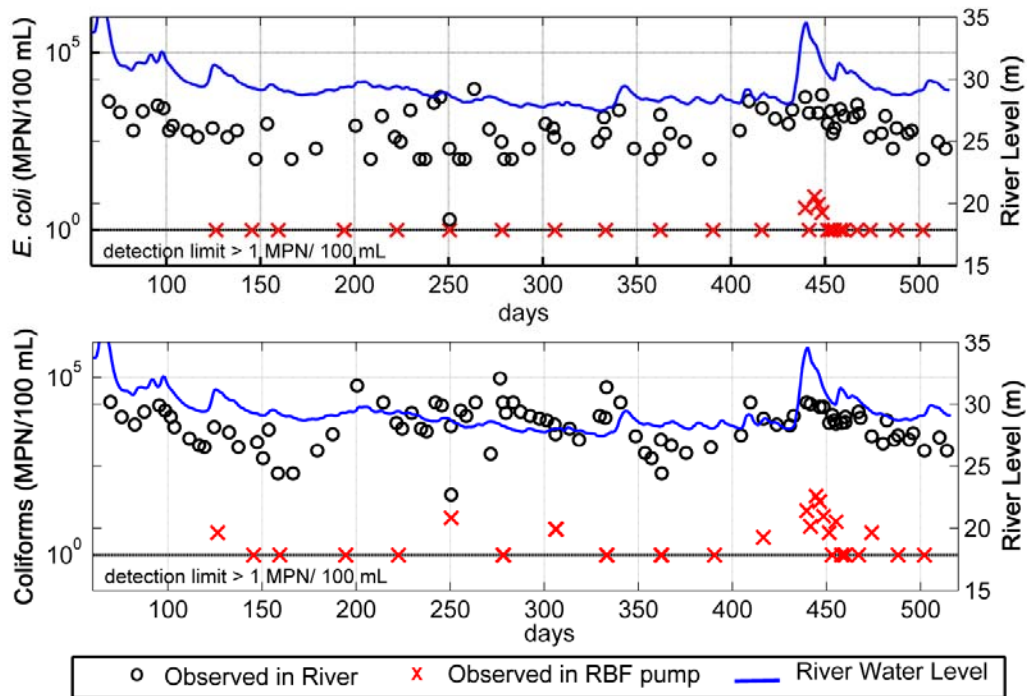


Fig. 18: *E. coli* and coliform concentrations measured in the river water and the observed values at the RBF well.

*Boundary conditions:* The hydraulic boundary conditions have been described in detail in Chapter 2, Section 2.3.1. The river cells below the low flood level were assigned transient heads representing the actual time series of river stage; and the right and left boundaries were defined as general head boundaries with reference to another observation well located farther inland. A time series data of microbes (*E. coli* and Coliforms) observed at the site in the Rhine River (Fig 18), observation wells and the pumping wells is obtained from the Flehe Water Works for the period of Jan 2003 to April 2004 and used for modeling. The river cells in the model domain were defined with time-variant specified

concentration corresponding to the measured time series data in the river. The *E. coli* and coliforms concentrations observed at a multi-level monitoring well (well C in Fig 5, Chapter 2) was used as the right side and left side boundary for reactive transport, no presence of microbes were reported. The observations on the right bank within the river and the pumping well is shown in Fig 18. These values have been imposed on the model to simulate the field condition. The aquifer is initially assumed free of any microbes.

*Reaction framework:* The attachment, detachment, straining and decay processes quantified by Equations (7) – (13) were written in PHT3D “RATE block” similar to the modeling of the 1-D benchmark problem in Section 3.3.2. For the RBF case, the kinetic mobile and immobile species of *E. coli* and coliforms were added and that of the MS2 phage removed. (See Appendix B). The parameters used in the calculations are listed in Table 8.

Table 8: Constant parameters used in modeling RBF microbial transport.

Median grain size $a_c$	$397 \times 10^{-6}$ m	Porosity, $\theta$	0.17
Boltzmann's Constant, $k$	$1.2806 \times 10^{-23}$ JK <sup>-1</sup>	<i>E. coli</i> diameter $a_p$ ,	$1.2 \times 10^{-6}$ m
Hamaker Constant	$6.5 \times 10^{-21}$ J	Coliforms diameter $a_p$ ,	$0.8 \times 10^{-6}$ m
Gravity acceleration, $g$	$9.81$ ms <sup>-2</sup>	$\alpha_f$	1
Particle density (microbe)	$1050$ kgm <sup>-3</sup>	$\alpha_u$	0.005
Fluid density (water)	$1000$ kgm <sup>-3</sup>	$\alpha_{STR}$	0.01

The multilevel observation point B is located at a distance of 20.4 m towards the river from the RBF well. The observation point B1 is located 18.75 m above sea level, while the points B2 and B3 are higher up at 23.25 m and 26.25 m level. The observation points B 4-6 are also active when the water level is higher; they are located at elevations of 28.75 m, 29.75 m and 30.75 m in the model, respectively.

### 3.4.3 Results and discussion

The RBF field scale microbial modeling result showed reasonably well fit, considering we are fitting microbial data. Most importantly, the model is able to simulate both the occurrence as well as the non-occurrence of microbial breakthrough as shown in Fig 19.

The parameters  $\lambda$ ,  $k_{det}$ ,  $\mu_l$  and  $\mu_s$  were varied successively to obtain a good fit of the

break-through curves at the observation points and the RBF well. The parameters are -  $\lambda = 0.0016$ ,  $k_{det} = 0.009 \text{ d}^{-1}$ ,  $k_{dec}(\text{aqueous}) = 0.30 \text{ d}^{-1}$ , and  $k_{dec}(\text{solid}) = 0.30 \text{ d}^{-1}$ .

The  $\lambda$  value denotes the heterogeneity factor describing the fraction of grains favoring attachment, so that there should be about 0.16 % of favourable grains for attaching the microbes. In the Flehe fields, total inorganic carbon was about 0.14% and sulfur was present less than 0.02% (mostly as pyrites). This would relate to a comparable fraction of sites favoring attachment. It is seen from Eq. (9) that  $\lambda$  primarily defines the attachment or sticking efficiency. The other parameters are also within the range reported in the literature (Foppen and Schijven, 2006; Pang, 2009; Sinton et al., 2010).

The Fig. 19 shows the simulated concentrations of *E. coli* and coliforms at the observation points B 1-3 and the RBF pump well. A breakthrough of the both the microbes occur after the peak flood observed in the Rhine River on 339<sup>th</sup> day. When the river water level rises well above the median flow levels, it bypasses the clogging layer of the river bed and the bank (located below 28 m elevation, see Fig 6) and travels rapidly towards the RBF well screens. The high flood level also increases the hydraulic gradient towards the RBF well. It pushes or provides the impulse so that the infiltrating water travels with higher velocities infiltrating deeper into the riverbank. Transport of microbes is also aided by size exclusion (Ginn et al., 2002) wherein the transported particles move faster than the mean pore water velocity. When the mean velocity of travel is increased, the velocity in the middle of the pore spaces would be even higher. This could also be a reason for the increased transport rate compromising further the microbial reduction capability during high floods.

A couple of other occasional single breakthroughs also occur as isolated events for coliforms between 200 and 350 days in the observation points B1, B2 and the RBF well. This may be due to the sheer high concentration in of the coliforms in the river, as the breakthroughs are synchronized with local peaks in concentration of coliforms in the river. The microbial removal capacity of the system with respect to the coliforms may have been achieved and the coliforms breakthrough. Such breakthroughs are occurring when the river water concentrations are reaching or exceeding 3.5 to 4 log units.

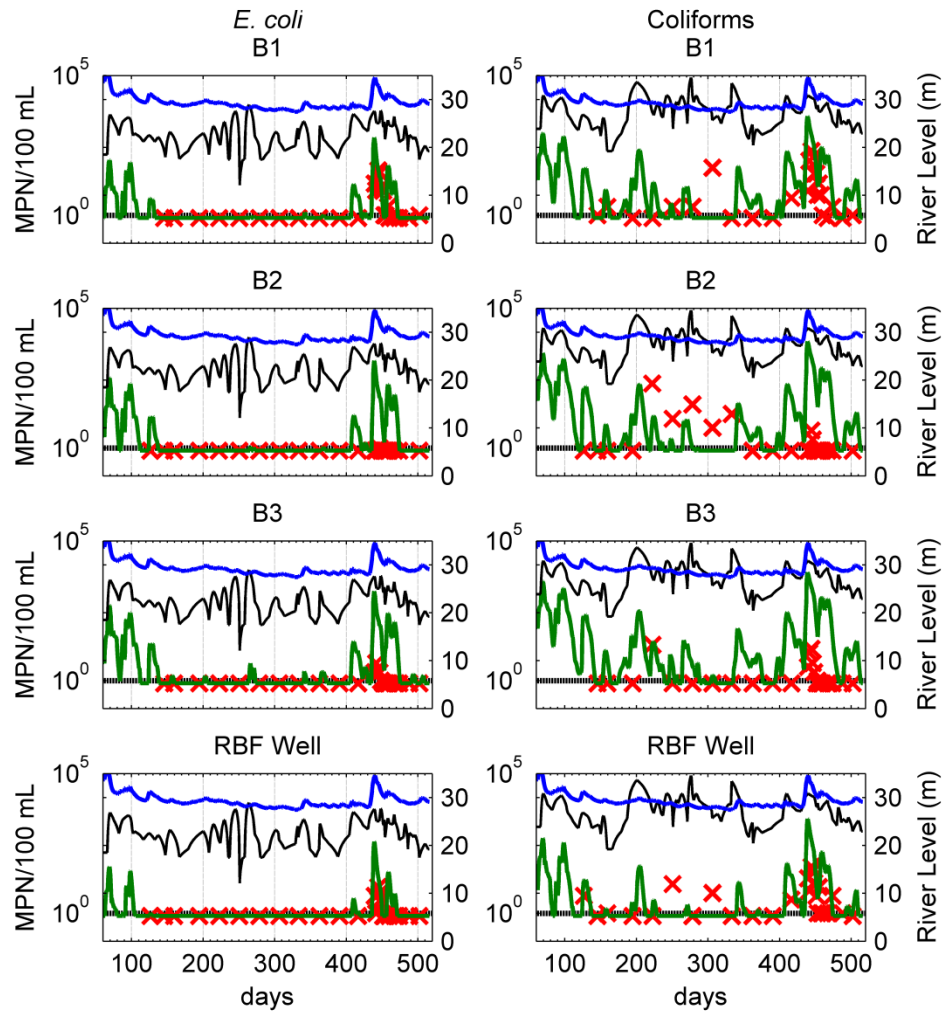


Fig. 19: Simulated (green lines) and observed (red  $\times$ ) *E. coli* and Coliforms shown in reference to the concentration in river (black line) in the observation points B 1- 3 and the changing river water level (blue lines). (Detection limit  $\geq 1$  MPN/100 mL)

There are other three observation points B 4-6 (Fig 20) that are intermittently under the phreatic line at high flood levels. Our results are mostly affirmative, apart from a single result at B4. These, locations are intermittently saturated - rapidly wetted and drained part of the aquifer - and our saturated zone modeling may not fully capture the processes in such locations where air-water interfaces and pathogens occur simultaneously. The transport behavior of pathogens in air-water interfaces may be different (Powelson and Mills, 2001).

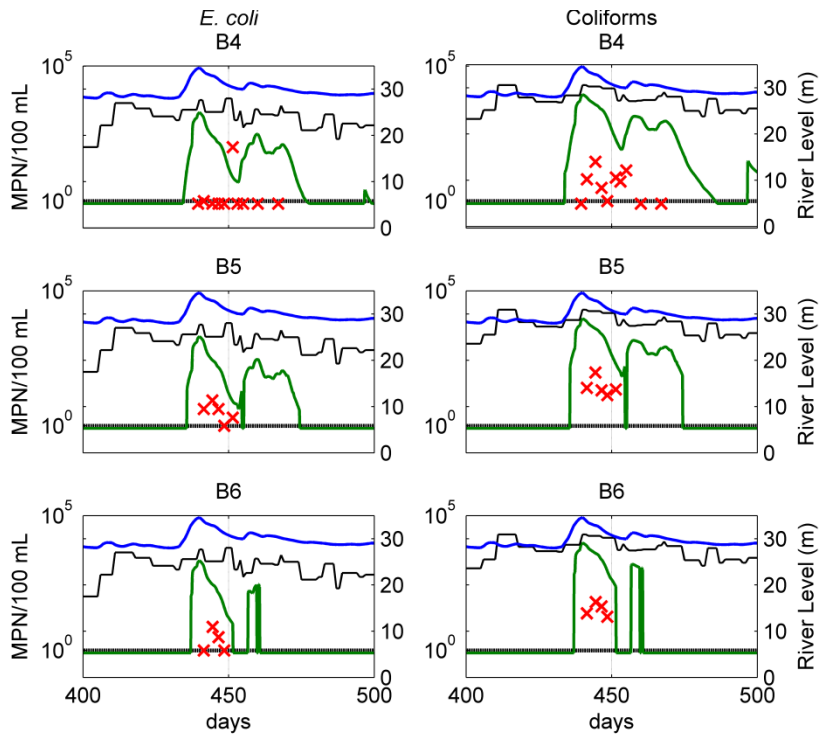


Fig. 20: Simulated (green lines) and observed (red  $\times$ ) *E. coli* and Coliforms shown in reference to the concentration in river (black line) in the intermittently saturated observation points B 4 - 6, and the changing river water level (blue lines). (Detection limit  $\geq 1$  MPN/100 mL)

Fig 21 and 22 show the concentrations of *E. coli* and coliforms, respectively at different time steps. In Fig. 21, it is modeled that the *E. coli* front reaches the well screen or breakthroughs at the well in 75, 100, 450 and 475 days. It is seen that the river water level at these times are higher, bypassing the clogging layers (shown by the bold line up to a level of about 28 m above sea level). The concentration of *E. coli* in the river at 100 and 300 days are comparable, but the concentration front of *E. coli* breakthroughs at the RBF well at 100 days but does not do so at 300 days. The front is contained within a few meters from the riverbed at 300 days. At 100 days, the river water level is receding from a flood wave and it is still above and bypasses the clogging layer. Similar observation can be seen at 450 days when a major flood is passing through the RBF site. At 250 days, when the *E. coli* concentration in the river is comparable to that at 450 days, no breakthrough of the bacteria occurs. At 300 days and 450 days the infiltrating water has to go through the clogging layer which attenuates the *E. coli* concentration.

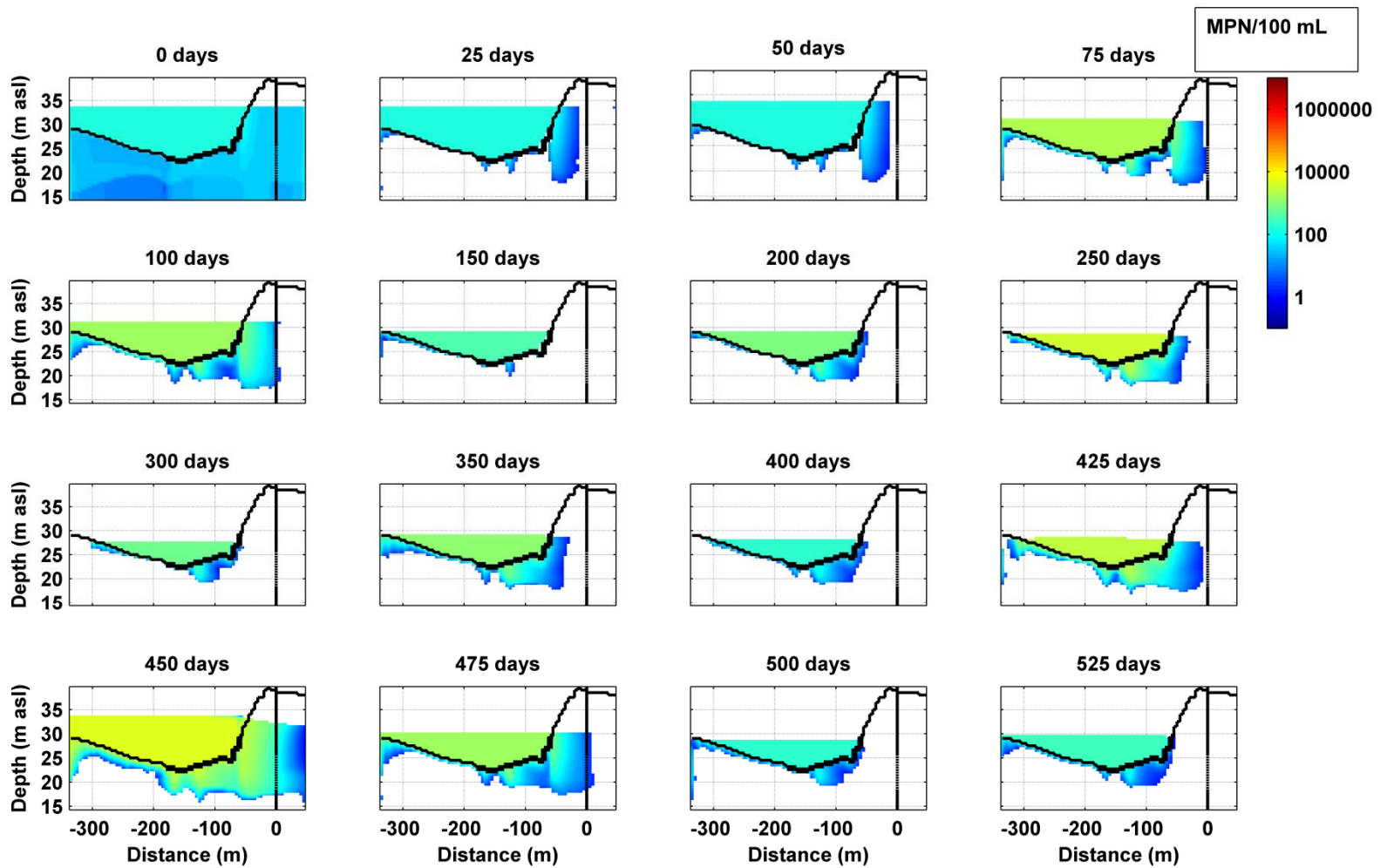


Fig. 21: *E. coli* concentration in the river and aquifer at different times.

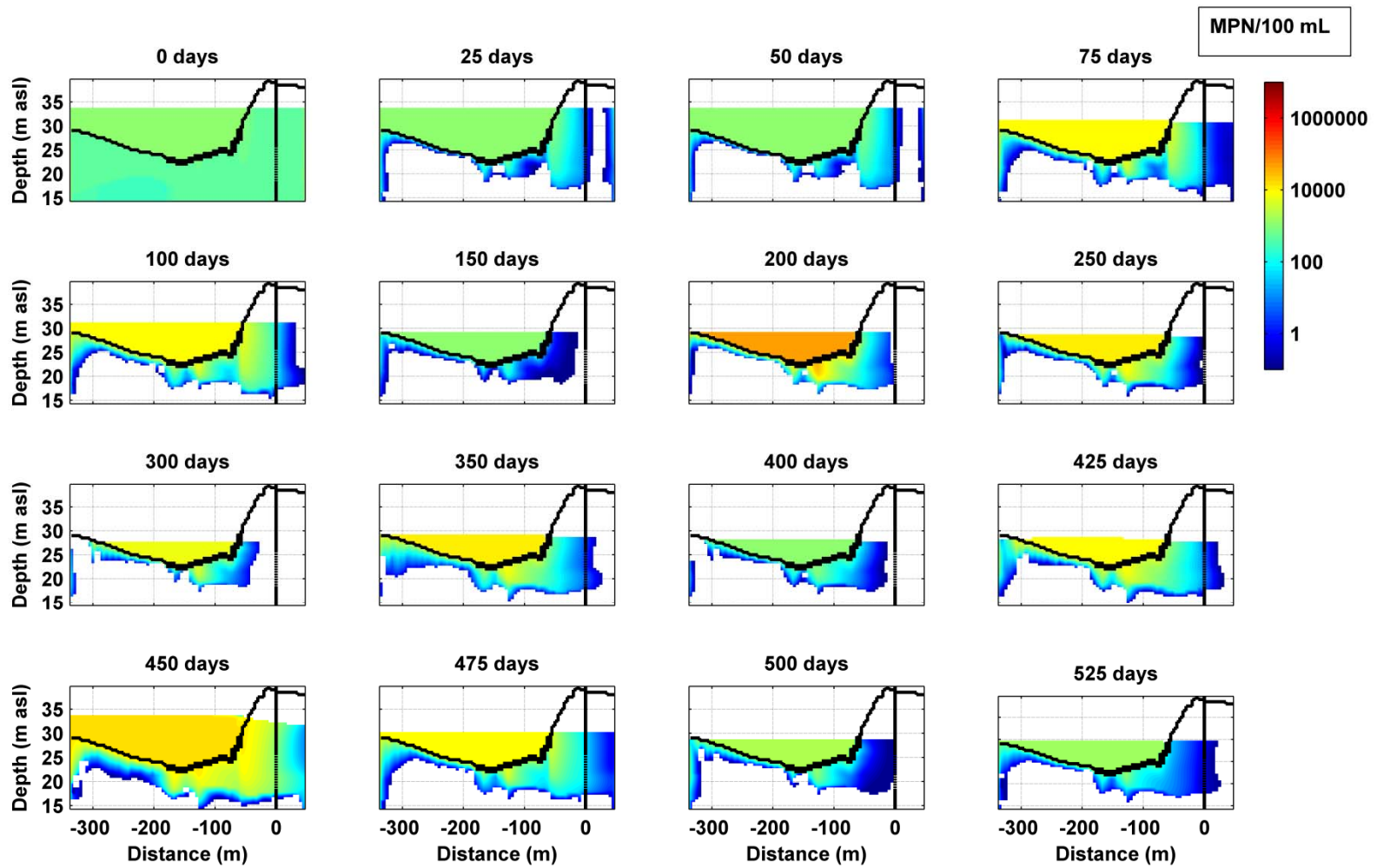


Fig. 22: Coliforms concentration in the river and aquifer at different times.

Similar results can be seen by analysing the coliforms concentration distribution at different time steps. For example, the coliform concentration levels in the river are similar at 100, 300 and 475 days, but the breakthroughs occur at the 100 and 475 days but not at 300 days. The river water levels at the 100 and 475 days are in flooding stage, above the clogging layer, and the infiltration from the recently inundated bank area without any clogging layer occurs in a rapid manner with a short travel (residence) time as discussed in Chapter 2 (see Sharma et al., 2012 also).

These results show the dynamic or transient nature of the *E. coli* and coliforms distribution in the riverbank aquifer have been adequately captured by our modeling efforts. The findings of flood levels compromising the microbial reduction capacities are similar to observations made by others also (Medema and Stuyfzand, 2002, Schijven et al., 2003).

### 3.5 Conclusions

Rivers and lakes, source waters for RBF systems, can contain high amounts of pathogenic concentrations so the fate and transport of pathogens in an RBF system is of common interest. Microbial transport is modeled in groundwater using the attachment rate the advection-dispersion transport equation adding on the mass-transfer processes of attachment, detachment and inactivation often approximated with linear kinetic reaction expressions. The rates defined by these processes are velocity dependent and could not be used directly for a transient RBF model where the velocity fields are constantly changing.

Modeling microbial transport in RBF systems required the transient nature of the boundary conditions and the flow fields within the system to be fully incorporated in the numerical schemes. The concepts of the classical colloid filtration theory and the advection dispersion transport equations were combined together to develop a procedure to incorporate transient conditions into a model for multicomponent reactive transport using PHT3D and MODFLOW. The approach was verified on a benchmark 1-D problem. The benchmark 1-D column modeling by our approach showed that we can use the same set of parameters to explain the breakthrough concentrations within a reasonable

degree, whether the velocity of flow is 0.46 m/d or doubled to 0.92 m/d. This has definite advantages for enabling modeling of transient conditions, such as in the RBF systems, where the velocities are constantly changing. Otherwise it would not have been possible to do so.

This new model is extended to model transport of *E. coli* and Coliforms in a large full-scale operating RBF scheme. The model was able to simulate the occurrence of the breakthrough during high floods as well as the non-occurrence during other times. The model was able to show that during high floods microbial reduction capability could be compromised where the reduction capacity was reduced to almost 1 log unit from an average value of about 4 log units compared to concentrations in the river.

The processes of detachment, straining, biological and physiological processes including microbial motility, mobility, predation, are components that have been simplified or excluded in the model. These could be gradually improved in the future. Neither the pathogen transport model used in the study nor the models discussed in the current literature, couple the aqueous chemistry of the groundwater with the microbes present therein. The temperature, pH, salinity, etc. are already noted to affect the microbe fate and transport, and these factors could be added on to the reactive transport model. This reactive transport model, being based on PHT3D, has the capability to be easily linked to aqueous chemistry other physico-chemical processes and can be a base case to which further developments can be easily added on.

A crucial part of the approach used here is the estimation of the attachment coefficient. Most pathogenic microorganisms have a low negative surface charge over a wide range of pH values; therefore, charge-based attachment to negatively charged soil, sediment, or rock surfaces is likely to be hindered and different from that with soils with some positively charged grains or fractions. This aspect needs to be addressed in the model through the heterogeneity factor ( $\lambda$ ), which may be difficult to define and needs further improvement.

## **CHAPTER 4. A Combined RBF and ASR System for Providing Drinking Water in Water Scarce Areas \***

### **Abstract**

A novel combination of riverbank filtration (RBF) and aquifer storage recovery (ASR) in the Albany region of Georgia (USA) was investigated in order to study possible changes in water quality. In areas where there are seasonal changes in water availability, seasonal excesses can be stored underground to meet short-term demands. Using RBF as a source water, rather than obtaining water directly from the surface water, would reduce treatment costs. The RBF site taps the Flint River through the Upper Floridan Aquifer producing water that can be injected into the deeper Clayton Aquifer for storage and subsequent recovery. This study tests the conceptual framework of having such RBF and ASR schemes coupled together and, more importantly, looks at the hydrogeochemical changes that are likely to occur. It was seen, in the scenarios considered, through numerical modeling, that acceptable water can be obtained from such coupled systems. Injection of the RBF water in an aquifer with arseniferous pyrite did not mobilize any significant arsenics.

**Keywords:** Riverbank filtration, aquifer storage recovery, drinking water, water scarcity, PHT3D, redox modeling.

---

\* This chapter is an updated reformatted version of a published chapter. Sharma, L. and Ray, C., 2011. A Combined RBF and ASR System for Providing Drinking Water in Water Scarce Areas. In: C. Ray and M. Shamrukh (Editors), Riverbank Filtration for Water Security in Desert Countries. NATO Science for Peace and Security Series C: Environmental Security. Springer Netherlands, pp. 29-49.

## 4.1 Introduction

Spatial and temporal variations in availability of fresh water resources necessitate diversion and storage of fresh water to meet demand. The increasing and competing demands of the residential, industrial, agricultural and environmental sectors make water a limiting or a scarce resource, which often constrains the development or economic growth of a region. The scarcity of water can exist not only in arid zones, but also in other climatic zones where there exist significant seasonal variations in water availability and use, and the present resources are already (over)allocated. A unique combination of riverbank filtration (RBF) and aquifer storage and recovery (ASR) is presented herein, where RBF is used to obtain a relatively better quality water to inject into a deeper aquifer for temporary storage, and then recover it to be used in times of water stress.

RBF (Kuehn and Mueller, 2000; Ray et al, 2002; Hubbs, 2004) is an efficient, yet low-cost water treatment technology for drinking water production. RBF wells for public water supply have been widely used in Europe for more than a century (Schubert, 2002) and more recently in the United States (Ray et al, 2002). While it has been shown that the quality improvement of the filtrate is significant compared to the source water (Stuyfzand et al. 1989; Stuyfzand, 1998; Tufenkji et al, 2002; Wang et al, 2002), very few studies have examined the feasibility of RBF for water banking or aquifer storage and recovering it later.

For example, in desert areas, rain occurs for a small duration of the year and the rivers run dry rest of the year. Surface storage is not feasible due to excessive evaporation. Increased evaporation limits the suitability of surface impoundments in these dry areas. In monsoon-driven climates, such as in India or Nepal, the river flows diminish greatly in post-monsoon seasons. River flows can be so low that storage impoundments must be constructed in order to allow water to be pumped to treatment plants. Even in wetter areas of the United States, high consumptive uses such as irrigation and municipal demands severely limit environmental flows. For example, in the Southeastern United States (particularly in South Georgia), several rivers cut into the large Floridian aquifer—a supraregional limestone aquifer in the area. There occurs significant pumping for irrigation during these low flow periods causing the groundwater table to drop so low that it even causes depletion of flows in the rivers.

This adversely affects the ecology of the downstream reaches. In an effort to maintain environmental flows, the state offers cash incentives to farmers to stop using the groundwater for irrigation so that the downstream impacts on the river can be minimized (Wilson, 2007).

In Santa Rosa, California, the Sonoma County Water Agency (SCWA) pumps its water from the Russian River where an inflatable dam is raised in summer months to impound the water so that its six collector wells can pump adequate amount of water to meet summer demand (Su et al., 2008). However, the operation of this dam and a reduction of flow affect threatened species of fish (salmon) and other biota. One of the potential solutions for South Georgia or the SCWA is to bank the water in aquifers during periods of high river flows and to release the stored water from the aquifer during times of high demand. This may enable SCWA to meet regulations regarding the minimum flow in the river. For Georgia, it will not only enable the state to meet the minimum flow requirements in the lower reaches of the rivers, it will also allow economic expansion for cities that are located in southern parts of the state thus attracting industry.

ASR is increasingly becoming a popular technique to augment drinking water supplies as well as to enhance the recharge of aquifers (Pyne, 2005). ASR is considered as a useful water management option in areas of water scarcity or where the seasonal demands fluctuate widely. The purpose of ASR is to store water in a suitable aquifer during times when water is available, and recover water from the same aquifer when it is needed (Dillon, 2005; Pyne, 2005). A large volume of water can be stored underground in suitable aquifers, reducing or eliminating the need to construct surface reservoirs and minimizing evaporation losses, saving resources (Khan et al, 2008) and without most of the undesirable environmental consequences associated with large surface reservoirs.

Using RBF water over surface water as a source for ASR has several other advantages too. RBF water is generally better than directly tapping surface water of polluted rivers. In general, it reduces turbidity, biodegradable compounds, bacteria, viruses, parasites, persistent organic contaminants and heavy metals, as well as attenuate shock loads to yield water of a relatively consistent quality as it is forced through the river bed and the bank.

There are several quality concerns when riverbank filtration and aquifer storage recovery systems are run in series. The quality of the filtrate must comply with local regulations before it can be injected into an aquifer. This is true for any source water for injection into potable aquifers. This paper looks at the possibility of a novel combination of riverbank filtration and aquifer storage recovery to address water shortage issues with reference to the Albany region of Georgia. The Georgia State Water Plan (EPD, 2008) outlines surface water storage, interbasin transfer, and aquifer storage and recovery (ASR) as three main water supply management practices to address water scarcity issues. RBF is sought to be used as source water for an ASR system which injects water into the deeper aquifer during times of excess flows in the Flint River and extract it during the drier seasons. Numerical modeling is done to investigate the possibility of such a scheme and model the possible water quality changes occurring therein.

## **4.2 Review of Past Relevant Work**

The surface water, as it flows through the river bed and the porous media, is subjected to a combination of physical, chemical, and biological processes such as filtration, dilution, sorption, and biodegradation that can significantly alter the filtrate water quality by the time it reaches the production wells (Stuyfzand, 1998; Kuehn and Mueller, 2000; Tufenkji et al, 2002). The passage of water through aquifers can introduce a number of water quality changes, such as attenuation or removal of organic carbon, microbes, pesticides, nitrate, and other contaminants or even leaching of minerals (Stuyfzand, this volume; Hiscock and Grischek, 2002; Tufenkji et al., 2002; Ray et al, 2002; Kuehn and Mueller, 2000; Doussan et al, 1997; Miettinen et al, 1994; Massman, 2008; Petrunic et al, 2005).

There are currently more than 300 ASR systems in operation (NRC, 2007). The injected water undergoes a complex set of geochemical reactions before it is recovered. The recovered water quality can change substantially during the cyclical processes of injection, storage within the aquifer, and subsequent withdrawal. Some of these changes are beneficial whereas others are adverse. The reactions may even alter the hydraulic properties (permeability and porosity) of the aquifer due to mineral precipitation/dissolution (Meyer, 1999) and/or by biological clogging (Rinck-Pfeiffer et al., 2000). Injecting oxygen-rich potable water and nutrient-rich reclaimed water

into an anaerobic aquifer leads to a variety of water quality changes (Greskowiak et al., 2005; Vanderzalm et al., 2006). This process leads to the production or consumption of protons and other reactants which in turn triggers the precipitation and dissolution of minerals, ion exchange, and surface complexation reactions (Eckert and Appelo, 2002). If dissolved organic carbon (DOC) is present in the injected water, microbial reactions will degrade the carbon and deplete oxygen in the process, making the aquifer more reducing. This result can affect processes such as denitrification and other redox reactions and lead to higher concentrations of redox sensitive species such as iron, manganese, arsenic and  $\text{SO}_4^{2-}$  in the recovered water.

In field settings, quality changes during the injection of high quality water have been observed by several authors. Stuyfzand (1998) gives an important overview of quality changes of injection water based on 11 deep well recharge experiments in The Netherlands; and the dissolution of calcite, dolomite and amorphous silica was reported by Mirecki et al. (1998). Effects of deep well recharge of oxic water into an anoxic pyrite-bearing aquifer was investigated and modeled by Saalnik et al. (2005). However, only a limited number of studies report water quality changes during the injection of reclaimed water. Australia and some western states in the U. S., most notably, such as California and Arizona employ ASR systems that use recycled waters exclusively. Greskowiak et al. (2005) simulated carbon cycling and biogeochemical changes during the operation of an ASR system at Bolivar, South Australia. Their models predict that dynamic changes in bacterial population during the storage phase can affect the local geochemistry around the injection/extraction wells. Farther away from the injection wells, breakthrough of cations was strongly affected by exchange reactions. Calcite dissolution substantially increased calcium concentrations in the recovered water.

Seasonal variations in redox reactions have also been looked at in a few cases in the context of ASR. Temperature-dependent pyrite oxidation in a deep (1000 ft) anaerobic aquifer in the Netherlands was simulated by Prommer and Stuyfzand (2005). Greskowiak et al. (2006) examined the variability in the degradation of pharmaceutical phenazone (present in the wastewater of Berlin, Germany) as a function of season. They found that the degradation was redox sensitive and

breakthrough of phenazone in monitoring wells occurred in warmer summer months when anaerobic conditions developed.

In terms of benefits, ASR has the potential to remove pathogens, disinfection byproducts (from chlorinated water), DOC, and pharmaceutical residues (NRC, 2007). The NRC report also points to case studies where tri-halomethanes have been formed by injecting chlorinated drinking water to aquifers that have some amount of DOC. Recently, arsenic (As) dissolution from the Floridan aquifer has been identified as a major problem inherent to ASR application there (Arthur et al, 2002 and 2005). At the Punta Gorda ASR site in Florida, these authors showed that arsenic concentrations significantly increased during the recovery periods, and exceeded the current EPA standards for presence of arsenic in water. Similar mobilization of arsenic has also been observed at the Peace River ASR site in Florida. The limestone matrix in the Floridan Aquifer contains small amounts of arsenic, mostly associated with arseniferous pyrite along with other trace metals (Price and Pichler, 2005). Under normal conditions, arsenic is in equilibrium with the native ground water. However, during ASR operation, especially when the system experiences iron-reducing conditions and the iron oxides dissolve, the adsorbed arsenic is released (Smedley and Kinniburgh, 2002). Jones and Pichler (2007) recently showed in the lab that the arsenic was immobile in ambient deep anoxic groundwater conditions, but became mobile as recharge water increased the redox potential of groundwater. EPA has lowered the maximum allowable limit of arsenic in drinking water supply/sources from 50 to 10  $\mu\text{g/L}$ . Thereby about 13 ASR systems in Florida are in violation of the drinking water standards (NRC, 2007) and are reportedly banned from operating. This underscores the importance of screening tools, such as numerical modeling, that can yield critical information a priori when it is backed by proper site investigations.

### **4.3 Methods and Procedures**

The study was carried out by collating information, analyzing data and literature from various sources, estimating parameters, building conceptual models, carrying out numerical modeling using the parameters for different scenarios.

For this study, we examined various areas of Georgia for ASR feasibility. The coastal zones were excluded as the current regulations do not allow for ASR systems in the immediate future (until the prohibition for ASR expires). Areas north of the “fall line”

that runs northeast from Columbus, GA to Augusta, GA were eliminated because of geological constraints. Most recently, the Flint and Chattahoochee basins experienced drought conditions that reduced stream flows significantly. In order to preserve base flow of the Flint River, the Georgia Environmental Protection Division (EPD) asked the farmers to stop withdrawing groundwater from this upper aquifer for irrigation in return for a cash rebate (Wilson, 2007).

Cities that are located in the area also face limitations of growth because of restrictions of additional withdrawal from surface or ground water sources. To mitigate this, a possible solution was to consider withdrawing water from the Flint or the Chattahoochee rivers during periods of high flows and then treating this water and storing it in a deeper aquifer for future use. The needed treatment before injection could be regular treatment of surface water in a conventional water treatment plant, natural filtration such as occurring during RBF without additional treatment, or a combination of both. Such systems would allow the cities to capture excess runoff at a period of no or minimal restrictions and store that water in deep aquifers for later use.

An area in the vicinity of the City of Albany, GA, USA was selected for the study. The Water Planning and Policy Center (<http://www.h20policycenter.org>) had previously developed a conceptual stage feasibility assessment of an ASR system for the extraction and injection scenario (Water Resource Solutions, 2006). It identified an area east/north-east of the City of Albany for a RBF and ASR scheme. It suggested extracting water from the Flint River and treating it before storing in a deeper aquifer so that the industry could pump it out at a sustained rate of 10 million gallons per day (MGD). Water for injection was to be obtained by directly pumping surface water or obtaining it from RBF schemes, the latter being the more attractive alternative. It was expected that the RBF scheme would have overall lower treatment costs, assuming that heavy metal concentrations do not increase substantially during subsurface passage. The proposed area is shown in Fig 23.

This area lies on the Floridan Aquifer system, having multiple aquifers and confining layers, and the geo-hydrology is well documented (Hicks et al., 1981). A generalized stratigraphy and the water-bearing properties of formations underlying the study area are shown in Fig 24. The aquifers included are (i) the Upper Floridan Aquifer of the Ocala Limestone formation, and (ii) the Clayton Aquifer of the Midway Group, which

is a deeper aquifer. Water from the shallower aquifer will be extracted when the surface water in the Flint River is in excess of demands. This extracted water will be used to recharge the lower aquifer. This in turn can be pumped to augment water supply during dry summer months.

For the simplified case of this study, water is extracted from the RBF part of the system for the six months of October to March and recharged into the deeper aquifer, and subsequently withdrawn from this storage for the remaining six months of April to September when the water demand is higher. The water from storage could be directly used for municipal or industrial uses, or released into the river which could augment the environmental flows and recharge the depleting aquifer.

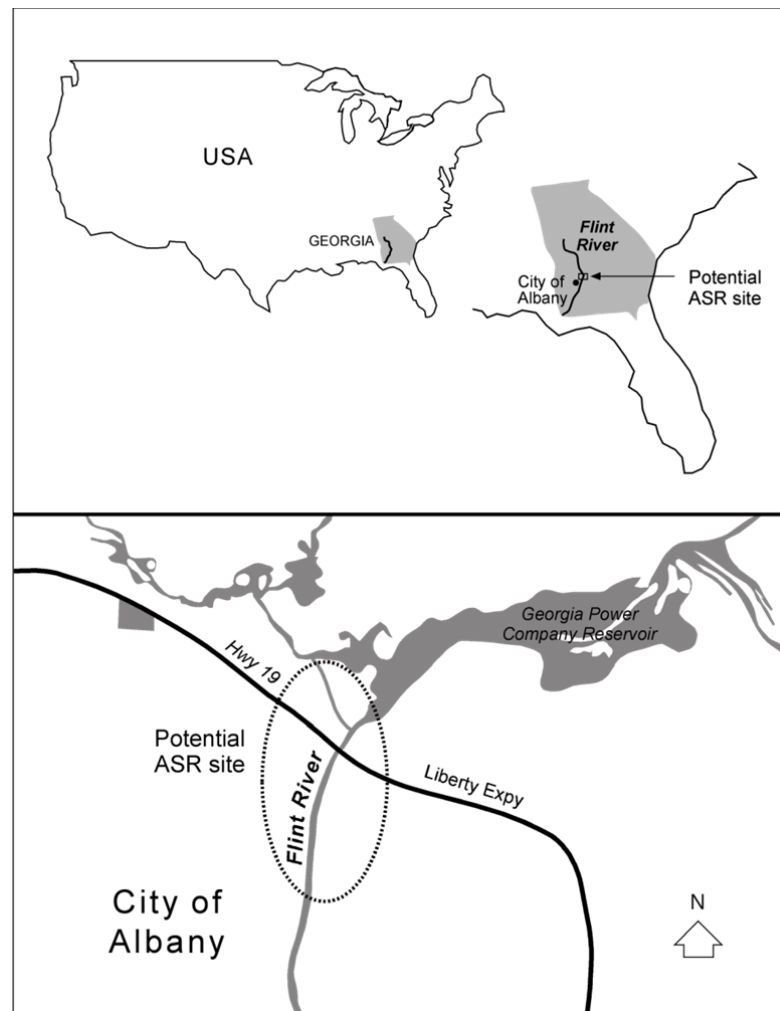


Fig. 23: Possible location of the ASR site east/north-east of the City of Albany, Georgia, USA.

Study of the available materials and maps indicate that suitable areas for the project would be located adjacent to the river, north of the City of Albany. A linear parcel along the river would facilitate placing about 10 RBF wells, each of about 1 MGD capacity, at a lateral spacing of 200 ft. This could draw water from Upper Floridan Aquifer (also called the Ocala aquifer; Fig 24) which is hydraulically connected to the Flint River.

A preliminary 3-D numerical model using MODFLOW (Harbaugh et al., 2000) was set up to explore the flow conditions in the aquifers and the information was used to prepare computationally more efficient 2-D models using MODFLOW. Separate models were set up for obtaining water from the river (named the RBF model) and for injection, storage and retrieval of the pumped water (named ASR model). Geochemical transport of different species in the models with reactions was carried out using the PHT3D (Prommer et al., 2003) which couples the transport simulator MT3DMS (Zheng and Wang, 1999) in MODFLOW with the geochemical model PHREEQC-2 (Parkhurst and Appelo, 1999).

The river water quality and stage data is obtained for the USGS Station ID 02352560 (Flint River at Albany) from the United States Geological Survey (USGS) surface water data inventory. The groundwater quality data were determined from the nearest wells, Well ID 12K129 in the Upper Floridan Aquifer and Well ID 12L020 for the Clayton aquifer. Water quality and hydrology data of the other adjacent wells (12M002, 13L002 and others) were also looked into to determine the regional flow and the required water chemistry.

The 2-D RBF model grid is set up 520 feet long and 160 feet deep with a unit thickness as shown in the upper part of Fig 25. The grid is divided into a total 14 layers and refined at the river portion so that the river hydrograph can be properly represented and the boundary head cells do not go dry at any time during simulations.

ERA	SYSTEM	SERIES	GROUP FORMATION AND MEMBER		AQUIFER OR CONFINING UNIT	
			Northwest	Southeast		
Cenozoic	Quaternary	Holocene	Undifferentiated Overburden	Undifferentiated Overburden	Surficial aquifer/upper semi-confining unit	
		Pliocene	Missing Rocks (?)	Missing Rocks (?)		Upper Floridan aquifer
				Undifferentiated sediments		
		Missing Rocks (?)				
		Suwannee Limestone				
	Oligocene	Missing Rocks (?)	Missing Rocks (?)	Upper water-bearing zone		
	Tertiary	Upper Eocene	Ocala Limestone	Ocala Limestone	Middle unit	
			Clinchfield Sand		Lower water-bearing zone	
		Eocene	Middle Eocene	Lisbon Formation		Lisbon confining zone
				(?)		Claiborne aquifer
		Talaahatta Formation (?)				
		Paleocene	Wilcox Group	Bashi Formation	Hatchetigbee Formation	Wilcox confining unit
				Tusahoma Formation		
				Baker Hill Formation		
				(?)		
			Midway Group	Porters Creek Clay	Clayton Formation	
				Confining Layer		Clayton -Providence confining zone

RBF Aquifer

ASR Aquifer

Fig. 24: Aquifers in the Albany area  
 (source: <http://ga.water.usgs.gov/projects/albany/stratcol.html>)

The pumping well is placed 120 feet away from the river bank. The river stage and aquifer data were obtained from USGS sites for surface water and groundwater data. The model is subjected to a time variant hydraulic boundary of the river defined by varying water stages, and with general head boundaries on either side defined with a hydraulic head of 154 ft at a distance of 6000 ft from the boundary corresponding to regional groundwater levels. For simulating aqueous species composition, the river boundary is defined with the observed river water chemistry; and the left and right boundaries are set as constant concentration boundaries - the aqueous chemistry being defined with that of the ambient aquifer water quality.

The ASR aquifer, 125 ft thick, is located between the depths of 625 ft and 750 ft below the ground surface level and is described by a grid as shown in the lower part of Fig 25. The confined aquifer is differentiated into 5 layers. It is depicted by a 2-D symmetrical model, set up with the well at the left end and a general head boundary at the right side. The left boundary cells are set as point sources for injecting and extracting water, i.e. a well with reversible pumps. The length of the model domain is selected in an iterative manner so that the right boundary chemistry remained relatively unchanged from ambient conditions. The vertical grids are closer spaced near the well and placed further apart towards the right boundary as more rapid reactions are assumed to take place in the vicinity of the wells.

Detailed site specific multi-species time series data was not available and only a few parameters such as river stage, temperature and dissolved oxygen in the river water and others for the groundwater were found to be recorded intermittently; and only one set of complete aquatic chemistry data could be constructed for other species. These data are used to emulate annual time series data. Errors in this data set was minimized by carrying out a charge balance of the ions using PHREEQC-2 (Parkhurst and Apello, 1999) adjusting the small errors to chloride concentrations. The aqueous chemistry data sets for the Flint River, Upper Floridan Aquifer (the RBF aquifer) and the Lower Floridan Aquifer (the ASR aquifer) are given in Table 9 and are used for the initial and boundary conditions in constraining the numerical model.

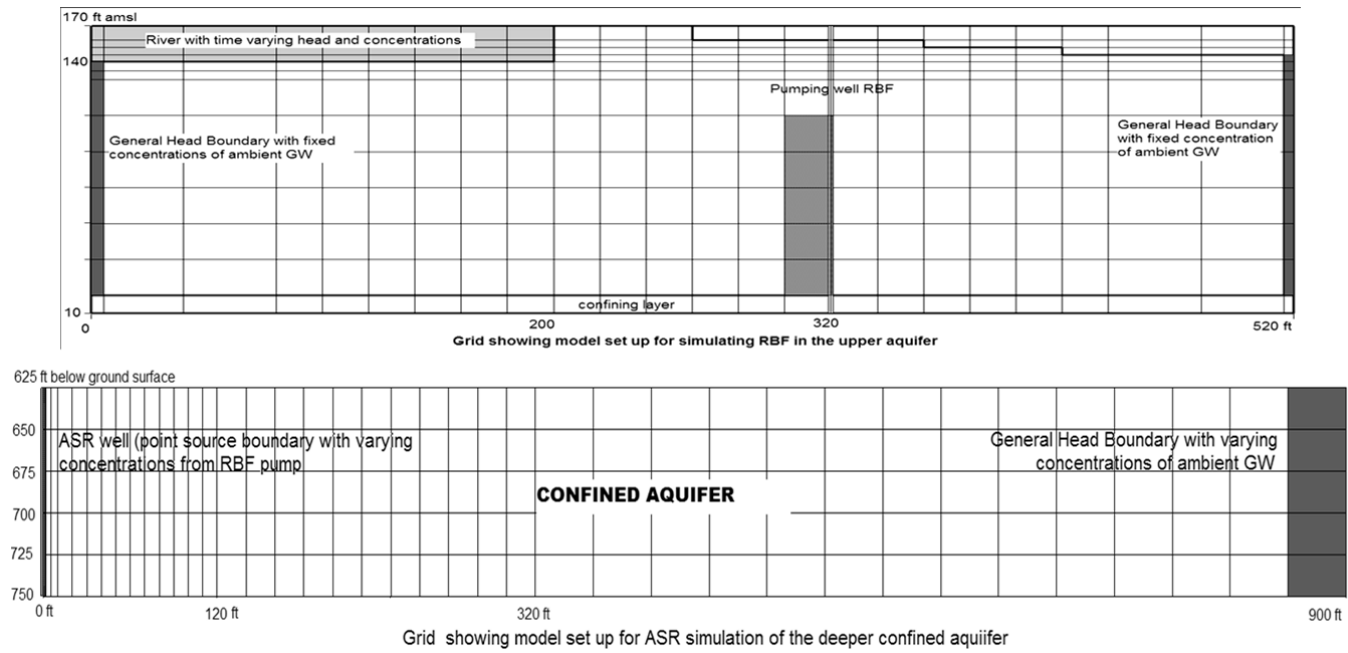


Fig. 25: Two dimensional grid models for depicting RBF (top) and ASR (bottom).

Table 9: Aqueous components as model inputs from charge balanced data set.

Component	Flint River (mol/L)	Upper Floridan Aquifer (mol/L)	Lower Floridan Aquifer (mol/L)
DOC	0.00035	0	0
Temperature	9.8 to 30.6	20.4	23
Dissolved Oxygen	4.4e-4 to 6.9e-4	5.44e-04	0
Ca(+2)	5.24e-04	9.68e-04	2.99e-04
Mg(+2)	5.76e-05	2.17e-05	2.47e-04
Na(+)	2.94e-04	9.18e-05	1.44e-03
K(+)	4.60e-05	8.19e-06	7.16e-05
Fe(+3)	1.38e-06	5.37e-08	3.22e-06
Mn(+3)	7.81e-07	1.82e-08	9.10e-08
Si	1.09e-04	1.33e-04	3.33e-04
Cl(-)	7.48e-04	1.44e-04	1.23e-03
C(+4)	5.98e-04	1.76e-03	1.34e-03
S(+6)	9.68e-05	1.87e-06	1.35e-04
N(+5)	2.71e-05	2.04e-04	2.86e-06
N(+3)	2.14e-07	7.14e-08	0
Ammonium (+)	1.61e-06	0	0
pH	7.3	7.9	7.2

Units: mol/L except temperature (°C) and pH is dimensionless.

The extraction rate per well is 1 MGD (million gallons per day). These wells are placed linearly along the river bank every 200 feet so a linear approximation is made to represent the system with a 2 D vertical model. The extraction rate per unit width is 5000 gallons per day (GPD). A simplified scenario of extraction from the RBF well for six months, starting October and lasting until March, is used to approximate the season when there would be excess flow in the river. The pump is turned off for the rest of the year.

The average hydraulic conductivity is assumed to be 450 ft/day in the upper aquifer, and 66 ft/day in the storage aquifer estimated from regional transmissivity values (Hicks et al., 1981; Miller, 1986). The ASR wells are placed 350 ft apart with reversible pumps operating at 2900 GPD. Equal injection and extraction rates are assumed for the ASR for a simple analysis. The model set up utilizes symmetry of the system simulating one half of the system imposing half the extraction or injection rates in the model. The actual pumping schedule is shown in Table 10. All simulations are run with a 50 day spin up period so as to remove any biases from arbitrarily

chosen starting conditions. The ambient aquifer head in the upper layers is taken as 154 feet below the ground surface. It is important to note that the hydraulic performance of the wells and the aquifer are assumed adequate in terms of aquifer storage, recovery and hydraulic heads on the aquifer and well-heads.

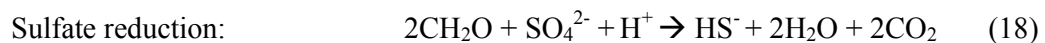
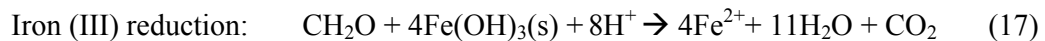
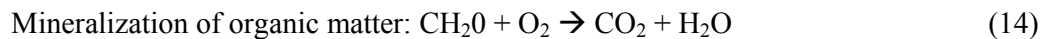
Table 10: Pumping Schedule

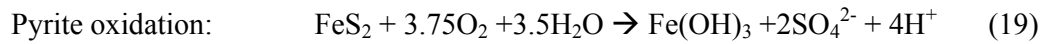
Start time (days)	End time (days)	RBF well (GPD)	ASR well (GPD)	Remarks
0	50	-5000	2900	Start up period
50	230	-5000	2900	to storage
230	410	0	-2900	to external supply
410	590	-5000	2900	to storage
590	770	0	-2900	to external supply

The MODFLOW/MT3DMS-based multi-component reactive transport model PHT3D was used. Both the upper aquifer and the lower aquifers are carbonate aquifers, so the model was first set up to run equilibrium and dissolution reactions with oxidation of the organic carbon and other species using PHT3D with sorption described by linear isotherms and the reaction module defined by the PhreeqC-2 database (Parkhurst and Appelo, 1999).

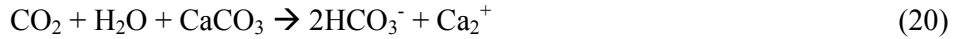
The DOC in river water as it infiltrates into the aquifer is initially degraded by the dissolved oxygen in presence of microbes and electron acceptors. Redox sensitive species such as O<sub>2</sub>, NO<sub>3</sub><sup>-</sup>, Mn<sup>4+</sup>, Fe<sup>3+</sup>, SO<sub>4</sub><sup>2-</sup> are present in the aquatic environment and these also sequentially act as electron receptors for degradation of dissolved organic matter.

**Key reactions involved in RBF and ASR**





The acidity generated by the dissolution of carbon dioxide in water or the excess protons are commonly expected to bring about calcite dissolution, i.e.,



The kinetics of the degradation is also dependent upon the aqueous temperature (Prommer and Stuyfzand, 2005; Greskowiak, 2006) for oxidation of pyrites and organic matter respectively. Modeling temperature of the influx water and the aquifer is also carried out considering temperature as a dummy species that undergoes sorption following a linear isotherm, as water travels through the aquifer. The reaction networks are described in detail in the PHT3D reaction module PHREEQC-2 database and follow on the lines of (Prommer and Stuyfzand, 2005; Greskowiak, 2006). It is often seen that a small amount of organic carbon does persist even when oxidizing agents are present. This is because the organic carbon may also consist of a more persistent form. So a basic persistent level of 2E-05 mol/L of organic carbon is modeled to remain in the aquifer.

The RBF and ASR models were first set to run for equilibrium and dissolution reactions with oxidation of organic carbon in a calcite aquifer, typical of the area considered. A second set of simulations was done injecting the water obtained from the carbonate RBF system into an ASR aquifer with arsenopyrites to check for mobility of arsenic. The pyritic aquifer was assumed to contain 0.1% arsenopyrite, and the simulations considered sole oxidation of pyrites by omitting the presence of the DOC in the filtrate water. If DOC was considered, it would be competing with pyrite for oxidation, and reducing the possibility of release minerals. As it is, the water obtained from the RBF would be low on degradable DOC, as most of it is likely to be consumed in the RBF process. The geochemical modeling of this latter scenario is done in a manner similar to that used by Prommer and Stuyfzand (2005) wherein pyrite oxidation is modeled to be depending upon the concentrations of oxygen, nitrate, proton concentrations, mineral surface area and the concentration of pyrites.

## 4.4 Results and Discussion

### 4.4.1 The RBF subsystem

The simulation results for investigation into organic carbon redox reactions, calcite dissolution and the general equilibrium reactions show that the organic carbon degradation is the first predominant reaction that takes place. The model allows for the presence of some dissolved organic carbon as refractory and some as readily degradable (Greskowiak et al., 2005). The simulation result of concentrations of different species in the RBF well is shown in Fig 26. It should be noted that the pump is stopped during the periods 230-410 days and 590-770 days.

The model showed that in the RBF well, consumption of DO is rapid as it enters the aquifer. The dissolved oxygen introduced with the infiltrating water is consumed in overcoming the initial anoxic situation in the aquifer as well as in oxidizing the DOC coming in through the river bed. The river water contains  $3.5\text{E-}04$  mol/L of DOC which is reduced to less than  $0.7\text{E-}04$  mol/L at the first phase of injection. There are seen initial increases in DOC and the  $\text{SO}_4^{2-}$  (denoted by S(+6) in the plot) during the early start up time in the plots shown. The small increase in DOC in the plot initially is due to the reason that no DOC was considered present in the aquifer at the start, so its concentration increases to the minimum level assumed to be present in the aquifer. The  $\text{SO}_4^{2-}$  and Fe(+3) also increase initially as they are also present in higher concentrations in the river than in the aquifer.

At around 200 days, aerobic degradation diminishes and denitrification takes place rapidly as shown by consumption all of the N(+5) and increase N(0) concentrations. It is seen that denitrification is not able to degrade the entire DOC coming in with the river water as the DOC concentration picks up slightly. At the end of the pumping period, at 230 days, N(+5) is exhausted and rapid iron reduction also takes place converting all the Fe(+3) present into Fe(+2). A strongly reducing situation then develops corresponding to higher electron activity, indicated by low pe. The degradation of remaining DOC is then gradually degraded to the minimum level due to sulfate reduction, wherein S(+6) in  $\text{SO}_4^{2-}$  is converted to S(-2). Some  $\text{SO}_4^{2-}$  is still present till the start of the next cycle showing that sulfate reduction is incomplete and no methane generation takes place.

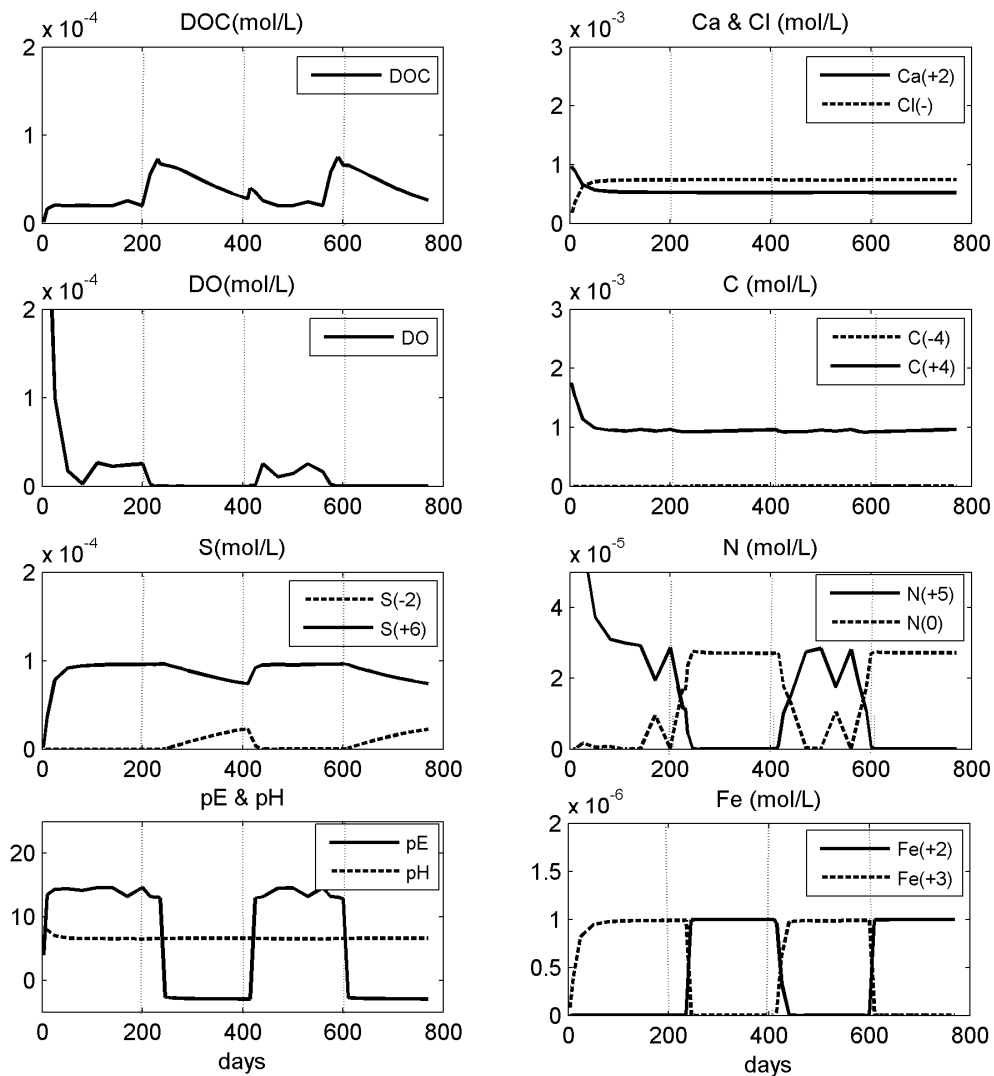


Fig. 26: Concentration time series data at the RBF pumping well. The pump is turned off during the periods 230-410 and 590-770 days.

In the next cycle of pumping from 410 to 590 days, the infiltrating water from the river supplies more DO and DOC so that aerobic reactions start taking place. The pE reverts to its higher value. The concentrations of N(+5) and  $\text{SO}_4^{2-}$  increase with corresponding decreases in N(0) and S(-2) respectively. At the end of the pumping period, denitrification, iron reduction also take place followed by some sulfate reduction when the pump is stopped. This cycle repeats itself subsequently.

The maximum concentrations of the aqueous species in the pumped RBF filtrate water are shown in Table 11 along with that of the Flint River and the final ASR

output. The concentrations of RBF extract are similar to the concentrations in the deeper aquifer and are taken to be within acceptable limits for injection into the ASR aquifer.

Table 11: Maximum concentration of various aqueous species in RBF and ASR water

Aqueous Component	Flint River (mol/L)	RBF Filtrate maximum values (mol/L)	ASR extracted water maximum values (mol/L)
DOC	0.00035	7.54E-05	6.25E-05
Temperature	9.8 to 30.6	19.1	14.2
Dissolved Oxygen	4.4E-4 to 6.9E-4	2.67E-05	5.66E-06
Ca(+2)	5.24E-04	5.33E-04	5.28E-04
Mg(+2)	5.76E-05	5.80E-05	8.68E-05
Na(+)	2.94E-04	2.94E-04	6.66E-04
K(+)	4.60E-05	4.60E-05	5.40E-05
Fe(+3)	1.38E-06	9.91E-07	9.94E-07
Fe(+2)	-	9.99E-07	1.63E-06
Mn(+3)	7.81E-07	-	
Mn(+2)	-	9.99E-07	9.87E-07
Si	1.09E-04	1.09E-04	1.82E-04
Cl(-)	7.48E-04	7.47E-04	8.97E-04
C(+4)	5.98E-04	9.65E-04	9.66E-04
C(-4)	-	6.24E-08	2.48E-04
S(+6)	9.68E-05	9.62E-05	9.61E-05
S(-2)	-	2.30E-05	1.07E-04
N(+5)	2.71E-05	3.00E-05	2.94E-05
N(0)	-	2.73E-05	2.94E-05
Ammonium(+)	1.61E-06	2.00E-06	1.98E-06
pH	7.3	6.6	7.38

Units: mol/L except Temperature (°C) and pH is dimensionless.

#### 4.4.2 The ASR subsystem

The RBF filtrate is of adequate quality to be allowed for injecting into the deeper aquifer. The injection periods into the ASR aquifer are 0-230 days and 410-590 days; and the extraction periods are 230-410 days and 590-770 days. The time series plot of the concentrations of various species in the ASR well is shown in Fig 27.

Anoxic conditions are fully developed in the aquifer; some DO seen at the start of the simulations is during the startup simulations. A closer look at the plot shows that complete denitrification occurs at around 230, 410 and 590 days at the ASR well, corresponding to times when the aquifer becomes strongly reducing with low  $pe$

values. Further degradation of organic carbon is caused by partial iron reduction at 230 and 590 days, whereas full iron reduction takes place around 410 days and after 750 days. The S(6) and S(-2) plots also show that reduction of  $\text{SO}_4^{2-}$  occurs at around 400 days, and 750 days when the  $pe$  is inverted to reducing conditions. All the sulfate is consumed briefly at the end of the extraction periods and extreme reducing conditions exist at those short intervals, with production of  $2.48 \times 10^{-4}$  mol/L of C(-4) for a short time. This situation is immediately corrected when RBF water is injected into the ASR well.

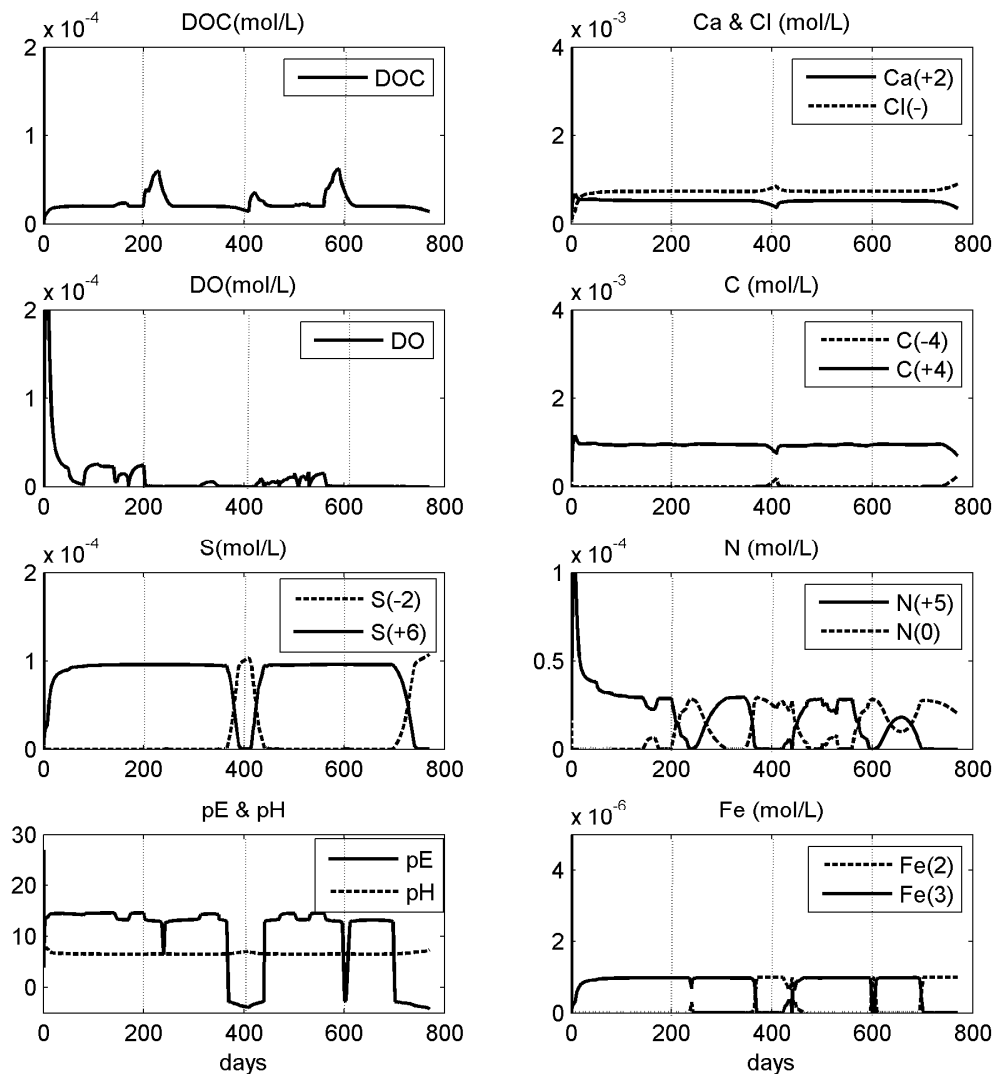


Fig. 27: Concentration time series data at the ASR well. The pump is injecting RBF water into the deeper aquifer in the periods 0- 230 days and 410-590 days, and extracting at other times.

One important aspect in limestone aquifers is that calcite dissolution can be triggered by repeated flow reversals and by lowered  $pH$ . Degradation of organic carbon is associated with an increase in acidity, which should, to some extent, promote carbonate dissolution. It was observed in the ASR model simulation (results not shown here) that the calcium concentration was slightly raised near the wells and the zone of this elevated concentration would expand outwards as the water was pumped in and decrease when it was extracted. This shows that there is some flux of calcium ions in the near vicinity of the wells and it could help increase porosity. It is understood that this mechanism can help offset the well clogging phenomenon that can occur due to precipitates near the well or deposition of other organic complexes. A more detailed qualitative analysis was not done here but there is considerable literature available on it (Mirecki et al, 1998; Greskowiak, 2005; Rinck-Pfieffer et al., 2000; Pyne, 2005).

#### **4.4.3 Pyrite Oxidation and Arsenic mobility**

Results from the set of runs modeling pyrite oxidation with kinetics are presented in Fig 28. The simulations assuming the absence of DOC did not yield any significant presence of Arsenic in the extracted water.

The figure shows that the aquifer remains anoxic, because the RBF water that is injected has already reduced levels of oxygen, due to oxidation of DOC in the RBF set up. So any remaining oxygen is rapidly used up in pyrite oxidation. The model shows that the rapid consumption of  $NO_3^-$  and  $SO_4^{2-}$  during the model run up period also occurs and it subsequently attains equilibrium at very low concentrations during the normal operation of the ASR system. It is seen that the pH averages around the near neutral range. The concentrations of As(3) and  $SO_4^{2-}$  start rising once the injection stops (230 days) and stop when it starts again (410 days). The peak concentration of As(3) and As(5) observed in the ASR well are  $5.27E-11$  mol/L and  $9.12E-11$  mol/L respectively, which are well below the EPA permissible limits in potable water. During pyrite dissolution, ferrous iron released from the pyrite is oxidized to hydrous ferric oxides and this precipitates out. Sorption of arsenic onto these neoformed oxides are known to occur and these further attenuate the arsenic concentration in water. If these conditions are prevalent, then any appreciable mobilization of As will probably not take place. Mobilization could be higher if more

electron acceptors are available. This would occur if more oxic waters were to be injected into the aquifer with pyrites.

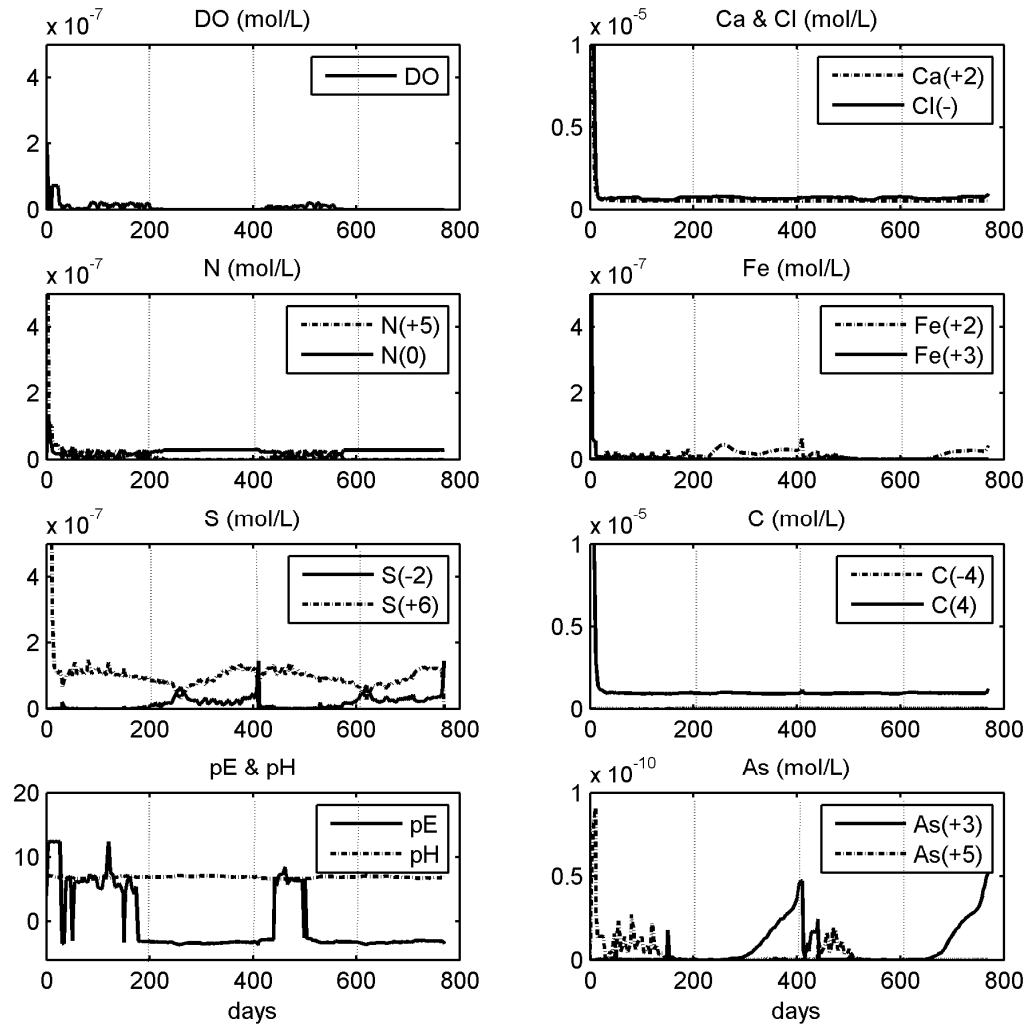


Fig. 28: Concentration time series plot at the ASR well for the second case when pyrite oxidation is considered. The pump is injecting RBF water into the deeper aquifer in the periods 0 - 230 days and 410-590 days, and extracting at other times.

#### 4.5 Conclusions and Future Research Recommendations

The study shows that a coupled RBF and ASR scheme is possible and would help alleviate the water scarcity problems in the drier seasons if there is an excess of water in the wetter seasons and suitable geo-hydrologic conditions exist. It was determined this would be a viable option to store and pump water. It was observed through

numerical modeling that the degradation of DOC reduces all of the Fe(+3) and nitrates, and some  $\text{SO}_4^{2-}$ . In our simplified case, there appeared no significant mobilization of arsenic and the ASR water was found to be of acceptable quality. Hydraulic aspects such as possible storage volume, recovery efficiency and rates of injection, permissible aquifer head build-ups and fluctuations of it also need to be carefully looked at.

Transport and fate of arsenic is an immediate concern for the field of RBF and ASR schemes. A better elucidation backed by benchmark studies is essential to restore confidence in these schemes. Mobilization of arsenic and other heavy trace elements in different scenarios could be modeled more accurately if it is backed by accurate in-situ geochemical data.

The modeling did not look at the aspects of transport and fate of microorganisms and other chemicals of concern such as disinfection by-products (DBPs) and pharmaceuticals and personal care products which are pressing issues that need to be looked at in the immediate future. The extent of dissolution and potential clogging of the wells also need to be carefully examined to estimate the ease of injection and efficiency of aquifer recovery.

An approach that could be useful for RBF ASR coupling, so that no metals are mobilized from the ASR aquifer, is to ensure that the RBF filtrate that is pumped into the ASR is as close to the ASR aquifer properties as possible. This would minimize the disturbance on the aquifer chemistry balance such that no disequilibrium occurs and setting off redox reactions. Recovered water from this type of bank-filtration ASR system, must comply with EPA standards before being distributed for drinking water purposes. It is expected that the water treatment costs would not only be minimized, but it would also provide water during drought seasons.

## **CHAPTER 5. CONCLUSION AND RECOMMENDATIONS**

Riverbank filtration is an accepted method of treatment for water from rivers (or lakes) which markedly improves the source water quality (Ray et al., 2002a). Riverbank filtration is a mechanism in which wells placed alongside rivers (or lakes) or driven below them are pumped to induce surface water to flow through the aquifer to the wells. As water is forced to travel through the aquifer, natural processes attenuate the contaminants and pathogens in the source water. This study used field data from an operating RBF scheme located along the Rhine River in Dusseldorf, Germany, and carried out focused research on the fate of dissolved organic carbon and on the transport of microbial pathogens. To complement this modeling study, a novel application of RBF and ASR was considered to address seasonal water scarcity in the Albany region of the Georgia in US.

A process-based reactive transport model was developed to analyze the dynamically changing hydro-geochemical processes of the fully functioning RBF site. Transient boundary conditions and flow fields within the aquifer were used to capture the dynamic behavior of RBF and model the degradation of the dissolved organic carbon as well as the transport of bacterial pathogens. The reactive transport model was established on the base of a conservative solute transport model for which temperature and chloride data served as calibration constraints. The major findings of the study are given below.

1. The results of our redox modelling show that aerobic respiration is the predominant process in the RBF subsurface. Anaerobic conditions with partial denitrification occurs within the system only for a short period leading to considerable variability in dissolved oxygen and nitrate concentrations at the monitoring and the production wells. Our results demonstrate that seasonal temperature changes in combination with rapid changes in residence time strongly affected the extent of biodegradation and thus electron acceptor consumption along the flow path.

2. Higher rates of biodegradation, and thus more reducing conditions, were evident at higher temperatures during summer, while low temperatures decreased the microbial activity and led to breakthroughs of dissolved oxygen at the monitoring and production wells. The observed strong seasonal changes in breakthrough of dissolved oxygen concentrations was better predicted when biodegradation rate constants were made dependent on temperature, compared to simulations where the effect of temperature variation was neglected.
3. Flood events in the Rhine River and ensuing higher hydraulic gradients between the river and the pumping wells drastically reduced travel times (~7 days) to the RBF well, compared to average travel times of 25-40 days. On the other hand, low-flow conditions increased the residence time of the infiltrating water to more than 60 days to emerge in the RBF well. The longer travel time in the latter case was responsible for the temporary shift to denitrifying conditions that developed during this period. In general, short term variations in the extent of electron acceptor consumption rates resulted from rapid changes in residence time rather than gradual changes in temperature.
4. The present study elucidates biodegradation of DOC and the development of redox zones along the flow paths of the infiltrating water. An understanding of the temporally changing extents of oxic and anoxic zones in RBF systems, as well as the residence time in these zones is crucial for assessing the breakthrough behavior of redox sensitive trace organic compounds.
5. Rivers and lakes, source waters for RBF systems, can contain high amounts of pathogenic concentrations so the fate and transport of pathogens in an RBF system is of common interest. Microbial transport is modeled in groundwater using the advection-dispersion equation adding on the mass-transfer processes of attachment, detachment and inactivation often approximated with linear kinetic reaction expressions. The rates defined by these processes were found to be velocity dependent, so a rate expression with constant values cannot be used in a

transient simulation of an RBF model where the velocity fields are constantly changing.

6. The concepts of the classical colloid filtration theory and the advection dispersion transport equations were combined together to develop a procedure to incorporate transient conditions into a model for multicomponent reactive transport using MODFLOW and PHT3D. The approach is verified on a benchmark 1-D problem. The results of verification were found acceptable. The ability to use a single set of parameters to describe the breakthrough or transport at different velocities present a unique opportunity. The benchmark 1-D column modeling by our approach showed that we can use the same set of parameters to explain the breakthrough concentrations within a reasonable degree, whether the flow velocity of water was 0.46 m/d or doubled to 0.92 m/d. This has definite advantages for carrying out modeling of transient conditions, such as in the RBF systems, where the velocities are constantly changing, and otherwise it would have been almost impossible.
7. This new model is extended to simulate transport of *E. coli* and Coliforms in a large full scale operating RBF scheme. The model successfully demonstrated both the occurrence as well as the non-occurrence of the breakthrough of *E. coli* and coliforms. The model was able to replicate the breakthrough that occurred during high floods, a moment when the microbial reduction capability of the RBF could be compromised. It also simulated correctly the non-occurrence of breakthrough of the pathogens. The model was successful in depicting the fate and transport of *E. coli* and coliforms in the aquifer.

To complement the study mentioned above a novel application of RBF was considered coupling it with aquifer storage and recovery to address seasonal water scarcity. In areas where there are seasonal changes in water availability, seasonal excesses can be stored underground to meet short-term demands. The Flint River in the Albany region of Georgia, US, was studied as cities located in that area face limitations of growth because of restrictions to additional withdrawal from surface or ground water sources. Using RBF as source water, rather than obtaining water directly from the surface water, would reduce

potentially treatment costs. The RBF site taps the Flint River through the Upper Floridan Aquifer producing water that can be injected into the deeper Clayton Aquifer for storage and subsequent recovery. This study tested the conceptual framework using literature values of having such a coupled system of RBF and ASR schemes and, more importantly, looked at the hydrogeochemical changes that are likely to occur.

1. The study showed that a coupled RBF and ASR scheme is possible and would help alleviate the water scarcity problems in the drier seasons if there is an excess of water in the wetter seasons and suitable geo-hydrologic conditions exist. It was determined this would be a viable option to store and pump water.
2. It was observed through numerical modeling that the degradation of DOC reduces all of the Fe(+3) and nitrate, and some sulfate. In our simplified case, there appeared no significant mobilization of arsenic and the ASR water was found to be of acceptable quality. It is expected it would provide water of adequate quality during seasons when water is in short supply.

## **Recommendations**

1. An approximation in the above-mentioned studies is the hydraulic modeling of the RBF and later the ASR system with MODFLOW using 2-D approximations. It can be argued that a full-scale 3-D model should have been used to model wells. These arguments are correct, yet a 3-D simulation would have required much more computational efforts, including further approximations in boundary conditions and assumptions in various processes. Improvements may be made to the numerical results by adopting a 3-D model.
2. The studies in RBF modeling above use MODFLOW and PHT3D for numerical modeling and therefore are restricted to saturated sub-surface flow. Due to the dynamic nature of river flows, some of the riverbanks will be intermittently wetted or saturated. Powelson et al. (2001) show the importance of air-water-interface in *E. coli* transport. Even the redox conditions on the capillary zones in shallow water tables may be different due to repeated lowering and rising of these

zones associated with possible exchange of gases with the atmosphere. An important improvement would be to incorporate unsaturated zone modeling to simulate better the processes happening in nature.

3. An important improvement would be to incorporate the transient conditions in the hydraulic conductivity in clogging layers in river and around well points. The response of the riverbed should be able to reflect the flow hydrodynamics, erosion of the clogging layer and or a low flow causing deposition. A full-fledged surface water hydrodynamic model may not be immediately coupled, but the model can be improved to include variations in hydraulic conductivity and porosity over time.
4. In the modeling of microbial transport, the estimation of attachment coefficient is a crucial element, which is related to heterogeneity coefficient ( $\lambda$ ). Most pathogenic microorganisms have a low net negative surface charge over a wide range of pH values; therefore, charge-based attachment to negatively charged soil, sediment, or rock surfaces is likely to be hindered and different from that on positively charged soils. This aspect needs to be addressed in the model.
5. The processes of detachment, straining, biological and physiological processes including microbial motility, mobility, predation, are components that have been simplified or excluded in the model. These could be gradually improved in the future. Neither the pathogen transport model used in the study nor the models discussed in the current literature, couple the aqueous chemistry of the groundwater with the microbes present therein. The temperature, pH, salinity, etc. are already noted to affect the microbe fate and transport, and these factors could be added on to the reactive transport model.

#### RBF ASR coupling study

1. The modeling was done using literature surveys and desk studies. Real field values, in-situ hydro-geological investigations, aquifer parameters etc. need to be done accurately to determine hydraulic aspects such as possible storage volume,

recovery efficiency and rates of injection and permissible aquifer head build-ups. The effect of the dynamic of repeated pressure reversals in the subsurface in particular also needs to be carefully addressed.

2. The extent of dissolution of calcite and potential clogging of the wells also need to be carefully examined backed by *in-situ* experiments.
3. Transport and fate of arsenic is an immediate concern for the field of RBF and ASR schemes. A better elucidation backed by benchmark studies is essential to restore confidence in these schemes. Mobilization of arsenic and other heavy metals in different scenarios could be modeled more accurately if it is backed by accurate in-situ geochemical data.
4. An approach that could be useful for RBF ASR coupling, so that no metals are mobilized from the ASR aquifer, is to ensure that the RBF filtrate that is pumped into the ASR is as close to the ASR aquifer properties as possible. This would minimize the disturbance on the aquifer chemistry balance such that no disequilibrium occurs and setting off redox reactions. Recovered water from this type of bank-filtration ASR system, must comply with EPA standards before being distributed for drinking water purposes. It is expected that the water treatment costs would not only be minimized, but it would also provide water during drought seasons.

## **APPENDIX A: PHT3D database modifications for modeling DOC transport**

The following is the part of the PHT3D database file that was written to include the redox modeling of dissolved organic carbon (Part 1). Dissolved organic carbon was written as “Orgc” and the sedimentary carbon as “Orgc\_sed\_1”.

The additional species are added into the list of solution master species in the database and the reaction rate is defined in the “rate” block subsequently. The interface file pht3d\_ph.dat is given in Part 2, where the parameter values are defined to be used in the reaction rate calculations.

Part 1: PHT3D Database modification for modeling the fate of DOC

Part 2: PHT3D\_PH.DAT the PHREEQC-2 interface package file used in PHT3D

## Part 1: PHT3D Database modification for modeling the fate of DOC

The following is the part of the regular database file of the PHT3D that was amended to include the redox modeling of dissolved organic carbon.

```
#####
# Description: PHREEQC-2 Database modified for Rhine RBF modeling
# (Laxman Sharma, 2012, JOH)
# modified organic carbon rate expression and renamed to "Orgc"
# Orgc_sed_l species added for recalcitrant dissolved organic carbon
#####
SOLUTION_MASTER_SPECIES
...
Orgc      Orgc      0.0  Orgc      30
Tracer    Tracer    0.0  Tracer    1
Tmp       Tmp       0.0  Tmp       1
Orgc_sed_l Orgc_sed_l 0.0  Orgc_sed_l 1

SOLUTION_SPECIES
...
RATES
...
#####
Orgc # (extended - see, e.g., Sharma et al. 2012, ES&T)
#####
-start
# 1      = parm(1) (not used)
  2  k1_ox = parm(2) # 1.57e-09
  3  k1_nit = parm(3) # 8.00e-10
  4  k1_sul = parm(4) # 5e-11
  5  k1_fe  = parm(5) # 5e-11
  6  k1_mn  = parm(6) # 2.00e-10
  7  resid  = parm(7) # 2e-05 residual (undegradable) fraction of DOC
 10  mOrgc = mol("Orgc")
 12  if (mOrgC < resid) then goto 15
 13  m_deg_OrgC = mOrgC - resid
 15  if (m_deg_OrgC <= 1e-10) then goto 200
 16  mTmp = 1000 * tot("Tmp")
 18  f_t  = EXP(-1.5 + 0.18 * mTmp * (1 - 0.5 * mTmp/35))
 19  put(f_t,7)
 20  mO2  = mol("O2")
 25  mNO3 = tot("N(5)")
# 30  mSO4 = tot("S(6)")
# 35  mFe1 = EQUI("Fe(OH)3(a)")
```

```

# 36 mFe2 = EQUI("Goethite")
# 37 mFe = mFe1 + mFe2
# 40 mMn1 = EQUI("Manganite")
# 41 mMn2 = EQUI("Pyrolusite")
# 42 mMn = mMn1 + mMn2
50 rate = f_t * k1_ox * mO2/(2.94e-4 + mO2)
52 k_inh_ox= 1e-5
55 rate = rate + f_t * k1_nit * mNO3/(1.55e-4 + mNO3)(k_inh_ox/(m_O2 +
    k_inh_ox))
# 60 rate = rate + k1_sul * mSO4/(1.e-4 + mSO4)
# 65 rate = rate + k1_fe * mFe/(1.e-4 + mFe)
# 70 rate = rate + k1_mn*mMn/(1.e-4 + mMn)
74 rate = rate * m_deg_OrgC / (1e-05 + m_deg_OrgC)
75 moles = rate * time
200 save moles
-end

#####
# Orgc_sed_l
#####
Orgc_sed_l
-start
3 temp_fac=get(7)
5 parm1= parm(1)*temp_fac
7 parm2= parm(2)*temp_fac
10 parm3= parm(3)*temp_fac
20 m_O2 = mol("O2")
30 m_NO3 = tot ("N(5)")
40 m_MnO2 = equi ("Pyrolusite")
45 m_orgc = tot("Orgc_sed_l")
47 if (m_orgc < 1e-9) then goto 200
50 r_ox=parm1/86400
51 k_ox=1e-5
52 k_inh_ox=1e-5
53 r_nitr=parm2/86400
54 k_nitr=1e-5
55 r_mn=parm3/86400
80 rate = r_ox*(m_O2/(m_O2 + k_ox))+
    r_nitr*(m_NO3/(m_NO3+k_nitr))*(k_inh_ox/(m_O2 + k_inh_ox)) #+ r_mn
90 moles = m_orgc/(m_orgc+1e-5)*rate*time
91 put(r_ox,1)
92 put(r_nitr,2)
93 put(r_mn,3)
94 put(k_ox,4)

```

```
95   put(k_nitr,5)
96   put(k_inh_ox,6)
100  if (moles > m) then moles = m
200  SAVE moles
-end
```

```
....
```

```
....
```

```
END
```

**Part 2: PHT3D Database modification for modeling the fate of DOC**

2 1 0 15 0 1e-10 0.001 4000

0

21

0

0 0 0 0 0 0 0 0 0 0

0

1 0 0 1

0 0

Orgc 7

0

1.3e-09

8e-10

2.4e-13

1e-13

1e-13

8.9e-05

-formula Orgc -1.0 CH2O 1.0

Tmp

O(0)

Ca

Mg

Na

K

Fe(2)

Fe(3)

Mn(2)

Mn(3)

Cl

C(4)

C(-4)

S(6)

S(-2)

N(5)

N(3)

N(0)

Amm

pH

pe

Orgc\_sed\_I 3

1.9e-11

1.2e-11

1e-13

-formula Orgc\_sed\_I -1 CH2O 1

## **APPENDIX B: PHT3D database modifications for modeling microbial transport**

- Part 1: Modeling MS2 with ADV equation and rate parameters directly (for validating Model with Hijnen 2005 data)
- Part 2: Modeling MS2 with filtration theory concept model (validation with Hijnen 2005 data) - This gives us a single set of parameters to model columns with different flow velocities.
- Part 3: Modeling E-coli and coliforms transport in a RBF in a full transient dynamic system
- Part 4: PHT3D\_PH.DAT the PHREEQC-2 interface package file used in PHT3D

**Part 1 : Modeling MS2 with ADV equation and rate paramters directly (for validating Model with Hijnen 2005 data)**

This database modification is done to model MS2 phage transport, Hijnen (2005) column experiment, using the advection dispersion transport equation, Eq. 6 (Chapter 3). Two species of MS2 is defined a mobile form and an immobile form.

**SOLUTION\_MASTER\_SPECIES**

```
#
#element      species      alk  gfw_formula  element_gfw
...
Mstwo_m      Mstwo_m      0.0  Mstwo_m      1
...
Mstwo_im     Mstwo_im     0.0  Mstwo_im     1
....
```

**SOLUTION\_SPECIES**

...

**RATES**

...

#####

Mstwo\_m

#####

-start

1 PR = parm(1)

2 DR = parm(2)

3 DC = parm(3)

4 DH = parm(4)

#-----

# TIME UNIT in MT3D = DAYS - TRANSLATE INTO SECONDS

#-----

5 qx = parm(5) /86400

6 qy = parm(6) /86400

7 qz = parm(7) /86400

8 k\_att = parm(8) / 3600 # parm data per 1/hour converted to 1/sec

9 k\_inact = parm(9)/3600 # parm data per 1/hour converted to 1/sec

#-----

# find rates

#-----

10 mMstwo\_m = TOT("Mstwo\_m") #units PFP/L

15 att\_rate = k\_att\* TOT("Mstwo\_m") #units 1/s\*PFP/L

20 inact\_rate = k\_inact\*TOT("Mstwo\_m") #units 1/s\*PFP/L

```

#save attachment rate for immobile Mstwo
25 put(att_rate,20)          #PFP/(L.s)
# retrieve detachment rate from rate expression of immobile Mstwo
26 det_rate = get(21)       #PFP/(L.s)

# negative sign is introduced to induce removal of mobile Mstwo
# atachment and inactivation decrease conc
# detachment increases concentrations of mobile Mstwo
30 rate = - att_rate - inact_rate + det_rate
40 moles = rate * TIME      #PFP/(L.s) * s
100 if (moles > m) then moles = m
200 SAVE moles              #PFP/L
-end

#####
# Mstwo attached
#####
Mstwo_im
-start
1 PR = parm(1)
2 k_det = parm(2)/3600      #parm data per 1/hour converted to 1/sec
3 k2_inact = parm(3)/3600  #parm data per 1/hour converted to 1/sec

5 mMstwo_im = TOT("Mstwo_im") #units PFP per gram
7 bulkdensity = 2600        # kg per cum, 1000g/1000L = g/L

10 att_rate = get(20)       #PFP/(L.s)
12 att2_rate = att_rate * PR/bulkdensity # units 1/s*PFP/L * L/g = PFP/(g.s)
13 det2_rate = k_det * TOT("Mstwo_im") # units 1/s*PFP/g = PFP/(g.s)
14 inact2_rate = k2_inact * TOT("Mstwo_im") # units 1/s*PFP/g = PFP/(g.s)

# save detachment rate for mobile phase change units
15 det_rate = det2_rate * bulkdensity/PR # units 1/s*PFP/g * g/L =PFP/(L.s)
16 put (det_rate, 21)      # PFP/(L.s)

# positive att2_rate causes immobile Mstwo to increase
# while positive inactivation rate decreases concentrations
20 rate = att2_rate - det2_rate - inact2_rate #units = PFP/(g.s)
95 moles = rate * TIME
100 if (moles > m) then moles = m
    200 VE moles
-end

```

**Part 2: Modeling MS2 with filtration theory concept model (validation with Hijnen 2005 data)** - This gives us a single set of parameters to model columns with different flow velocities.

**SOLUTION\_MASTER\_SPECIES**

```
#
#element    species      alk  gfw_formula  element_gfw
...
Mstwo_m    Mstwo_m      0.0  Mstwo_m      1
...
Mstwo_im    Mstwo_im      0.0  Mstwo_im      1
....
```

**SOLUTION\_SPECIES**

...  
**RATES**

```
...
#####
Mstwo_m
#####
-start
 1 PR = parm(1)
 2 DR = parm(2)
 3 DC = parm(3)
 4 DH = parm(4)
#-----
# TIME UNIT in MT3D = DAYS - TRANSLATE INTO SECONDS
#-----
 5 qx = parm(5) /86400
 6 qy = parm(6) /86400
 7 qz = parm(7) /86400
 8 lambda = parm(8)
 9 k_dec = parm(9)/3600 #inactivation rate inaqueous phase
#-----
# Get fluxes, cell dimensions and porosity from mt3d
#-----
11 vx = qx / (DH * DC) / PR
12 vy = qy / (DH * DR) / PR
13 vz = qz / (DC * DR) / PR
14 print "qx,qy,qz, DH,DR,DC,PR = ",qx,qy,qz, DH,DR,DC,PR
15 print "vx,vy,vz ",vx,vy,vz
17 v_abs = sqrt(vx*v_x+vy*v_y+vz*v_z)
18 print "v_abs [m/d] = ", v_abs * 86400
#-----
```

```

19 p = (1-PR)^(1/3)
20 As = 2*(1-p^5)/(2- 3*p + 3*p^2 - 2*p^6)
21 Ap = 2.1*1e-08 # Hijnen's paper
22 Ac = 180*1e-06 #(median of grain size distribution, 0.18 mm)
24 NR = Ap/Ac
25 mTmp = mol("Tmp")*1000
26 T = 273.15+mTmp # T = absolute temp in Kelvin
27 omega = 9.85*10^15 * T^(-7.7) # omega= dynamic viscosity
28 k = 1.3806E-23 # Boltzmann'd Constant JK^(-1)
29 Db = k*T/(3*(22/7)*omega*Ap) # Db = Coeficient of Brownian Motion
30 NPe = v_abs*Ac/Db # Peclet nr
31 print "T, omega, Db, NPe =", T, omega, Db, Npe

#-----
# Calculating van der Waal's number
#-----
39 H = 6.20E-21
40 NvdW = H/(k*T) # H = Hamaker Constant = 6.5*10^(-21) changed specific to
site
42 sp_area = 6*(1-PR)/(PR*Ac) # specific surface area unit per m
# Calculating Attraction number
50 NA = H/(12*(22/7)*omega*(Ap*Ap)*v_abs*PR) # omega= dynamic viscosity
51 print "As, NR, NPe, NvdW =", As, NR, NPe, NvdW

# Calculating the Gravity number
# grav =accln due to gravity m/s^2
52 grav = 9.81
53 paden = 1085 # kg/m3 particle density
54 fluden = 999.7 # kg/m3 fluid density
55 NG = 2*grav*((Ap)^2)*(paden-fluden)/(9*omega*v_abs*PR)
56 print " sp_area, NA, NG =", sp_area, NA, NG

#Calculating Efficiency Factor
60 n01 = 2.4 *As^(1/3)*NR^(-0.081)*NPe^(-0.715)*NvdW^(0.052)
61 n02 = 0.55*As*NR^(1.675)*NA^(0.125)
62 n03 = 0.22*NR^(-0.24)*NG^(1.11)*NvdW^(0.053)
63 n0 = n01 + n02 + n03
64 print "n0, n01, n02, n03 =", n0, n01, n02, n03

#Overall sticking efficiency
65 alpha_f = 1.0 # sticking eff at favorable sites = 1
66 alpha_u = 0.0007 # sticking eff at unfavorable sites
68 alpha_tot = lambda*alpha_f+(1-lambda)*alpha_u

```

```

# straining efficiency
71 nstr = 2.7*(Ap/Ac)^(3/2) #ok
72 alpha_str = 0.01 #straining correction factor #ok
73 print "alpha_tot, nstr =", alpha_tot, nstr

80 k_str = (sp_area*v_abs*PR/4)*(nstr*alpha_str)
82 k_stick = (sp_area*v_abs*PR/4)*(n0*alpha_tot)
83 mMstwo_m = TOT("Mstwo_m")
84 print "mMstwo_m, k_dec =", TOT("Mstwo_m"), k_dec

# straining rate (= irreversible)
85 str_rate = k_str * TOT("Mstwo_m")

# stick rate (= attachment to sediments)
86 stick_rate = k_stick * TOT("Mstwo_m")

# decay rate in aqueous phase: default k_dec = ~ 0.2 per day
90 dec_rate = k_dec * TOT("Mstwo_m")

# save sticking (attachment) rate for use
# in rate expression of immobile Mstwo
91 put(stick_rate,20)

# retrieve detachment rate from rate
# expression of immobile Mstwo
92 det_rate = get(21)

# negative sign is introduced to induce removal of mobile Mstwo
# straining and decay decrease conc, detachment increases
# concentrations of mobile Mstwo
93 rate = - stick_rate - dec_rate - str_rate + det_rate
94 print "rate Ms2: - stick_rate - dec_rate - str_rate + det_rate", stick_rate, dec_rate,
str_rate, det_rate
95 moles = rate * TIME
96 print "moles = rate * time =", moles, rate, time
#100 if (moles > m) then moles = m
# This is to make sure that the mole removal is not more than that present (not valid
here)
200 SAVE moles
-end

#####
# Mstwo attached
#####

```

```

Mstwo_im
-start
  1 mMstwo_im = TOT("Mstwo_im")
  2 print "mMstwo_im = ", TOT("Mstwo_im")

# 2 if (mMstwo_im <= 1e-14) then goto 200
  7 k_det = parm(2)/3600 #rate per hour input convert to seconds for Pht3d
  8 k_dec = parm(3)/3600 #inact. rate per hour input convert to seconds for Pht3d
  20 det_rate = k_det * TOT("Mstwo_im")
  25 dec_rate = k_dec * TOT("Mstwo_im")

# save detachment rate so it can be used in the
# rate expression for the mobile Mstwo
  28 put(det_rate,21)

# retrieve straining_rate from rate
# expression for mobile Mstwo
  30 stick_rate = get(20)

# positive stick_rate causes immobile Mstwo to increase
# while positive decay rate decreases concentrations
  40 rate = stick_rate - dec_rate - det_rate
  45 print "Mstwo (attached): stick_rate - dec_rate - det_rate" , stick_rate, dec_rate,
det_rate
  95 moles = rate * TIME
  96 print "moles = rate * time = ", moles, rate, time

#100 if (moles > m) then moles = m
200 SAVE moles
-end

```

### Part 3: Modeling E-coli and coliforms transport in a RBF in a full transient dynamic system

```
#####  
# Description: PHREEQC-2 Database modified for microbial modeling  
# Laxman Sharma  
# added Coliforms and Ecoli in mobile and immobile forms for RBF modeling  
#####
```

#### SOLUTION\_MASTER\_SPECIES

```
#  
#element species      alk                gfw_formula        element_gfw  
...  
Coliforms_m          Coliforms_m        0.0  Coliforms_m        1  
Ecoli_m              Ecoli_m            0.0  Ecoli_m            1  
Coliforms_im         Coliforms_im       0.0  Coliforms_im       1  
Ecoli_im             Ecoli_im           0.0  Ecoli_im           1
```

#### SOLUTION\_SPECIES

...

#### RATES

...

```
#####
```

Ecoli\_m

```
#####
```

-start

1 PR = parm(1)

2 DR = parm(2)

3 DC = parm(3)

4 DH = parm(4)

```
#-----
```

# TIME UNIT in MT3D = DAYS - TRANSLATE INTO SECONDS

```
#-----
```

5 qx = parm(5) /86400

6 qy = parm(6) /86400

7 qz = parm(7) /86400

8 lambda = parm(8)

9 k\_dec = parm(9)/86400

```

#-----
# Get fluxes, cell dimensions and porosity from mt3d
#-----
11 vx = qx / (DH * DC) / PR
12 vy = qy / (DH * DR) / PR
13 vz = qz / (DC * DR) / PR
14 v_abs = sqrt(vx*vx+vy*vy+vz*vz)
#15 print "qx,qy,qz, DH,DR,DC,PR = ",qx,qy,qz, DH,DR,DC,PR
#16 print "vx,vy,vz ",vx,vy,vz
#18 print "v_abs [m/d] = ", v_abs * 86400
#-----
19 p = (1-PR)^(1/3)
20 As = 2*(1-p^5)/(2- 3*p + 3*p^2 - 2*p^6)
21 Ap = 1.2*1e-06 # 0.5 micron (dia of bacteria 0.5 X 2 L)
22 Ac = 397*1e-06 #(median of grain size distribution)
24 NR = Ap/Ac
25 mTmp = mol("Tmp")*1000
26 T = 273.15+mTmp # T = absolute temp in Kelvin
27 omega = 9.85*10^15 * T^(-7.7) # omega= dynamic viscosity
28 k = 1.2806*10^(-23) # Boltzmann'd Constant JK^(-1)
29 Db = k*T/(3*(22/7)*omega*Ap) # Db = Coeficient of Brownian Motion
30 NPe = v_abs*Ac/Db # Peclet nr
#31 print "T, omega, Db, NPe =", T, omega, Db, NPe
#-----
# Calculating van der Waal's number
#-----
39 H = 6.5*10^(-21)
40 NvdW = H/(k*T) # H = Hamaker Constant = 6.5*10^(-21)
# k = 1.2806*10^(-23) Boltzmann'd Constant JK^(-1)
42 sp_area = 6*(1-PR)/(PR*Ac) # specific surface area unit per m
# Calculating Attraction number
50 NA = H/(12*(22/7)*omega*((Ap)^2)*v_abs*PR) # omega= dynamic viscosity
#51 print "As, NR, NPe, NvdW =", As, NR, NPe, NvdW

# Calculating the Gravity number
# grav =accln due to gravity m/s^2
52 grav = 9.81
53 paden = 1050 # kg/m3 particle density
54 fluden = 1000 # kg/m3 fluid density
55 NG = 2*grav*((Ap)^2)*(paden-fluden)/(9*omega*v_abs*PR)
#56 print " sp_area, NA, NG =", sp_area, NA, NG

```

```

#Calculating Efficiency Factor
60 n01 = 2.4 *As^(1/3)*NR^(-0.081)*NPe^(-0.715)*NvdW^(0.052)
61 n02 = 0.55*As*NR^(1.675)*NA^(0.125)
62 n03 = 0.22*NR^(-0.24)*NG^(1.11)*NvdW^(0.053)
63 n0 = n01 + n02 + n03
#64 print "n0, n01, n02, n03 =" , n0, n01, n02, n03

#Overall sticking efficiency
65 alpha_f = 1.0 # sticking eff at favorable sites = 1
66 alpha_u = 0.005 # sticking eff at unfavorable sites
68 alpha_tot = lambda*alpha_f+(1-lambda)*alpha_u

# straining efficiency
71 nstr = 2.7*(Ap/Ac)^(3/2) #ok
72 alpha_str = 0.01 #straining correction factor #ok
#73 print "alpha_tot, nstr =", alpha_tot, nstr
80 k_str = (sp_area*v_abs*PR/4)*(nstr*alpha_str)
82 k_stick = (sp_area*v_abs*PR/4)*(n0*alpha_tot)
# 83 print "Ecoli_m, k_dec = ", TOT("Ecoli_m"), k_dec

# straining rate (= irreversible)
84 str_rate = k_str * TOT("Ecoli_m")
# stick rate (= attachment to sediments)
85 stick_rate = k_stick * TOT("Ecoli_m")
# decay rate in aqueous phase: default k_dec = ~ 0.2 per day
90 dec_rate = k_dec * TOT("Ecoli_m")

# save sticking (attachment) rate for use
# in rate expression of immobile Ecoli
91 put(stick_rate,10)
# retrieve detachment rate from rate
# expression of immobile Ecoli
92 det_rate = get(11)
# negative sign is introduced to induce removal of mobile Coliforms
# straining and decay decrease conc, detachment increases
# concentrations of mobile Ecoli
93 rate = - stick_rate - dec_rate - str_rate + det_rate
#94 print "rate Ecoli_m: - stick_rate - dec_rate - str_rate + det_rate" , stick_rate,
dec_rate, str_rate, det_rate
95 moles = rate * TIME
#96 print "moles = rate * time = ", moles, rate, time
100 if (moles > m) then moles = m
200 SAVE moles

```

```

-end
#####
# Ecoli attached
#####
Ecoli_im
-start
  1 mEcoli_im = TOT("Ecoli_im")
  # 2 print "mEcoli_im = ", mEcoli_im
  # 2 if (mEcoli_im <= 0.0) then goto 200
  7 k_det = parm(1)/86400 #rate per day converted to per sec
  8 k_dec = parm(2)/86400 #rate per day converted to per sec
  20 det_rate = mEcoli_im * k_det
  25 dec_rate = mEcoli_im * k_dec
  28 put(det_rate,11)
  30 stick_rate = get(10)
# positive stick_rate causes immobile Ecoli to increase
# while positive decay rate decreases concentrations
  40 rate = stick_rate - dec_rate - det_rate
  #45 print "Ecoli_m (attached): stick_rate - dec_rate - det_rate" , stick_rate, dec_rate,
det_rate
  95 moles = rate * TIME
  #96 print "moles = rate * time = ", moles, rate, time
  100 if (moles > m) then moles = m
  200 SAVE moles
-end

```

```

#####
Coliforms_m
#####
-start
  1 PR = parm(1)
  2 DR = parm(2)
  3 DC = parm(3)
  4 DH = parm(4)
#-----
# TIME UNIT in MT3D = DAYS - TRANSLATE INTO SECONDS
#-----
  5 qx = parm(5) /86400
  6 qy = parm(6) /86400
  7 qz = parm(7) /86400
  8 lambda = parm(8)
  9 k_dec = parm(9)/86400

```

```

#-----
# Get fluxes, cell dimensions and porosity from mt3d
#-----
11 vx = qx / (DH * DC) / PR
12 vy = qy / (DH * DR) / PR
13 vz = qz / (DC * DR) / PR
14 v_abs = sqrt(vx*vx+vy*vy+vz*vz)
#-----
19 p = (1-PR)^(1/3)
20 As = 2*(1-p^5)/(2- 3*p + 3*p^2 - 2*p^6)
21 Ap = 0.8e-06 # 0.8 micron (dia of bacteria 0.5 X 2 L)
22 Ac = 397*1e-06 #(median of grain size distribution)
24 NR = Ap/Ac
25 mTmp = mol("Tmp")*1000
26 T = 273.15+mTmp # T = absolute temp in Kelvin
27 omega = 9.85*10^15 * T^(-7.7) # omega= dynamic viscosity
28 k = 1.2806*10^(-23) # Boltzmann'd Constant JK^(-1)
29 Db = k*T/(3*(22/7)*omega*Ap) # Db = Coeficient of Brownian Motion
30 NPe = v_abs*Ac/Db # Peclet nr
#-----
# Calculating van der Waal's number
#-----
39 H = 6.5*10^(-21)
40 NvdW = H/(k*T) # H = Hamaker Constant = 6.5*10^(-21)
# k = 1.2806*10^(-23) Boltzmann'd Constant JK^(-1)
42 sp_area = 6*(1-PR)/(PR*Ac) # specific surface area unit per m
# Calculating Attraction number
51 NA = H/(12*(22/7)*omega*((Ap)^2)*v_abs*PR) # omega= dynamic viscosity

# Calculating the Gravity number
# grav =accln due to gravity m/s^2
52 grav = 9.81
53 paden = 1050 # kg/m3 particle density
54 fluden = 1000 # kg/m3 fluid density
55 NG = 2*grav*((Ap)^2)*(paden-fluden)/(9*omega*v_abs*PR)

#Calculating Efficiency Factor
60 n01 = 2.4 *As^(1/3)*NR^(-0.081)*NPe^(-0.715)*NvdW^(0.052)
61 n02 = 0.55*As*NR^(1.675)*NA^(0.125)
62 n03 = 0.22*NR^(-0.24)*NG^(1.11)*NvdW^(0.053)
63 n0 = n01 + n02 + n03

```

```

#Overall sticking efficiency
65 alpha_f = 1.0 # sticking eff at favorable sites = 1
66 alpha_u = 0.005 # sticking eff at unfavorable sites
68 alpha_tot = lambda*alpha_f+(1-lambda)*alpha_u

# straining efficiency
71 nstr = 2.7*(Ap/Ac)^(3/2) #ok
72 alpha_str = 0.01 #straining correction factor #ok

80 k_str = (sp_area*v_abs*PR/4)*(nstr*alpha_str)
82 k_stick = (sp_area*v_abs*PR/4)*(n0*alpha_tot)

# straining rate (= irreversible)
84 str_rate = k_str * TOT("Coliforms_m")
# stick rate (= attachment to sediments)
85 stick_rate = k_stick * TOT("Coliforms_m")
# decay rate in aqueous phase: default k_dec = ~ 0.2 per day
90 dec_rate = k_dec * TOT("Coliforms_m")

# save sticking (attachment) rate for use
# in rate expression of immobile Coliforms
91 put(stick_rate,20)
# retrieve detachment rate from rate
# expression of immobile Coliforms
92 det_rate = get(21)
# negative sign is introduced to induce removal of mobile Coliforms
# straining and decay decrease conc, detachment increases
# concentrations of mobile Coliforms
94 rate = - stick_rate - dec_rate - str_rate + det_rate
95 moles = rate * TIME
#100 if (moles > m) then moles = m
200 SAVE moles
-end

```

```

#####
# Coliforms attached
#####
Coliforms_im
-start
  1 mColif_im = TOT("Coliforms_im")
# 2 if (mColif_im <= 1e-14) then goto 200
  7 k_det = parm(1)/86400
  8 k_dec = parm(2)/86400
  20 dec_rate = mColif_im * k_dec
  25 det_rate = mColif_im * k_det
# save detachment rate so it can be used in the
# rate expression for the mobile Coliforms
  28 put(det_rate,21)
# retrieve sticking rate from rate
# expression for mobile Coliforms
  30 stick_rate = get(20)
# positive stick_rate causes immobile Coliforms to increase
# while positive decay rate decreases concentrations
  40 rate = stick_rate - dec_rate - det_rate
# 45 print "Coliforms: str_rate - dec_rate - det_rate" , str_rate, -dec_rate, -det_rate
  95 moles = rate * TIME
  100 if (moles > m) then moles = m
  200 SAVE moles
-end

END

```

**Part 4: PHT3D\_PH.DAT the PHREEQC-2 interface package file used in PHT3D**

2 1 0      15 1    1e-10    0.001 4000

0

5

0

0 0 0 0 0 0 0 0 0 0

0

2 0 0 2

0 0

Coliforms\_m 9

PR

DR

DC

DH

qx

qy

qz

0.0016

0.3

-formula Coliforms\_m 1.0

Ecoli\_m 9

PR

DR

DC

DH

qx

qy

qz

0.0016

0.3

-formula Ecoli\_m 1.0

Tmp

Na

Cl

pH

pe

Coliforms\_im 3

0.009

0.3

0

-formula Coliforms\_im 1.0

Ecoli\_im 3  
0.009  
0.3  
0  
-formula Ecoli\_im 1.0

## REFERENCES

- Anderson, E.I., 2005. Modeling groundwater-surface water interactions using the Dupuit approximation. *Adv. Water Resour.*, 28(4): 315-327.
- Appelo, C.A.J. and Postma, D., 2006. *Geochemistry, groundwater and pollution*. A. A. Balkema Publishers, Leiden, xviii, 649 pp.
- Arthur, J.D., Dabous A.A., and Cowart J.B., 2002. Mobilization of arsenic and other trace elements during aquifer storage and recovery, Southwest Florida. *US Geological Survey Artificial Recharge Workshop Proceedings*, Sacramento, CA, pp 2-4
- Arthur, J.D., Dabous A.A., and Cowart J.B., 2005. Water-Rock Geochemical Consideration for Aquifer Storage and Recovery: Florida Case Studies. In: Tsang CF, Apps JA (ed) *Underground Injection Science and Technology, Developments in Water Science*, Elsevier, Amsterdam, vol 52, pp 327-339
- Barry, D.A. et al., 2002. Modelling the fate of oxidisable organic contaminants in groundwater. *Advances in Water Resources*, 25(8-12): 945-983.
- Blaschke, A.P., Steiner, K.H., Schmalfuss, R., Gutknecht, D. and Sengschmitt, D., 2003. Clogging processes in hyporheic interstices of an impounded river, the Danube at Vienna, Austria. *International Review of Hydrobiology*, 88(3-4): 397-413.
- Bolster, C. H., Walker, S. L. and Cook, K. L., 2006. Comparison of *Escherichia coli* and *Campylobacter jejuni* transport in saturated porous media. *Journal of Environmental Quality* 35(4), 1018-1025.
- Bourg, A.C.M. and Bertin, C., 1993. Biogeochemical Processes During The Infiltration Of River Water Into An Alluvial Aquifer. *Environ. Sci. Technol.*, 27(4): 661-666.

- Bourg, A.C.M., Kedziorek, M.A.M. and Darmendrail, D., 2002. Organic matter as the driving force in the solubilisation of Fe and Mn during river water infiltration. In: C. Ray (ed.), *Understanding Contaminant Biogeochemistry and Pathogen Removal*. NATO Science Series: IV: Earth and Environmental Sciences. Kluwer.
- Bradford, S. A., Simunek, J. and Walker, S. L., 2006a. Transport and straining of E-coli O157 : H7 in saturated porous media. *Water Resources Research* 42(12).
- Bradford, S. A., Torkzaban, S. and Simunek, J., 2011. Modeling colloid transport and retention in saturated porous media under unfavorable attachment conditions. *Water Resources Research* 47.
- Bradford, S. A., Torkzaban, S. and Walker, S. L., 2007. Coupling of physical and chemical mechanisms of colloid straining in saturated porous media. *Water Research* 41(13), 3012-3024.
- Bradford, S.A., Simunek, J., Bettahar, M., Van Genuchten, M.T. and Yates, S.R., 2003. Modeling colloid attachment, straining, and exclusion in saturated porous media. *Environmental Science & Technology*, 37(10): 2242-2250.
- Bradford, S.A., Simunek, J., Bettahar, M., van Genuchten, M.T. and Yates, S.R., 2006b. Significance of straining in colloid deposition: Evidence and implications. *Water Resources Research*, 42(12).
- Brun, A. and Engesgaard, P., 2002. Modelling of transport and biogeochemical processes in pollution plumes: literature review and model development. *Journal of Hydrology*, 256(3-4): 211-227.
- Champ, D.R., Gulens, J. and Jackson, R.E., 1979. Oxidation–reduction sequences in groundwater flow systems. *Can. J. Earth Sci.*, 16: 12–23.
- Constantz, J., 2008. Heat as a tracer to determine streambed water exchanges. *Water Resources Research*, 44: 20.

- Corapcioglu, M. Y. and Haridas, A. , 1984. Transport and fate of microorganisms in porous-media: a theoretical investigation. *Journal of Hydrology* 72(1-2), 149-169.
- DeFlaun, M.F. et al., 1997. Preliminary observations on bacterial transport in a coastal plain aquifer. *Fems Microbiology Reviews*, 20(3-4): 473-487.
- Dillon, P., 2005. Future management of aquifer recharge. *Hydrogeology Journal*, 13(1): 313-316.
- Ding, D., 2010. Transport of bacteria in aquifer sediment: experiments and modeling. *Hydrogeology Journal* 18(3), 669-679.
- Doppler, T., Franssen, H.J.H., Kaiser, H.P., Kuhlman, U. and Stauffer, F., 2007. Field evidence of a dynamic leakage coefficient for modelling river-aquifer interactions. *Journal of Hydrology*, 347(1-2): 177-187.
- Doussan, C., et al., 1994. Coupled use of thermal and hydraulic head data to characterize river-groundwater exchanges. *Journal of Hydrology*, 153(1-4): 215-229.
- Doussan, C., Poitevin, G., Ledoux, E., and Detay, M., 1997. River bank filtration: Modeling of the changes in water chemistry with emphasis on nitrogen species. *J Contam Hydrol*, 25:129
- Eckert, P. and Irmischer, R., 2006. Over 130 years of experience with Riverbank filtration in Dusseldorf, Germany. *Journal of Water Supply Research and Technology-Aqua*, 55(4): 283-291.
- Eckert, P., and Appelo, C.A.J., 2002. Hydrogeochemical modeling of enhanced benzene, toluene, ethylbenzene, xylene (BTEX) remediation with nitrate. *Water Resources Research*. 38(8): 1130
- Eckert, P., Irmischer, R. and Rohns, H.P., 2005. Dynamic processes during bank filtration and their impact on raw water quality, 5th International Symposium on Managed Aquifer Recharge (ISMAR5), Berlin, Germany, 11-16 June 2005. IHP-VI, Series on Groundwater No. 13. UNESCO, pp. 16-21.

- Edberg, S. C., Rice, E. W., Karlin, R. J. and Allen, M. J., 2000. *Escherichia coli*: the best biological drinking water indicator for public health protection. *Journal of Applied Microbiology* 88, 106S.
- EPA, 2009. National Primary Drinking Water Regulations, U.S. Environmental Protection Agency, EPA 816-F-09-0004.
- EPA, 2010. Watershed Assessment, Tracking & Environmental Results, U.S. Environmental Protection Agency, Washington DC, USA
- EPD, 2008. Georgia Comprehensive State-wide Water Management Plan. Georgia Water Council, Environmental Protection Directorate, GA, USA
- Ferguson, C., Husman, A. M. D. R., Altavilla, N., Deere, D. and Ashbolt, N., 2003. Fate and Transport of Surface Water Pathogens in Watersheds. *Critical Reviews in Environmental Science and Technology* 33(3), 299-361.
- Fong, T. T., Mansfield, L. S., Wilson, D. L., Schwab, D. J., Molloy, S. L. and Rose, J. B., 2007. Massive microbiological groundwater contamination associated with a waterborne outbreak in Lake Erie, South Bass Island, Ohio. *Environ Health Perspect* 115(6), 856-864.
- Foppen, J. W. A., Mporokoso, A. and Schijven, J. F., 2005. Determining straining of *Escherichia coli* from breakthrough curves. *Journal of Contaminant Hydrology* 76(3-4), 191-210.
- Foppen, J. W., Lutterodt, G., Röling, W. F. M. and Uhlenbrook, S., 2010. Towards understanding inter-strain attachment variations of *Escherichia coli* during transport in saturated quartz sand. *Water Research* 44(4), 1202-1212.
- Foppen, J. W., Van Herwerden, M. and Schijven, J., 2007. Measuring and modelling straining of *Escherichia coli* in saturated porous media. *Journal of Contaminant Hydrology* 93(1-4), 236-254.

- Foppen, J.W.A. and Schijven, J.F., 2006. Evaluation of data from the literature on the transport and survival of *Escherichia coli* and thermotolerant coliforms in aquifers under saturated conditions. *Water Research*, 40(3): 401-426.
- Geldreich, E. E., 1996. Pathogenic agents in freshwater resources. *Hydrological Processes* 10(2), 315-333.
- Ginn, T. R., Wood, B. D., Nelson, K. E., Scheibe, T. D., Murphy, E. M. and Clement, T. P., 2002. Processes in microbial transport in the natural subsurface. *Advances in Water Resources* 25(8-12), 1017-1042.
- Gollnitz, W.D., Clancy, J.L., Whitteberry, B.L. and Vogt, J.A., 2003. RBF as a microbial treatment process. *Journal American Water Works Association*, 95(12): 56-66.
- Greskowiak, J., Prommer, H., Massmann, G., Johnston, C. D., Nützmann G., Pekdeger, A. 2005a. The impact of variably saturated conditions on hydrogeochemical changes during artificial recharge of groundwater. *Applied Geochemistry*, 20(7): 1409-1426.
- Greskowiak, J., Prommer, H., Massmann, G. and Nützmann, G., 2006. Modeling seasonal redox dynamics and the corresponding fate of the pharmaceutical residue phenazone during artificial recharge of groundwater. *Environmental Science & Technology*, 40(21): 6615-6621.
- Greskowiak, J., Prommer, H., Vanderzalm, J., Pavelic, P. and Dillon, P., 2005b. Modeling of carbon cycling and biogeochemical changes during injection and recovery of reclaimed water at Bolivar, South Australia. *Water Resources Research*, 41(10).
- Grischek, T., Schoenhein, D., Eckert, P. and Ray, C., 2010. Sustainability of river bank filtration. In: A. Zuber, J. Kania and E. Kmiecik (Editors), XXXVIII IAH Congress: Groundwater Quality Sustainability. University of Silesia Press, Krakow.
- Grünheid, S., Amy, G. and Jekel, M., 2005. Removal of bulk dissolved organic carbon (DOC) and trace organic compounds by bank filtration and artificial recharge. *Water Research*, 39(14): 3219-3228.

- Hall, J. A., Mailloux, B. J., Onstott, T. C., Scheibe, T. D., Fuller, M. E., Dong, H. and DeFlaun, M. F., 2005. Physical versus chemical effects on bacterial and bromide transport as determined from on site sediment column pulse experiments. *Journal of Contaminant Hydrology* 76(3-4), 295-314.
- Harbaugh, A.W., Banta, E.R., Hill, M.C. and McDonald, M.G., 2000. MODFLOW-2000, the U.S. Geological Survey Modular Ground-Water Model—User Guide to Modularization Concepts and the Ground-Water Flow Process. US Geological Survey Open-File Report 00-92, 121 pp.
- Harvey, R.W. and Garabedian, S.P., 1991. Use of colloid filtration theory in modeling movement of bacteria through a contaminated sandy aquifer. *Environmental Science & Technology* 25(1), 178-185.
- Harvey, R.W., 1997. Microorganisms as tracers in groundwater injection and recovery experiments: a review. *Fems Microbiology Reviews* 20(3-4), 461-472.
- Harvey, R.W., Kinner, N.E., Macdonald, D., Metge, D.W. and Bunn, A., 1993. Role of physical heterogeneity in the interpretation of small-scale laboratory and field observations of bacteria, microbial-sized microsphere, and bromide transport through aquifer sediments. *Water Resources Research*, 29(8): 2713-2721.
- Hendry, M. J., Lawrence, J. R. and Maloszewski, P., 1999. Effects of velocity on the transport of two bacteria through saturated sand. *Ground Water* 37(1), 103-112.
- Hermansson, M., 1999. The DLVO theory in microbial adhesion. *Colloids and Surfaces B-Biointerfaces*, 14(1-4): 105-119.
- Hicks D.W., Krause, R.E. and Clarke, J.S., 1981. *Geohydrology of the Albany Area, Georgia*. Prepared in cooperation with the US Geological Survey and the Albany Water, Gas, and Light Commission, Georgia Geologic Survey, Environmental Protection Division, Department of Natural Resources, Atlanta, GA
- Hijnen, W.A.M., Brouwer-Hanzens, A.J., Charles, K.J. and Medema, G.J., 2005. Transport of MS2 Phage, *Escherichia coli*, *Clostridium perfringens*, *Cryptosporidium*

- parvum, and *Giardia intestinalis* in a Gravel and a Sandy Soil. *Environmental Science & Technology*, 39(20): 7860-7868.
- Hiscock, K.M. and Grischek, T., 2002. Attenuation of groundwater pollution by bank filtration. *Journal of Hydrology*, 266(3-4): 139-144.
- Hubbs, S.A., (ed) 2006. Riverbank filtration hydrology; impacts on system capacity and water quality. Proc. NATO Advanced Research Workshop on Riverbank Filtration Hydrology, Bratislava, 7-10 Sept. 2004, Springer NATO Science Series IV, Earth and Envir Sciences 60, 344p.
- Jacobs, L.A., von Gunten, H.R., Keil, R. and Kuslys, M., 1988. Geochemical changes along a river-groundwater infiltration flow path: Glattfelden, Switzerland. *Geochimica Et Cosmochimica Acta*, 52(11): 2693-2706.
- John, D.E. and Rose, J.B., 2005. Review of Factors Affecting Microbial Survival in Groundwater. *Environmental Science & Technology* 39(19), 7345-7356.
- Johnson, W.P., Zhang, P., Gardner, P.M., Fuller, M.E. and DeFlaun, M.F., 2001. Evidence for detachment of indigenous bacteria from aquifer sediment in response to arrival of injected bacteria. *Applied and Environmental Microbiology*, 67(10): 4908-4913.
- Jones G.W., and Pichler, T., 2007. Relationship between pyrite stability and arsenic mobility during aquifer storage and recovery in Southwest Central Florida. *Environ Sci Technol.* 41, 723-730
- Keast, G. and Johnston, R., 2008. UNICEF handbook on water quality. UNICEF, New York.
- Kedziorek, M.A.M., Geoffriau, S. and Bourg, A.C.M., 2008. Organic Matter and Modeling Redox Reactions during River Bank Filtration in an Alluvial Aquifer of the Lot River, France. *Environ. Sci. Technol.*, 42(8): 2793-2798.

- Khan, S., Mushtaq, S., Hanjra, M.A., Schaeffer, J., 2008. Estimating potential costs and gains from an aquifer storage and recovery program in Australia. *Agricultural Water Management*. Volume 95, Issue 4, April 2008, Pages 477-488
- Kim, H. N. and Walker, S. L., 2009. Escherichia coli transport in porous media: Influence of cell strain, solution chemistry, and temperature. *Colloids and Surfaces B-Biointerfaces* 71(1), 160-167.
- Kirschbaum, M.U.F., 1995. The temperature dependence of soil organic matter decomposition, and the effect of global warming on soil organic C storage. *Soil Biology and Biochemistry*, 27(6): 753-760.
- Kuehn, W. and Mueller, U., 2000. Riverbank filtration - An overview. *Journal American Water Works Association*, 92(12): 60-69.
- Lawrence, J.R. and Hendry, M.J., 1996. Transport of bacteria through geologic media. *Canadian Journal of Microbiology*, 42(4): 410-422.
- Lensing, H.J., Vogt, M. and Herrling, B., 1994. Modeling of biologically mediated redox processes in the subsurface. *Journal of Hydrology*, 159(1-4): 125-143.
- Levy, J., Sun, K., Findlay, R. H., Farruggia, F. T., Porter, J., Mumy, K. L., Tomaras, J. and Tomaras, A., 2007. Transport of Escherichia coli bacteria through laboratory columns of glacial-outwash sediments: Estimating model parameter values based on sediment characteristics. *Journal of Contaminant Hydrology* 89(1-2), 71-106.
- Lovley, D.R. and Chapelle, F.H., 1995. Deep subsurface microbial processes. *Reviews of Geophysics*, 33(3): 365-381.
- Lutterodt, G., Basnet, M., Foppen, J.W.A. and Uhlenbrook, S., 2009. The effect of surface characteristics on the transport of multiple Escherichia coli isolates in large scale columns of quartz sand. *Water Research* 43(3), 595-604.
- Ma, R. and Zheng, C., 2010. Effects of Density and Viscosity in Modeling Heat as a Groundwater Tracer. *Ground Water*, 48(3): 380-389.

- Massmann, G., Greskowiak, J., Dünnbier, U., Knappe, A., Pekdeger, A. 2006. The impact of variable temperatures on the redox conditions and the behaviour of pharmaceutical residues during artificial recharge. *J. Hydrol.*, 328(1-2): 141-156.
- Massmann, G., Nogeitzig, A., Taute, T. and Pekdeger, A., 2008. Seasonal and spatial distribution of redox zones during lake bank filtration in Berlin, Germany. *Environmental Geology*, 54(1): 53-65.
- Matthess, G., 1982. *The Properties of Groundwater*. Wiley, New York.
- McNab, W.W., Jr. and Narasimhan, T.N., 1994. Modeling reactive transport of organic compounds in groundwater using a partial redox disequilibrium approach. *Water Resour. Res.*, 30(9): 2619-2635.
- Medema, G. J. and Stuyfzand, P. J., 2002. Removal of microorganisms upon basin recharge, deep well injection and river bank filtration in the Netherlands. Dillon, P. (ed), pp. 125-131, Balkema, Adelaide, Australia.
- Meyer, K.U., 1999. A numerical model for multicomponent reactive transport in variable saturated porous media. University of Waterloo, Waterloo, Canada.
- Miettinen, I.T., Martikainen, P.J., and Vartiainen, T., 1994. Humus Transformation At The Bank Filtration Water-Plant. 30(10): 179-187.
- Miller J.A., 1986. Hydrogeologic Framework of the Floridan Aquifer System in Florida and in Parts of Georgia, Alabama, and South Carolina. US Geological Survey Professional Paper 1403-B
- Mirecki, J.E., Campbell, B.G., Conlon, K.J. and Petkewich, M.D., 1998. Solute changes during aquifer storage and recovery testing in a limestone/clastic aquifer. *Ground Water*, 36(3): 394-403
- NRC, 2007. Prospects of Managed Underground Storage of Recoverable Water. Committee on Sustainable Underground Storage of Recoverable Water. Water Science

and Technology Board, National Research Council, The National Academies Press, Washington, DC.

Oliver, D.M., Clegg, C.D., Haygarth, P.M. and Heathwaite, A.L., 2005. Advances in Agronomy, pp. 125-180, Academic Press.

Pachepsky, Y. A., Sadeghi, A. M., Bradford, S. A., Shelton, D.R., Guber, A.K. and Dao, T. 2006. Transport and fate of manure-borne pathogens: Modeling perspective. *Agricultural Water Management* 86(1-2), 81-92.

Pang, L. P., 2009. Microbial Removal Rates in Subsurface Media Estimated From Published Studies of Field Experiments and Large Intact Soil Cores. *Journal of Environmental Quality* 38(4), 1531-1559.

Pang, L., Close, M., Goltz, M., Sinton, L., Davies, H., Hall, C. and Stanton, G., 2004. Estimation of septic tank setback distances based on transport of E. coli and F-RNA phages. *Environment International* 29(7), 907-921.

Parkhurst, D.L. and Appelo, C.A.J., 1999. User's guide to PHREEQC (version 2): A computer program for speciation, batch-reaction, one-dimensional transport, and inverse geochemical calculations, Water-Resources Investigations Report 99-4259. US Geological Survey, Denver, CO, 326 pp.

Partinoudi, V. and Collins, M.R., 2007. Assessing RBF reduction/removal mechanisms for microbial and organic DBP precursors. *American Water Works Association Journal* 99(12), 61-71.

Petrovic, M. et al., 2009. Fate and removal of pharmaceuticals and illicit drugs in conventional and membrane bioreactor wastewater treatment plants and by riverbank filtration. *Philosophical Transactions of the Royal Society A: Mathematical, Physical and Engineering Sciences*, 367(1904): 3979-4003.

Petrunic, B.M., MacQuarrie, K.T.B. and Al, T.A., 2005. Reductive dissolution of Mn oxides in river-recharged aquifers: a laboratory column study. *Journal of Hydrology*, 301(1-4): 163-181.

- Phanikumar, M.S., Hyndman, D.W., Zhao, X.D. and Dybas, M.J., 2005. A three-dimensional model of microbial transport and biodegradation at the Schoolcraft, Michigan, site. *Water Resources Research*, 41(5).
- Postma, D. and Jakobsen, R., 1996. Redox zonation: Equilibrium constraints on the Fe(III)/SO<sub>4</sub>-reduction interface. *Geochimica Et Cosmochimica Acta*, 60(17): 3169-3175.
- Powelson, D.K. and Mills, A.L., 2001. Transport of in Escherichia Coli in Sand Columns with Constant and Changing Water Contents. *J. Environ. Qual.* 30(1), 238-245.
- Prescott, L.M., Harley, J.P. and Klein, D.A., 1996. *Microbiology*. Wm. C. Brown Publishers, Dubuque, IA.
- Price R.E., Pichler, T., 2005. Abundance and Mineralogic Association of Arsenic in the Suwannee Limestone (Florida): Implications for Arsenic Release During Water-Rock Interaction. *Chem Geol* 228, 44-56
- Prommer, H. and Stuyfzand, P.J., 2005. Identification of temperature-dependent water quality changes during a deep well injection experiment in a pyritic aquifer. *Environmental Science & Technology*, 39(7): 2200-2209.
- Prommer, H., Barry, D.A. and Zheng, C., 2003. MODFLOW/MT3DMS-Based Reactive Multicomponent Transport Modeling. *Ground Water*, 41(2): 247-257.
- Prommer, H., Tuxen, N. and Bjerg, P.L., 2006. Fringe-controlled natural attenuation of phenoxy acids in a landfill plume: Integration of field-scale processes by reactive transport modeling. *Environmental Science & Technology*, 40(15): 4732-4738.
- Pyne, D., 2005. *Aquifer storage recovery: A guide to groundwater recharge through wells* ASR Systems. CRC Press, FL, USA
- Rajagopalan, R. and Tien, C., 1976. Trajectory analysis of deep-bed filtration with the sphere-in-cell porous media model. *AIChE Journal* 22(3), 523-533.

- Ray, C., 2002. Effects of biogeochemical, hydrological, and well construction factors on riverbank filtrate quality. In: C. Ray (Editor), *Riverbank Filtration: Understanding Contaminant Biogeochemistry and Pathogen Removal*. NATO Science Series. Kluwer Academic Publishers, Tihany, Hungary.
- Ray, C., 2004. Modeling RBF efficacy for mitigating chemical shock loads *JAWWA* 96(5), 114-128
- Ray, C., 2008. Worldwide potential of riverbank filtration. *Clean Technologies and Environmental Policy*, 10(3): 223-225.
- Ray, C., Grischek, T., Schubert, J., Wang, J.Z. and Speth, T.F., 2002a. A perspective of riverbank filtration. *Journal American Water Works Association*, 94(4): 149-+.
- Ray, C., Schubert, J., Linsky, R. and Melin, G., 2002b. Introduction: Riverbank Filtration. In: C. Ray, R. Linsky and G. Melin (Editors), *Riverbank filtration improving source water quality*. Water Science and Technology Library. Springer Netherlands, pp. 1-15.
- Ray, C., Soong, T.W., Lian, Y.Q. and Roadcap, G.S., 2002c. Effect of flood-induced chemical load on filtrate quality at bank filtration sites. *Journal of Hydrology*, 266(3-4): 235-258.
- Rinck-Pfeiffer, S., Ragusa, S., Sztajn bok, P. and Vandevelde T., 2000. Interrelationships between biological, chemical, and physical processes as an analog to clogging in aquifer storage and recovery (ASR) wells. *Water Research*, 34(7): 2110-2118
- Ryan, J.N. and Elimelech, M., 1996. Colloid mobilization and transport in groundwater. *Colloids and Surfaces A: Physicochemical and Engineering Aspects*, 107(0): 1-56.
- Saaltink, M.W., Ayora, C., Stuyfzand, P.J., and Timmer, H., 2003. Analysis of a deep well recharge experiment by calibrating a reactive transport model with field data. *J Contam Hydrol* 65(0169-7722)

- Scheibe, T.D., Dong, H. and Xie, Y., 2007. Correlation between bacterial attachment rate coefficients and hydraulic conductivity and its effect on field-scale bacterial transport. *Advances in Water Resources*, 30(6-7): 1571-1582.
- Scheibe, T.D., Hubbard, S.S., Onstott, T.C. and DeFlaun, M.F., 2011. Lessons Learned from Bacterial Transport Research at the South Oyster Site. *Ground Water* 49(5), 745-763.
- Schijven, J., Berger, P. and Miettinen, I., 2002. Removal of Pathogens, Surrogates, Indicators, and Toxins Using Riverbank Filtration. In: C. Ray, G. Melin and R. Linsky (ed.), *Riverbank filtration: Improving source-water quality*. Water Science and Technology Library. Springer Netherlands, pp. 73-116.
- Schijven, J.F. and Hassanizadeh, S.M., 2000. Removal of viruses by soil passage: Overview of modeling, processes, and parameters. *Critical Reviews in Environmental Science and Technology*, 30(1): 49-127.
- Schijven, J.F., Hoogenboezem, W., Nobel, P.J., Medema, G.J. and Stakelbeek, A., 1998. Reduction of FRNA-bacteriophages and faecal indicator bacteria by dune infiltration and estimation of sticking efficiencies. *Water Science and Technology* 38(12), 127-131.
- Schinner, T., Letzner, A., Liedtke, S., Castro, F. D., Eydelnant, I. A. and Tufenkji, N., 2010. Transport of selected bacterial pathogens in agricultural soil and quartz sand. *Water Research* 44(4), 1182-1192.
- Schubert, J., 2002a. German experience with riverbank filtration systems. In: C. Ray, G. Melin and R.B. Linsky (Editors), *Riverbank filtration improving source water quality*. Water Science and Technology Library. Kluwer Academic Publishers, pp. 35-48.
- Schubert, J., 2002b. Hydraulic aspects of riverbank filtration - field studies. *Journal of Hydrology*, 266(3-4): 145-161.

- Sen, T.K., 2011. Processes in Pathogenic Biocolloidal Contaminants Transport in Saturated and Unsaturated Porous Media: A Review. *Water Air and Soil Pollution*, 216(1-4): 239-256.
- Sharma, L., Greskowiak, J., Ray, C., Eckert, P. and Prommer, H., 2012. Elucidating temperature effects on seasonal variations of biogeochemical turnover rates during riverbank filtration. *Journal of Hydrology* 428-429, 104-115.
- Simoni, S. F., Harms, H., Bosma, T. N. P. and Zehnder, A. J. B. (1998) Population heterogeneity affects transport of bacteria through sand columns at low flow rates. *Environmental Science & Technology* 32(14), 2100-2105.
- Sinton, L.W., Mackenzie, M.L., Karki, N., Braithwaite, R.R., Hall, C.H. and Flintoft, M.J., 2010. Transport of *Escherichia coli* and F-RNA bacteriophages in a 5 m column of saturated pea gravel. *Journal of Contaminant Hydrology* 117(1-4), 71-81.
- Smedley, P.L., and Kinniburgh, G.D., 2002. A review of the source behavior, and distribution of arsenic in natural waters. *Applied Geochemistry*, 17: 517-668
- Sontheimer, H., 1980. Experience with Riverbank Filtration Along the Rhine River. *Journal American Water Works Association*, 72(7): 386-390.
- Stonestrom, D.A. and Constantz, J., 2003. Heat as a tool for studying the movement of ground water near streams, U.S. Geological Survey, Reston, VA.
- Stuyfzand, P.J., 1989. Hydrology and water quality aspects of Rhine bank ground water in The Netherlands. *J. Hydrol.* 106, 341-363.
- Stuyfzand, P.J., 2010. Hydrogeochemical processes during river bank filtration and artificial recharge of polluted surface waters: zonation, identification and quantification. This volume.
- Su, G.W., Jasperse, J., Seymour, D., Constantz, J. and Zhou, Q., 2007. Analysis of pumping-induced unsaturated regions beneath a perennial river. *Water Resources Research*, 43(8).

- Syngouna, V.I. and Chrysikopoulos, C.V., 2011. Transport of biocolloids in water saturated columns packed with sand: Effect of grain size and pore water velocity. *Journal of Contaminant Hydrology*, 126(3-4): 301-314.
- Tan, Y., Gannon, J.T., Baveye, P. and Alexander, M., 1994. Transport of bacteria in an aquifer sand: Experiments and model simulations. *Water Resour. Res.* 30(12), 3243-3252.
- Torkzaban, S., Bradford, S.A. and Walker, S.L., 2007. Resolving the Coupled Effects of Hydrodynamics and DLVO Forces on Colloid Attachment in Porous Media. *Langmuir* 23(19), 9652-9660.
- Torkzaban, S., Bradford, S.A., van Genuchten, M.T. and Walker, S.L., 2008. Colloid transport in unsaturated porous media: The role of water content and ionic strength on particle straining. *Journal of Contaminant Hydrology* 96(1-4), 113-127.
- Tufenkji, N. and Elimelech, M., 2003. Correlation Equation for Predicting Single-Collector Efficiency in Physicochemical Filtration in Saturated Porous Media. *Environmental Science & Technology*, 38(2): 529-536.
- Tufenkji, N. and Elimelech, M., 2004. Deviation from the classical colloid filtration theory in the presence of repulsive DLVO interactions. *Langmuir* 20(25), 10818-10828.
- Tufenkji, N., 2007. Modeling microbial transport in porous media: Traditional approaches and recent developments. *Advances in Water Resources*, 30(6-7): 1455-1469.
- Tufenkji, N., Ryan, J.N. and Elimelech, M., 2002. The promise of bank filtration. *Environ. Sci. Technol.*, 36(21): 422A-428A.
- Vanderzalm, J.L., Le Gal La Salle, C., and Dillon P.J., 2006. Fate of organic matter during aquifer storage and recovery (ASR) of reclaimed water in a carbonate aquifer. *Applied Geochemistry*, 21(7): 1204-1215

- Verstraeten, I.M. et al., 1999. Surface water-ground water interaction: Herbicide transport into municipal collector wells. 28(5): 1396-1405.
- Wall, K., Pang, L., Sinton, L. and Close, M., 2008. Transport and attenuation of microbial tracers and effluent microorganisms in saturated pumice sand aquifer material. *Water Air and Soil Pollution* 188(1-4), 213-224.
- Wallis, I., Prommer, H., Simmons, C.T., Post, V. and Stuyfzand, P.J., 2010. Evaluation of Conceptual and Numerical Models for Arsenic Mobilization and Attenuation during Managed Aquifer Recharge. *Environmental Science & Technology*, 44(13): 5035-5041.
- Wang, J., 2002. Riverbank Filtration Case Study at Louisville, Kentucky. In: C. Ray, G. Melin and R.B. Linsky (Editors), *Riverbank Filtration Case Study at Louisville, Kentucky*. In *Riverbank Filtration Improving Source-Water Quality*. Water Science and Technology Library. Springer Netherlands, pp. 117-145.
- Wang, J.Z., Hubbs, S.A. and Song, R., 2002. Evaluation of Riverbank Filtration as a Drinking Water Treatment Process. AWWA Research Foundation and American Water Works Association, Denver, CO, USA.
- Water Resource Solutions, 2006. Flint River Basin Near Albany, Georgia Aquifer Storage and Recovery (ASR) Feasibility Assessment, Water Policy Working Paper #2006-005, The Georgia Water Planning and Policy Center, Albany, GA
- Weiss, R.F., 1970. The solubility of nitrogen, oxygen and argon in water and seawater. *Deep Sea Research and Oceanographic Abstracts*, 17(4): 721-735.
- Weiss, W.J. et al., 2004. Riverbank filtration: Effect of ground passage on NOM character. *Journal of Water Supply Research and Technology-Aqua*, 53(2): 61-83.
- Weiss, W.J. et al., 2005. Riverbank filtration for control of microorganisms: Results from field monitoring. *Water Research*, 39(10): 1990-2001.

- Wilson, B.A., Smith, V.H., deNoyelles, F. and Larive, C.K., 2003. Effects of Three Pharmaceutical and Personal Care Products on Natural Freshwater Algal Assemblages. *Environmental Science & Technology*, 37(9): 1713-1719.
- Wilson, D., 2007. The feasibility of using aquifer storage and recovery to manage water supplies in Georgia. In: T Rasmussen (Editor) *Proceedings of the 2007 Georgia Water Resources Conference* University of Georgia, Athens, GA, USA
- Yao, K.-M., Habibian, M.T. and O'Melia, C.R., 1971. Water and waste water filtration. Concepts and applications. *Environmental Science & Technology*, 5(11): 1105-1112.
- Zhang, P.F., Johnson, W.P., Scheibe, T.D., Choi, K.H., Dobbs, F.C. and Mailloux, B.J., 2001. Extended tailing of bacteria following breakthrough at the Narrow Channel focus area, Oyster, Virginia. *Water Resources Research* 37(11), 2687-2698.
- Zheng, C. and Wang, P.P., 1999. MT3DMS: A modular three-dimensional multi-species transport model for simulation of advection, dispersion, and chemical reactions of contaminants in ground water systems. SERDP-99-1, US Army Corps of Engineers Research and Development Centre, Vicksburg, MS.
- Zheng, C., 2010. MT3DMS v5.3 - A modular three-dimensional multispecies transport model for simulation of advection, dispersion and chemical reactions of contaminants in groundwater systems: Supplemental User's Guide, The University of Alabama, Tuscaloosa, Alabama.